CHARACTERIZATION OF ELECTROSTATIC CHARGES IN GAS-SOLID FLUIDIZED BEDS

by

POUPAK MEHRANI

B.Sc., The University of British Columbia, 2001

A THESIS SUBMITTED IN PARTIAL FULFILMENT OF
THE REQUIREMENTS FOR THE DEGREE OF

DOCTOR OF PHILOSOPHY

in

THE FACULTY OF GRADUATE STUDIES

(Chemical and Biological Engineering)

THE UNIVERSITY OF BRITISH COLUMBIA

June 2005

ABSTRACT

A novel on-line measurement technique was developed in this work based on the Faraday cup method by constructing a copper fluidization column of diameter 0.1 m as the inner cup and a second surrounding copper column as the outer cup to gain better understanding of charge generation inside gas-solid fluidized beds. Net charges generated inside fluidized beds were investigated for relatively large glass beads (566 μm mean diameter) fluidized by extra dry air. It was concluded that particle-gas contacting had negligible effect on the particle charging mechanism for the conditions studied. Also, air ionization is expected to have played a negligible role with respect to dissipation of charges on the particles.

Free bubbling fluidization of mono-sized and binary mixtures of particles consisting of relatively large glass beads (566 μm mean diameter) and fine glass beads (30 μm mean diameter) showed that the net charges generated inside the fluidized bed were caused by entrained charged fine particles from the fluidization column.

The effect of adding different varieties of fine (<45 μm) particles (Larostat 519, glass beads, silver-coated glass beads, a catalyst and silica) on charge generation/dissipation inside beds of the relatively large glass beads and 558 μm polyethylene particles was studied by investigating the change of the electrostatic behaviour of fines after their addition to the fluidized bed. It was found that fine Larostat 519, two types of glass beads and two types of silver-coated glass beads carried positive charges out of the fluidized bed of relatively coarse glass beads at different relative humidities of the fluidizing air (0, 15, 35 and 60%). Comparison of charge-to-mass ratios of different fines showed that the finer the particles, the higher the charges carried per unit mass. The Larostat fines helped to dissipate the initial bed charges by attaching themselves to the large glass beads. It was found that the higher the surface conductivity of the fines, the easier it was for them to lose their charges to the column walls, thereby dissipating the initial bed charges. As the relative humidity of the fluidizing gas increased, the charge-to-mass ratios decreased, as

expected. Free bubbling fluidization of binary mixtures of fines (Larostat 519, catalyst, silica and silver-coated glass beads) with relatively large polyethylene particles showed that the polarity of the charges transported out of the fluidized bed depended on the relative humidity of the fluidizing gas. It was concluded that the relative humidity of the fluidizing gas can affect the bed material (polyethylene particles) and/or the electrical behaviour of added fines. Fine catalyst and silver-coated glass beads behaved similarly, probably due to having high surface electrical conductivities. Charge-to-mass ratios were higher for the catalyst and silica particles than for the other fines. Observations after fluidizing the binary particles mixtures confirmed that there were fewer polyethylene particles clinging to the column walls when Larostat 519 and silver-coated glass bead fines were present. Bi-polar charging was also investigated. For both the coarse glass beads and polyethylene particles tested, smaller particles were charged positively and larger particles negatively.

Different fines charging mechanisms, charge transfer and charge separation between the fines and the coarse particles, as well as the column wall, and their significance were investigated. For different added fines, different leading charging mechanisms were determined. The fines charging mechanisms considered in this study included particle-particle, as well as particle-wall, interactions. The latter were important here because the fluidization column in this study was of laboratory scale, so that particle-wall contacts were significant. In industrial-scale units, particle-particle interactions are likely to be dominant. Such factors as the material, physical and chemical surface properties of the solid phases, as well as the moisture content of the fluidizing gas are also important. Overall fines added to an initially charged fluidized bed carry significant charges from the column. This is a significant finding since fines are always elutriated in fluidized bed processes. It also suggests that since electrostatic forces play a role in determining the flux of entrained fines from a fluidized bed, they should be incorporated into models developed to predict entrainment flux and, perhaps also, transport disengagement height.

Table of Contents

List of Tables

List of Figures

Nomenclature

A_s	Total particles surface area (m^2)
d_P	Particle diameter (m)
D_L	Diameter of the smallest circumscribing circle of a particle (m)
D_s	Diameter of the largest inscribed circle of a particle (m)
m	Mass (kg)
N	Number of particles (-)
Q	Charge (C)
Q_o	Initial charge (C) or initial charge-to-mass ratio (C/kg)
Q_f	Final charge (C) or final charge-to-mass ratio (C/kg)
Q_F	Charges on fine particles (C)
Q_L	Charges on large particles (C)
Q_W	Charges on column wall (C)
$Q_{o,L}$	Initial charges of large particles (C)
$Q_{o,W}$	Initial charges of the column wall (C)
Q/m	Charge-to-mass ratio, (C/kg)
U_{mf}	Minimum fluidization velocity (m/s)

Greek Letters

ρ_p	Particle density (kg/m^3)
φ	Particle sphericity (-)

Acknowledgments

I would like to first express my sincere gratitude to my supervisors, Dr. John Grace and Dr. Xiaotao Bi, for their excellent guidance and continuous support throughout this challenging investigation. Special thanks to Dr. John Grace in believing in me and giving me the opportunity to be part of his fluidization group.

I would like to acknowledge Dr. K.D. Srivastava for the valuable discussions. I also wish to thank Dr. Aihua Chen for her time and always being available to help me with running the experiments.

I would like to acknowledge the staff of The Chemical Engineering Department, Peter Roberts, Graham Liebelt, Geoff Corbet, Doug Yuen, Alex Thang, Horace Lam, Qi Chen, Lori Tanaka, Helsa Leong and Amber Lee, for their expertise, experience, help and friendship. Special thanks to Graham Liebelt and Geoff Corbet whom the completion of this project would not have been possible without their excellent effort in building the experimental set up.

I wish to thank NOVA Chemicals. for their contribution, for providing samples and helping to understand the industrial aspect of this project. Many thanks to Dr. James Muir and Dr. Bob Quaiattini for all the informative discussions.

I am grateful to my fellow graduate students and friends for their love and support. My special thanks to my dear friend, Dr. Phillip Servio, for his ongoing support and encouragement throughout my Ph.D. Many thanks to my dear friends, Eman Al-atar and Sevan Bedrossian who made my life at UBC such an enjoyable experience.

Finally, I would like to thank my family for believing in me, and their love and encouragement during the difficult times.

Dedication

I wish to dedicate this thesis with love to the memory of my mother, Farkhondeh Parsa (1945-2000), who has been a source of encouragement and inspiration to me throughout my life. It is also dedicated to my father, Alireza Mehrani, who I could not have achieved this goal without his love and support, especially after the loss of my mother.

Chapter 1. Introduction

In gas-solid fluidization, solid particles are transformed into a fluid-like state by being suspended in a gas. Gas-solid fluidization has numerous important industrial applications such as drying, granulation, gas-solid reactions and solid-catalyzed gas reactions. For instance, a gas-phase fluidized bed process has been the dominant means for carrying out catalytic polymerization to produce polyethylene since the 1980s.

One of the major problems in some gas-solid fluidization processes is the electrostatic charge build-up inside the bed. Electrostatic charges are generated due to repeated particle-particle and particle-wall contact and separation, plus the friction of particles against each other and the vessel wall. The charge build-up results in particle agglomeration, particle-wall adhesion and generation of high-voltage electrical fields which could cause explosions and therefore be a major hazard. The electrostatic charging mechanism and distribution of charges in gas-solid fluidized beds have received minimal attention over the years relative to other aspects of fluidization. The main goal of this thesis is to gain a better understanding of electrostatic phenomena in gas-solid fluidized beds.

1.1. Electrostatic Phenomena

As early as the 1940s, researchers encountered electrostatic effects in fluidized beds by observing the adhesion of particles to vessel walls and its influence on fluidization conditions (Jones, 1997). Problems associated with fluidized bed electrification include particle-wall adhesion, inter-particle cohesion and electrostatic discharges. Particle-wall adhesion is a major problem because the charged particles can coat vessel walls, requiring frequent cleaning. They can also interfere with sensors and with bed internals. Electrostatic cohesion can cause the formation of undesired particle agglomerates that affect the fluidization conditions and reduce the overall production rate. Electrostatic discharges can result in serious problems such as electrical interference, adversely

affecting process instrumentation, physical shocks to operating personal and, most significantly, fires and explosions.

1.2. Charge Generation Mechanisms

The generation of static electricity in gas-solid fluidization has been known for a long time. However, the charge generation mechanism is not well understood due to its complexity. In a gas-solid fluidized bed, particles can be charged due to surface contact during collisions (triboelectrification), frictional charging and thermionic emission in high-temperature processes.

1.2.1. Triboelectrification

When two solid bodies (including particles) come into contact with each other, charges move from one to the other based on the energy of the electrons and ions at the surfaces of the two materials until charge equilibrium occurs (Fan and Zhu, 1998). Upon separation, particles that have lost electrons become positively charged, whereas those that have gained electrons acquire negative charges (Figure 1.1).

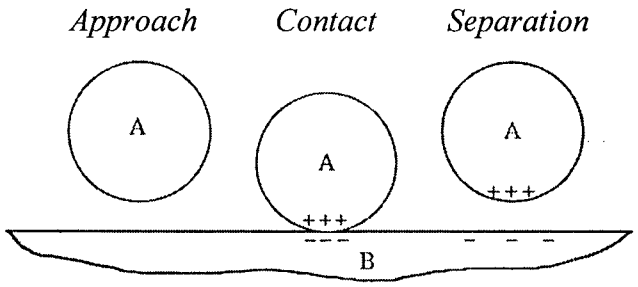

Figure 1.1. Triboelectrification charging mechanism. (Adapted from Jones, 1997)

In other words, triboelectrification, also known as contact electrification, occurs due to the difference in the initial Fermi energy levels of the materials at the contact surface until the energy levels are equalized. The Fermi energy level is the highest occupied energy level at absolute zero temperature (Cross, 1987). The energy required to move an electron from the top of the energy distribution, out of the metal to infinity, is called the

work function, which for the majority of metals is approximately 4 eV and depends on surface impurity (Cross, 1987). In metal-insulator contact, it has been determined that the amount of charge transferred to an insulator by a metal is proportional to the metal work function. Therefore, insulators such as polymers can be arranged in a work function series. A comparison of the results of two researchers is presented in Table 1.1.

Table 1.1. Polymer work function series of two studies provided by Cross (1987).

		Work Function (eV)	
	Material	***Davies (1969)***	***Strella (1970)***
-	PVC	4.85 ± 0.2	5.13
	Polyimide	4.36 ± 0.06	
	Polycarbonate	4.26 ± 0.13	4.80
	PTFE	4.26 ± 0.05	5.75
	PET	4.25 ± 0.10	
	Polystyrene	4.22 ± 0.07	
+	Nylon 66	4.08 ± 0.06	4.30-4.54
-	Teflon (PTFE)		5.75
	Polychlorotrifluoethylene		5.30
	Polychlorinated propylene		5.14
	PVC		5.13
	Polychlorinated ether		5.11
	Poly-4-chlorostyrene		5.11
	Poly-4-chloro-4-methoxy-styrene		5.02
	Polysulphone		4.95
	Polyepichlorohydrin		4.95
	Polystyrene		4.90
	Polyethylene		4.90
	Polycarbonate		4.80
	Polyethylene-vinyl acetate		4.79
	Polymethylmethacrylate		4.68
	Polyvinylacetate		4.38
	Polyvinylbutyral		4.30
	Poly-2-vinylpyrindine-styrene		4.27
	Nylon 66		4.30-4.54
+	Polyethylene oxide		3.95-4.50

Work function series values represent the charging polarity of two surfaces due to tribocharging. The higher the work function, the more negative the polarity of the charge. However, it can be seen from Table 1.1 that there are some differences in magnitude of the work function and in the order of materials in the series between the two investigators. According to Cross (1987), electron energies in an insulator are a function of position, surface impurities and local atomic structure, as well as the chemical nature of the material. Therefore, the work function of an insulating material should be determined experimentally. Triboelectrification is very sensitive to the electronic surface states of the materials in contact. Therefore, any surface changes at the time and point of contact may influence both the polarity and the magnitude of tribocharging. Trigwell et al. (2001) investigated the effect of surface contamination and environment (air at 22°C and 40% relative humidity) on the work function of different materials and compared their results with those reported in the literature measured in a vacuum with normally clean materials. They concluded that the actual work functions of material surfaces can differ significantly from their expected values due to the surface composition (contamination) and exposure to the environment. Their results indicated that surface contamination increases the surface work function of metals and polymers.

Charge polarities of different materials have been determined by numerous researchers and have been arranged in triboelectric series. Table 1.2 summarizes a number of triboelectric series (Cross, 1987).

The charge polarity can be influenced by different factors such as surface finish, preconditioning, material purity, particle shape and particle moisture content (Cross, 1987; Jones, 1997). For instance, Figure 1.2 represents an exception to the triboelectric series determined by some researchers by changing the rubbing manner of surfaces (Harper, 1967). As a result, it is impossible to predict with certainty the charge polarity of industrial solids based on published triboelectric and work function series.

Table 1.2. Triboelectric series as presented by Cross (1987).

	Material	Polymer Type	Source
Montgomery (1959)	+ Wool		
	Nylon		
	Viscose	Cellulose	
	Cotton		
	Silk		
	Acetate rayon	Cellulose acetate	
	Lucite or Perspex	PMMA	
	Polyvinyl alcohol		
	Dacron	Copolyester of ethylene glycol and terephthalic acid	
	Orlon	Polyacrylonitrile	
	PVC		
	Dynel	Copolymer acrylonitrile/vinyl chloride	
	Velon	Copolymer vinylidene chloride/vinyl chloride	
	Polyethylene		
	- Teflon	PTFE	
Webers (1963)	+ Polyox	Polyethylene oxide	Union Carbide
	Polyethylene amine		Chemirad
	Gelatin		
	Vinac	Polyninyl acetate	Colton chemicals
	Lucite 44	Polybutyl methacrylate	Du Pont
	Lucite 42	Polymethyl methacrylate	Du Pont
	Acryloid A101	Polymethyl methacrylate	Rohm and Haas
	Zelec DX	Polycation	Du Pont
	Polyacrylamide		Cyanamid
	Cellulose acetate/butyrate		Eastman
	Acysol		Rohm and Haas
	Carbopol	Polyacrylic acid	BF Goodrich
	Polyethylene terephthalate	Polyacid	
	Polyvinyl butyral		Du Pont
	- Polyethyelen		
Williams (1976)	+ Lucite 2041	Methyl methacrylate	Du Pont
	Dapon	Diallyl phthalate	
	Lexan 105	Poly-bishenol-A-carbonate	GE
	Formvar	Polyvinylformal	Monsanto
	Estane	Polyurethane	Goodrich
	Du Pont 49000	Polyester	Du Pont
	Durez	Phenol formaldehyde	Durez
	Ethocel 10	Ethyl cellulose	Hercules
	Polystyrene 8X	Polystyrene	Kopper
	Epolene C	Polyethylene	Eastman
	Polysulphone P-3500	A diphenyl suphone	Uion Carbide
	Hypalon 30	Chlorosulphonated PE	Du Pont
	Cyclolac H-1000	Acrylonitrile-butadiene-styrene terpolymer	Borg Warner
	Uncoated iron		
	Cellulose acetate butyral		
	Epon 828/V125	Epoxy amine curing agent	Shell/General Mills
	Polysuphone P-1700		
	Cellulose nitrate	Polyvinyldene fluoride	Penwalt
	- Kyna		

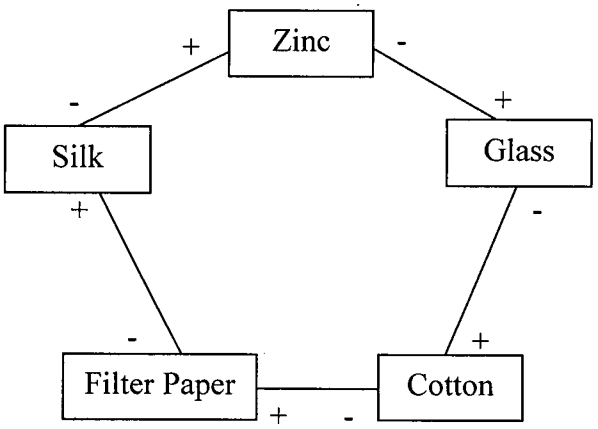

Figure 1.2. Closed triboelectric series. (Copied from Harper, 1967)

1.2.2. Frictional charging

Charging by friction occurs when the surfaces of solid particles rub against each other and/or against the walls of a containing vessel. Therefore, in industrial gas-solid fluidized beds, frictional charging between gas, particles and reactor walls is recognized to be the principal mechanism of charging. In cases where the column is large enough to neglect wall effects, particle-particle frictional charging is likely to be the dominant source of net charges generated inside the reactor.

Frictional charging can occur between similar and dissimilar materials. Cross (1987) reports that the charges generated between two similar materials can be as great as those from dissimilar materials. Frictional charging is known to be most sensitive to such factors as rubbing energy and velocity. Montgomery (1959) concluded that charges increase as the rubbing velocity increases. Zimmer (1970) reported that the charge polarity of polymers rubbed against a metal can change as the rubbing velocity and temperature vary. According to Cross (1987), charge transfer is affected more by the energy of rubbing than by the nature of the material. This clearly indicates that frictional charging is different in nature from triboelectrification. Hence, these two mechanisms should be distinguished in order to better understand the charging mechanisms in

fluidized beds.

1.2.3. Thermionic emission

Thermionic emission or thermal electrification can occur in very high-temperature environments. At T>1,000 K, electrons inside solid particles can gain energy from the high-temperature field to overcome the energy barriers and be freed, therefore becoming thermally electrified (Fan and Zhu, 1998). The charge build-up on the particles occurs due to the tendency of the electrons to escape from the solid particles by thermionic emission and increases as the freed electrons are captured by attracting Coulomb forces (Fan and Zhu, 1998).

1.3. Measurement Techniques

Different experimental techniques have been employed by previous researchers to measure electrostatic charges generated in gas-solid fluidized beds. The two main techniques involve Faraday cups and electrostatic probes. The Faraday cup is used for direct measurement of charge build-up on particles surfaces, whereas electrostatic probes determine the cumulative potential generated inside the bed and on the walls of the column.

1.3.1. Faraday cup

A Faraday cup consists of two concentric vessels of any suitable shape insulated from each other as illustrated schematically in Figure 1.3. The outer cup is grounded and functions as a screen to prevent generation of any induced charges on the inner cup by external sources. The inner or measurement cup (often referred to as a pail) is connected to an electrometer that measures charge by monitoring the voltage produced across a known capacitor. When a charged object enters the inner cup, an equal and opposite charge is induced on the walls of the inner cup. This charge is stored on the capacitor in the electrometer and measured (Cross, 1987).

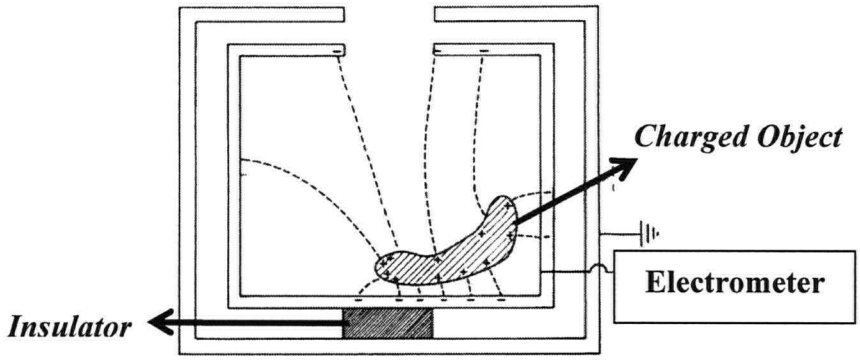

Figure 1.3. A Faraday cup. (Copied from Cross, 1987)

The Faraday cup method has been used by several previous researchers for direct measurement of the net electrostatic charge build-up on particles inside fluidized beds. Ali et al. (1998) used a Faraday pail system that could perform both charge measurement and separation by particle size. As shown in Figure 1.4a, their system consisted of nine Faraday cups, in a cross formation. A scooper, shown in Figure 1.4b, removed particle samples from the fluidized bed. The scooper was positioned a certain height above the Faraday pail system, and the sample was poured over the central pail (Figure 1.4c). Particles spread into the pails as they fell.

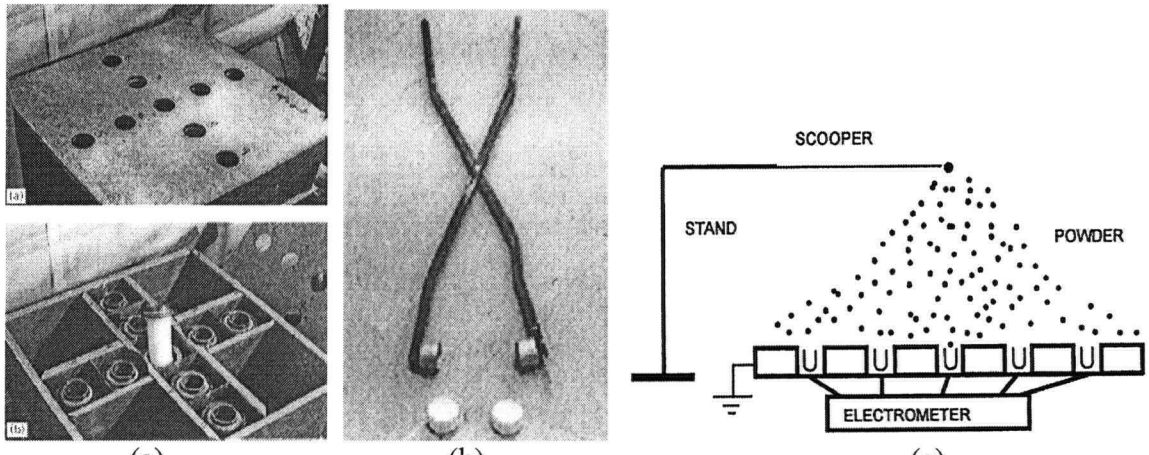

(a) (b) (c)

Figure 1.4. Faraday pail system of Ali et al. (1998): (a) nine-Faraday-pail system, (b) scooper to take samples from the bed, (c) pouring sample over the Faraday cups.

To minimize any additional charging during the handling of particles before entering the Faraday cup, Tardos and Pfeffer (1980) and Zhao et al. (2000) installed vertical grounded metallic tubes in the centre of the bed to sample the particles (Figures 1.5a and 1.5b). Tardos and Pfeffer used a 0.05 m diameter plastic tube as the fluidized bed. Zhao et al. performed their experiments in a grounded steel fluidized bed with a cross-sectional area of 0.025 m x 0.25 m and a height of 0.60 m from the distributor plate. Their tube had a series of holes equipped with a plug that could be opened to initiate sampling and be closed at other times. The tube and plug were coated with particles of the same type as those being sampled to eliminate extra charging. This method of particle sampling has the disadvantage of disturbing the flow and causing charge build-up.

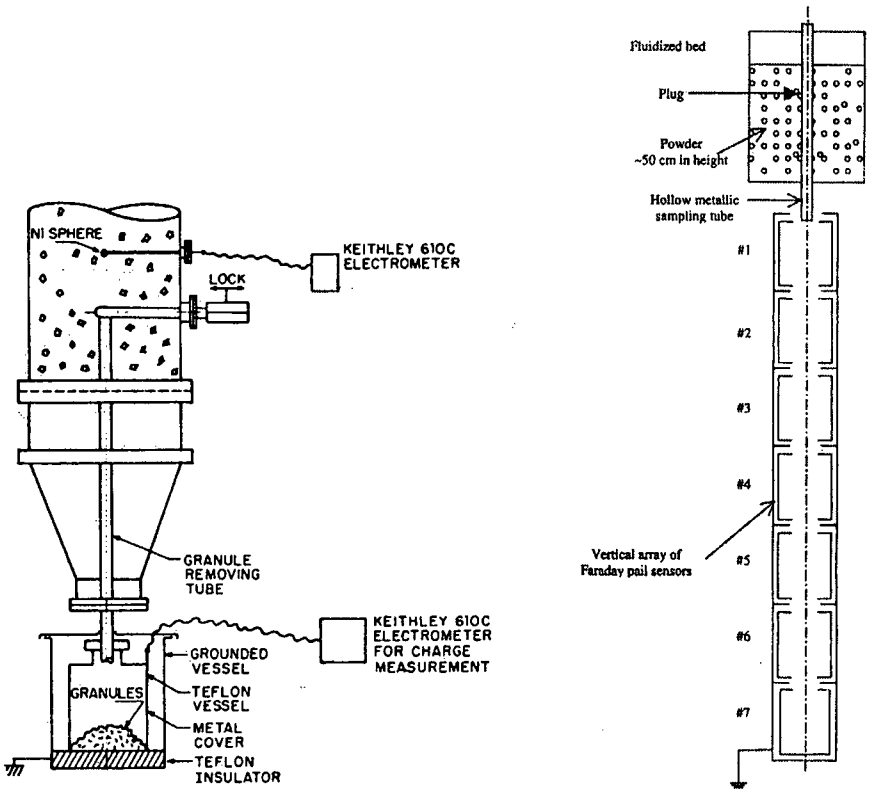

(a) (b)

Figure 1.5. Particle sampling methods in the literature, (a) Copied from Tardos and Pfeffer (1980), (b) Copied from Zhao et al. (2000).

Tardos and Pfeffer (1980) placed the Faraday cup below the fluidized bed in order to collect samples that drop from the tube. The Faraday pail used by Zhao et al. (2000)

consisted of seven Faraday cups mounted vertically as a cascade as shown in Figure 1.5b. An array of pails was used to separate the particles in the vertical and radial directions based on their size and charge. Fasso et al. (1982) placed a Faraday cup beside a fluidized bed (0.0952 m in diameter and 1.25 m tall), close to the flow system (Figure 1.6). The cup was connected to the wall of the column by two concentric thin copper tubes that passed through the wall and ended at the axis of the column. The particles were conveyed into the tubes by a vacuum pump and were collected in the cup. Wolny and Opalinski (1983) employed a similar set-up to determine the charge of single particles removed from a perspex fluidized bed with a square cross-sectional area of 0.04 m x 0.04 m, and 0.250 m tall.

It is apparent that the Faraday cup methods employed by all these researchers have had disadvantages such as additional charging during handling of particles before entering the cup, disturbance of the flow, and the ability to measure only local charges inside the fluidized bed.

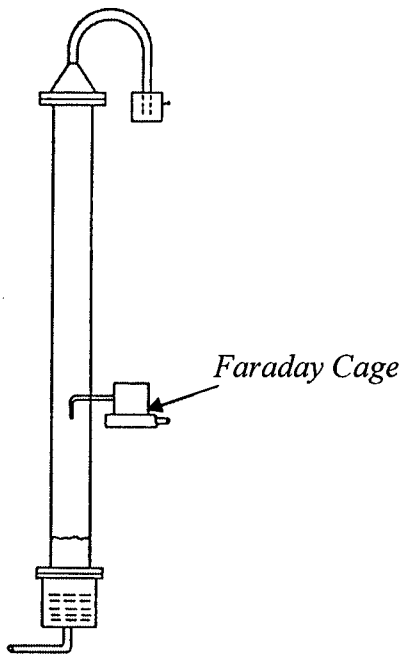

Figure 1.6. Faraday cup mounted on side of bed. (Copied from Fasso et al., 1982)

1.3.2. Electrostatic probes

The overall electrostatic charge build-ups inside a fluidized bed and on its walls have been measured by electrostatic probes by several previous researchers. The fundamental principle behind these measurement techniques is that a real charge induces an image of itself on a conducting surface.

Boland and Geldart (1971/1972) developed a probe based on this principle, as shown in Figure 1.7. This type of probe is generally mounted on the wall of the column with part of the wall between the tip of the probe and the inner surface of the column. They utilized a two-dimensional fluidized bed made of Perspex with cross-sectional dimensions of 0.50 m by 0.013 m. These non-contacting probes have the advantage of not disturbing the flow since they are not directly exposed to the fluidized material. However, the disadvantage is that they mainly measure the charge build-up on the column walls, rather than the charges generated inside the bed.

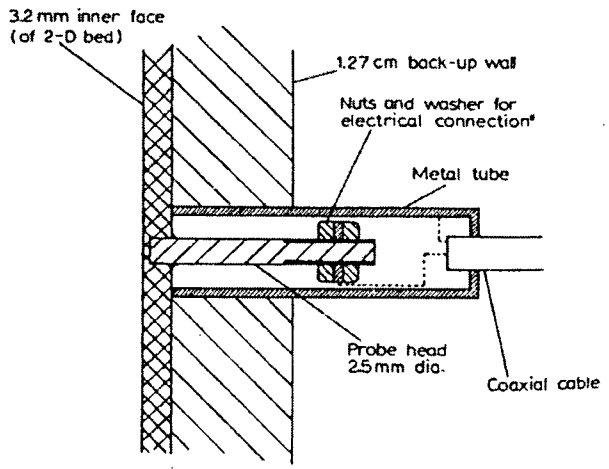

Figure 1.7. Non-contacting electrostatic probe (Copied from Boland and Geldart, 1972)

Other researchers have used the same principle of induction and have developed contacting probes made of highly conductive materials inserted along the central axis of the bed and connected to electrometers to read the current or potential generated inside the fluidized bed. Ciborowski and Wlodarski (1962) developed an electrode (Figure 1.8) made of platinum wire shaped as a ball mounted inside the bed by a silk thread connected

to an electrometer that measured the potential within the bed. The fluidization column was a glass tube, 0.06 m in diameter and 0.555 m tall, with a grounded steel distributor plate. In order to stabilize the electrical measurements, the whole column was surrounded by a grounded metal screen.

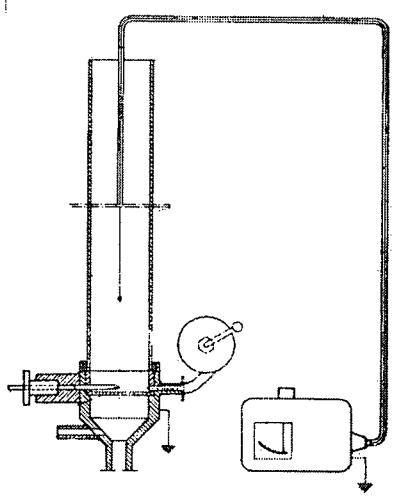

Figure 1.8. Contacting electrostatic probe. (Copied from Ciborowski and Wlodarski, 1962).

Fujino et al. (1985) adopted a similar approach by inserting a spherical brass terminal of 6 mm diameter into the fluidized bed (similar to that employed by Ciborowski and Wlodarski, 1962) supported by a nylon thread and connected to an electrometer (Figure 1.9a). A grounded brass perforated distributor was used to eliminate external induced charges. Guardiola et al. (1992) measured the degree of electrification by determining the potential difference between a metallic probe in contact with the bed and a metallic distributor. Shown schematically in Figure 1.9b, the fluidization column was made of Perspex tube 0.052 m in diameter, whereas the probe was made from a copper bar 5 mm in diameter, except at the tip covered by a silicone rubber coating. The distributor was a grounded stainless steel screen.

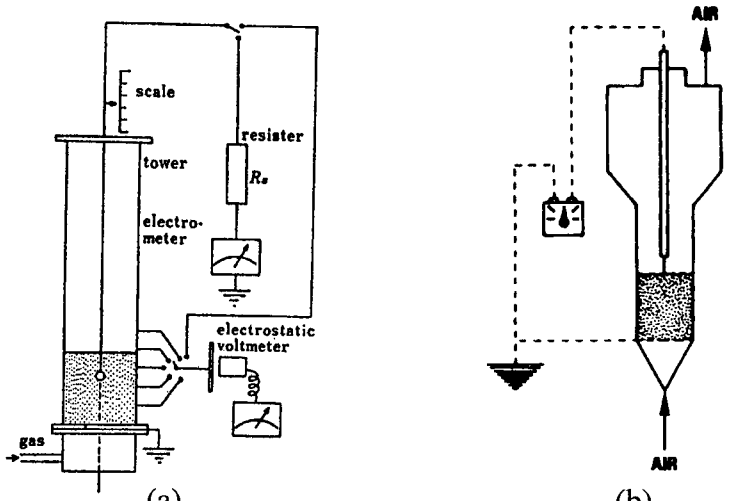

(a) (b)

Figure 1.9. Contacting electrostatic probes: (a) Copied from Fujino et al. (1985), (b) Copied from Guardiola et al. (1992).

Wolny and Kazmierczak (1989) used a different approach. They developed a capacitance probe consisting of an air-plate capacitor that could measure the electric field generated inside the fluidized bed (Figure 1.10). The fluidization apparatus was a 2-D column with a cross-section of 0.200 m x 0.200 m. The capacitor consisted of two brass plates of 0.060 m x 0.108 m cross-section, 0.07 m apart.

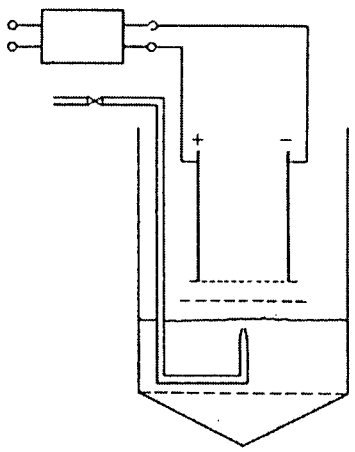

Figure 1.10. Capacitance probe. (Copied from Wolny and Kazmierczak, 1989)

A major disadvantage of contacting induction probes is their low accuracy. Due to the electrostatic charges generated inside the bed, particles can adhere to the tip of the probe, resulting in potentials lower than the true potential (Fujino et al., 1985). The dependence

of the measured potential on the adhesion of particles to the probe in one study is shown in Figure 1.11.

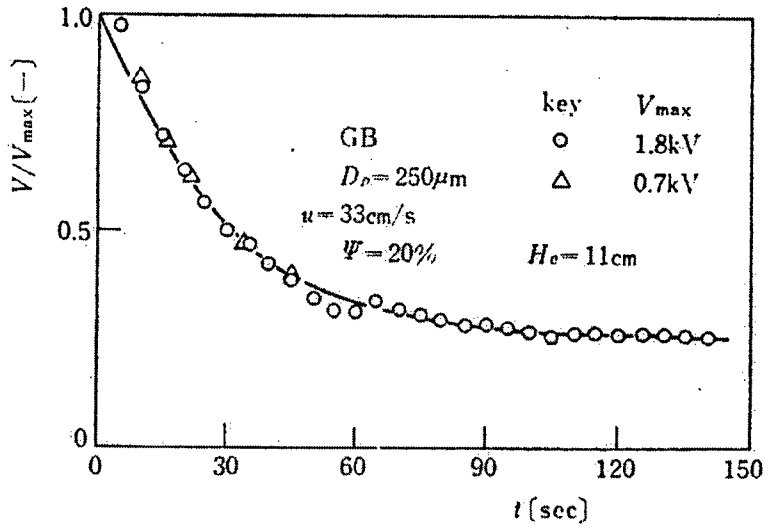

Figure 1.11. Decrease in measured potential due to adhesion of charged particles on spherical probe tip. (Copied from Fujino et al., 1985)

Other disadvantages include disturbing the flow, since the probes are suspended inside the bed, and introducing extra charging due to particle collisions with the probe. Some investigators, e.g. Park et al. (2002) and Tardos and Pfeffer (1980), used wall-mounted probes instead of suspended probes (Figure 4(a)). Park et al. performed their experiments in a two-dimensional Plexiglas fluidization column, 0.307 m x 0.022 m in cross-section and 1.24 m high, and in a three-dimensional Plexiglas column of diameter 0.0889 m and height 1.21 m. The wall-mounted probes measure the field rather than electrostatic potential and may be better than suspended probes which disturb the flow. However, they again cause particles to adhere to the probes, thereby affecting the accuracy of the measurements.

1.4. Methods of Charge Reduction

Some previous research has been performed to investigate ways to prevent or reduce electrostatic charges in gas-solid fluidized beds. Methods investigated include gas humidification, addition of antistatic agents, usage of more conductive particles, ionization of the gas and grounding the column.

1.4.1. Gas humidification

The influence of the relative humidity of the fluidizing gas on bed electrification has been investigated for many years. The research goes back as far as the 1960s when Ciborowski and Wlodarski (1962) concluded that decreasing the fluidizing gas humidity results in a rapid increase in bed potential. Over the years a number of researchers (Katz and Sears, 1969; Boland and Geldart, 1972; Tardos and Pfeffer, 1980; Smeltzer et al., 1982; Wolny et al., 1989; Ham et al. 1992; Guardiola et al., 1996; Hori, 2000; Revel et al., 2002; Park et al., 2002) have concluded that increasing the gas humidity to 60% or higher increases the surface conductivity of solids resulting in greater charge dissipation. Katz and Sears (1969) found that the surface conductivity of particles can be increased by a factor of 10^6 by adding moisture to the gas. It is important to note that increasing the gas humidity mostly affects charge dissipation, not charge generation.

One of the problems of this method is that at very high gas humidity, fluidization of hydrophilic particles such as glass beads may become impossible due to formation of a thin liquid layer around the particles that strengthens mutual cohesion (Guardiola et al. 1996). Also this technique is unlikely to be applicable to gas-solid catalytic industrial fluidized reactors since humidity often poisons catalysts. Furthermore, increasing the relative humidity is not effective in high-temperature processes.

1.4.2. Addition of antistatic agents

Another common method of reducing electrostatic charge is to add fine particles to the fluidized bed. According to Wolny and Opalinski (1983), the fines change the contact conditions between particles causing transfer of electrical charges among particles. The added fines surround the bed particles, thereby decreasing the number of contacts between bed particles, and between the column wall and the bed particles. Wolny and Opalinski (1983) also performed experiments by adding conductive, semi-conductive and dielectric fine materials to the bed and concluded that the electrical nature of the fines has negligible influence on the charge of the bed. The effect of the commonly-employed antistatic agent, Larostat 519, on the electrostatic charges in freely bubbling fluidized

beds of polyethylene particles was investigated by Park et al. (2002). They reported that the addition of the antistatic fines reduces the electrostatic charge build-up in the bed, causing particle accumulation on the column walls to disappear within one minute after adding the antistatic powder. For cases where the fluidized particles need to remain pure or mono-dispersed, addition of fines to the fluidized bed is inappropriate.

Goode et al. (1989) and Song et al. (1995) found a group of chemical additives that can be added to gas-phase polymerization reactors to reduce or prevent "sheeting", a problem commonly blamed on electrostatic charging. The authors claim that these additives generate either positive or negative charges in the reactor and therefore, depending on the initial charges in the reactor, they can maintain electrostatic charges at neutral levels. However, the exact charging mechanism was not described.

1.4.3. More conductive particles

The effect of binary dielectric/conductor (glass/steel) mixtures of similar size particles on the degree of electrification of a fluidized bed was studied by Guardiola et al. (1992). The addition of conducting materials such as steel was found to reduce the charge build-up in the fluidized bed.

1.4.4. Ionized gas

Some researchers have investigated the effect of injecting ions into the bed to neutralize the static electricity generated on fluidized particles. Revel et al. (2002) studied this technique by injecting ions into a bed of polyethylene particles fluidized by air. The addition of ions to the bed eliminated adherence of particles to the column walls and greatly reduced the generation of charges.

1.4.5. Grounding the column

Grounding the whole fluidization column has also been considered a means of helping to dissipate electrostatic charges. Even in small columns, this method is generally not

regarded as being very helpful (Grace and Baeyens, 1986). Grounding large industrial units or columns made of non-conducting materials (e.g. plastics) is also known to be ineffective.

1.5. Influence of Particle Size (Bi-Polar Charging)

Bi-polar charging has been explained as contact charging between particles of the same material but different sizes in which larger particles gain charge polarity opposite to those of the smaller particles (Ali et al., 1998; Zhao et al., 2000). Ali et al. (1998) found that for one type of particles, the large particles charged positively and the small particles negatively, whereas in other cases the polarity was reversed. Zhao et al. (2000) investigated the relation between particle size and polarities for some polymer particles and concluded that smaller particles charged negatively and larger particles positively, so that both positively and negatively charged particles existed within the fluidized bed.

1.6. Thesis Objectives

The occurrence of electrostatic charges is almost unavoidable in gas-solid fluidization. Industries involving gas-solid fluidized beds have suffered from this phenomenon for decades. The ultimate goal of our research is to determine ways to prevent or eliminate generation of electrostatic charges. In order to find methods of charge reduction or prevention, the relevant phenomena and mechanism need to be thoroughly understood. Therefore, the first step is to gain a better understanding of how the charges are generated, i.e. the charge generation mechanisms. Although the generation of static electricity in gas-solid fluidization has been reported for many years, the mechanism of charge generation is still not well understood.

The first step in investigating and understanding the charge generation mechanisms is to establish an adequate measurement technique. As explained above, there are significant deficiencies in the measurement techniques employed in previous work, mainly involving Faraday cups and electrostatic probes.

The goal of this thesis is to gain a better understanding of the mechanism of charge generation inside gas-solid fluidized beds by employing an on-line measurement technique. Rather than having a separate external Faraday cup as in previous work, a novel on-line Faraday cup measurement technique was developed in the present study. The specific objectives were:

- To develop and examine a new on-line measurement technique.
- To investigate the net charges generated inside a fluidized bed due to particle-gas contacting and gas ionization.
- To determine the effect of entrained fines leaving the top of the fluidization column on the build-up of net charges inside the bed.
- To establish the effect of addition of fine particles on electrostatic charge generation/dissipation inside the bed and the relevant mechanisms.
- To find the influence of operating conditions such as particle type, size and fluidizing gas relative humidity.

1.7. Thesis Outline

The first section of Chapter 2 focuses on the heart of the project, the development of a new on-line Faraday cup measurement technique to measure electrostatic charge generation in gas-solid fluidized beds. It describes the principles behind the method, the structural details of the unit, the types of measurements that can be performed by the unit, its abilities and limitations. The second section describes in detail the fluidization apparatus which includes the Faraday cup fluidized bed, digital electrometer, gas humidification system and data logging system. The third section provides details of the gas and solid phases used in the experiments. Further, it describes the experimental procedure. This chapter mainly focuses on the experimental equipment and methodology for the measurement of charges carried by different fines out of the fluidization column.

Chapter 3 presents and analyses the experimental results. Results show the charges carried out of the fluidized bed by different fines and thereby their effects on the electrostatic charge generation/dissipation inside gas-solid fluidized beds.

Chapter 4 focuses on additional laboratory experiments undertaken in an effort to achieve an understanding of the charging mechanisms and to explain some of the findings of the experiments in the Faraday cup fluidization column. This chapter includes bench-scale shaking experiments and particle-copper plate contacting experiments. In both cases, the chapter covers the experimental apparatus, procedure, results obtained and an interpretation of the results.

Chapter 5 summarizes and discusses the possible charging mechanisms involved in the Faraday cup fluidization column in the present work and thereby in gas-solid fluidized beds in general. The final chapter, Chapter 6, presents overall conclusions and recommendations for future research. Additional experimental results and photographs of the equipment appear in the appendices.

Chapter 2. Experimental Equipment and Method

This chapter describes the Faraday cup fluidization column employed to achieve the objectives of this research and the experimental procedures followed.

2.1. On-line Faraday Cup Fluidization Column

A novel on-line measurement technique was developed in the present work. The Faraday cup method was applied by considering the fluidization column as the inner cup and mounting a second column outside the fluidization column as the outer cup, as illustrated in Figure 2.1.

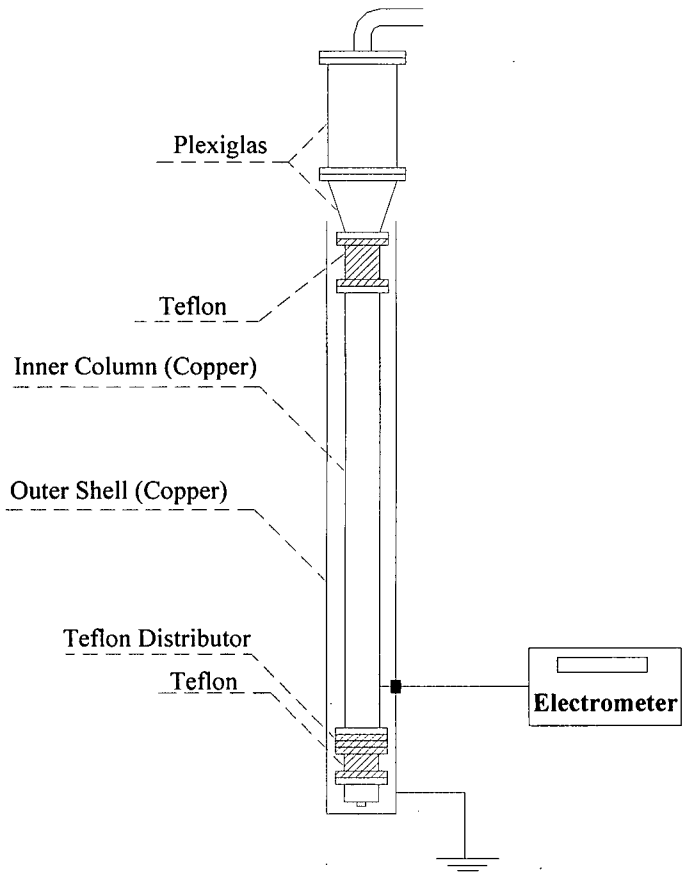

Figure 2.1. Schematic diagram of Faraday cup fluidization column.

Both the fluidization and the outer column are made of copper, which is electrically highly conductive. The outer column is grounded to eliminate external electrical interference. The fluidization column is insulated from other parts of the inner column and the outer column by Teflon cylinders and Teflon distributor plates. The fluidization column is directly connected to an electrometer to measure the charges induced on the column wall.

Negative and positive charges are generated inside a fluidized bed due to particle-particle and particle-wall interactions. However, unless charges are removed from the wall or carried out of the column, the net charge of the bed remains zero. Therefore in order to measure a net charge inside the fluidized bed by means of the proposed Faraday cup method, there must be a way for charges to either leave the system or be neutralized, thereby resulting in a net charge. Possibilities include charges leaving the system with entrained fines or being carried by the gas leaving the top of the column.

2.2. Faraday Cup Fluidized Bed System

The experiments were performed in a fully three-dimensional gas-solid fluidization column. The experimental set-up is shown schematically in Figure 2.2.

The main unit is a fluidization column consisting of two concentric vessels as illustrated in Figure 2.1. The outer copper shell is 0.2 m in diameter, 1.7 m high and 0.0016 m thick. The inner column, 0.1 m in diameter, 2.1 m high and 0.01 m thick, consists of three sections made of different materials. As shown in Figure 2.1, the middle part is made of copper, insulated at both ends with Teflon sections, and the top expanded section is made of Plexiglas. The distributor consists of two Teflon perforated plates, each containing 44 holes of 2 mm diameter on the top plate aligned with an equal number of 4 mm diameter holes on the bottom plate. A nylon screen with 38 μm openings is sandwiched between the two Teflon perforated plates to prevent particles from dropping into the windbox. Nine pressure taps (made of copper) are located at various heights in the column where three of them connected to three differential pressure transducers in order to measure

pressure gradients and overall pressure drops. Photographs of the experimental set-up are presented in Appendix A (Figures A.1-A.6).

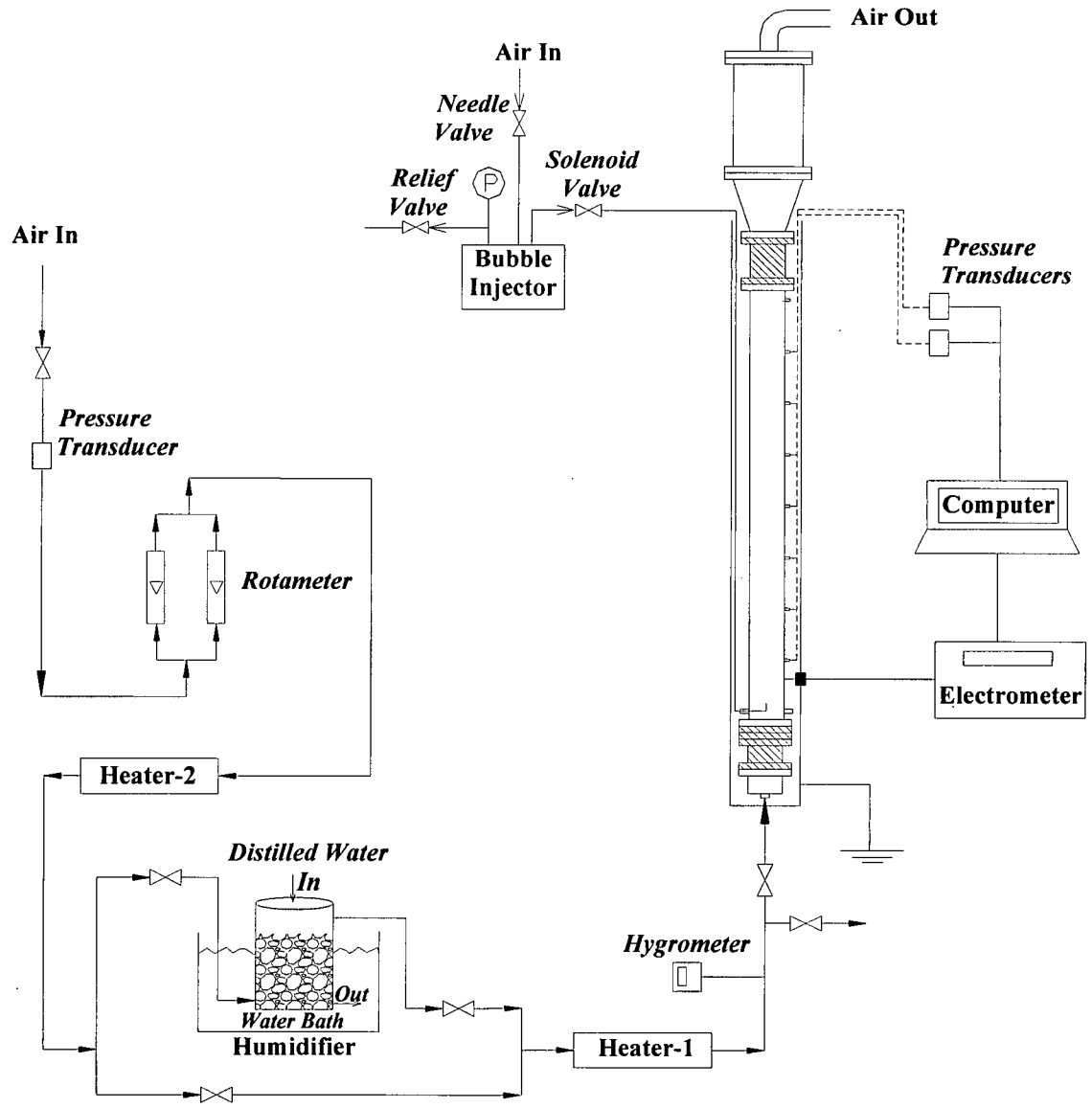

Figure 2.2. Schematic diagram of the experimental apparatus.

Two rotameters were employed to determine the fluidizing gas flow rate, with valves used to adjust to the desired value. A packed water column (humidifier) humidified the gas to the desired relative humidity. The humidifier was charged with distilled water to eliminate contamination of the gas passing through this unit. The humidifier was placed in a water bath at 25°C to keep the relative humidity of the gas constant. The relative humidity of the gas was varied by changing the gas temperature by means of Heater-2 (see Figure 2.2) and the gas flow rate by adjusting the valve prior to the humidifier. The gas leaving this unit was then reheated by Heater-1 to maintain the temperature in the fluidized bed at a pre-set value. The relative humidity and the temperature of the gas were monitored by a Vaisala Model HMP238 Humidity Transmitter (hygrometer) before the gas entered the fluidization column. This instrument is able to measure relative humidity from 0% to 100%, and temperature from -40°C to +180°C, with accuracies of ±1% and ±0.2°C, respectively. This unit was calibrated by the supplier.

A closed vessel of volume 1.01×10^5 mm^3 was provided to inject single and multiple gas bubbles through an orifice of diameter 0.0064 m located on the axis of the fluidization column, 0.025 m above the distributor and pointing upwards (see Figure 2.2). Nylon tubing of diameter 0.0064 m connected the vessel to the orifice. Nylon, which is non-conductive, was used to prevent charge leakage from the inner copper column.

The middle copper section of the fluidization column is connected directly to a Keithley Model 6514 Digital Electrometer to measure the charges induced on the inner copper column with the electrometer set to the Coulomb mode. This instrument is able to measure charges ranging from 1×10^{-13} to 20×10^{-6} C, current from 1×10^{-16} to 20×10^{-3} A and voltage from 1 to 20 μV. This unit was sent back to the manufacturer for calibration every year. The electrometer was connected to a computer through a USB port to record the measured signals. The signals were measured by the electrometer at a sampling rate of 2 Hz. The background noise of the electrometer was determined experimentally to be $\pm 10^{-11}$ C. It was confirmed that the fluidization column was functioning properly as a Faraday cup by showing that it gave the same response to immersion of a small charged sphere as did a small Faraday cup. The small Faraday cup consisted of two concentric

cups made of copper, insulated from each other by a Teflon piece as shown in Figure 2.3. The inner cup was 0.127 m tall and 0.152 m in diameter, whereas the outer cup was 0.152 m tall and 0.203 in diameter. The Faraday cup was connected to a Keithley Model 6514 digital electrometer. The results of the charges measured in both the fluidization column and the small Faraday cup are shown in Figure 2.4.

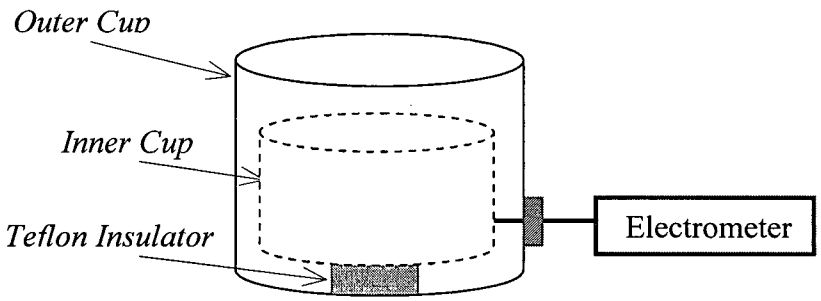

Figure 2.3. Schematic diagram of small Faraday cup.

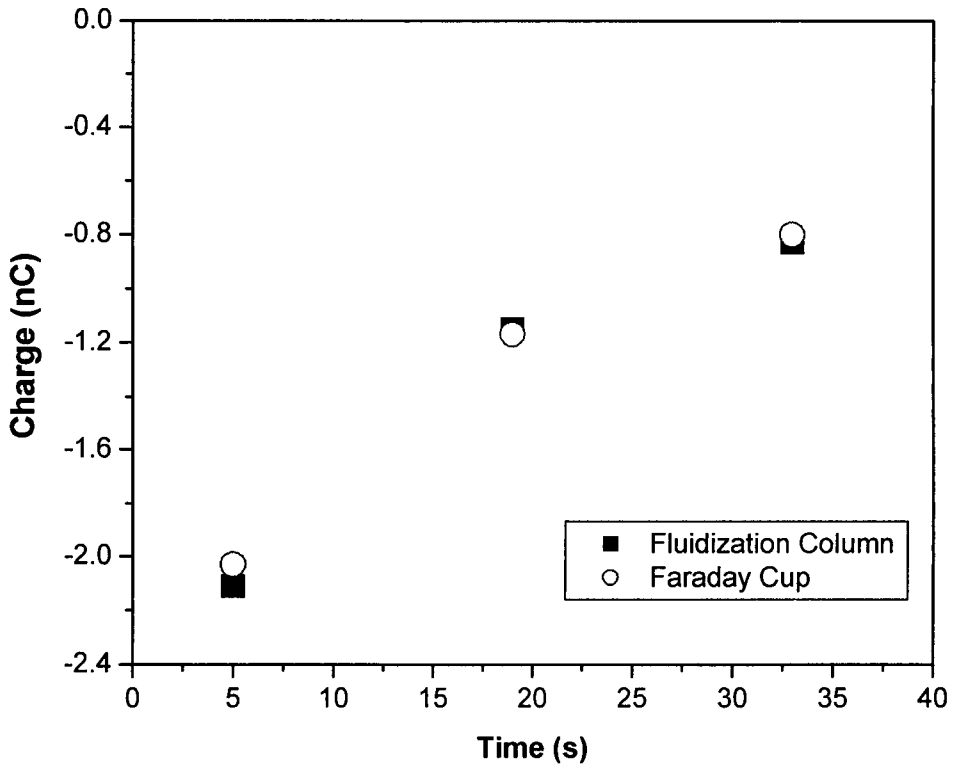

Figure 2.4. Charge responses of Faraday cup and fluidization column to a charged ball.

2.3. Gas and Particulates

2.3.1. Gas

The experiments employed extra dry air from gas cylinders to ensure the purity of the gas from any contamination that might affect the generation of charges inside the fluidized bed. Air was supplied in compressed gas cylinders by Praxair with the composition provided by the supplier shown in Table 2.1.

Table 2.1. Fluidizing gas properties.

Product Grade	**O_2**	**H_2O**
Extra Dry Air	19.5%-23.5%	<10 ppm

*The compositions of other elements are not provided by supplier.

2.3.2. Bed material

Solid particles used in the experiments included relatively large glass beads (soda lime glass) and polyethylene, with properties shown in Table 2.2.

Table 2.2. Relevant properties of the large particles.

Particles	**Glass beads**	**Original Polyethylene**	**Sieved Polyethylene**
Particle density (kg/m^3)	2500	797	797
Size range (μm)	420-752	38-876	500-600
Vol. weighted mean diameter (μm)	566	575	558
Loose packed bed voidage (-)	0.392	0.458	0.458
Sphericity (-)	~1	~0.77	~0.77
Minimum fluidization velocity (m/s)	0.209	0.096	0.096

The glass beads, which are smooth and very nearly spherical, represent ideal particles, whereas the polyethylene particles are non-spherical and porous with non-smooth surfaces, more typical of industrial particulates. The glass beads were supplied by Potter

Industries Inc., Vally Forge, PA, USA. The polyethylene particles were provided by NOVA Chemicals of Calgary in their original resin form directly from their fluidized bed reactors. The polyethylene particles were sieved to separate the preferred size range.

The particle densities were provided by the suppliers. The size distributions and the volume weighted mean diameter of particles were obtained using a Malvern Mastersizer 2000 equipped with a wet cell (see Appendix B for size distribution graphs). This instrument uses laser diffraction to measure particle size distributions from 0.02 to 2000 μm. Glass bead samples were suspended in distilled water and polyethylene particles in ethanol for the measurements. Loose packed bed voidages were determined by pouring known weights of the bulk materials into a 25 ml pycnometer. Water (ethanol was utilized for polyethylene particles) was then added to the pycnometer to make up the total volume to 25 ml. The total mass of the pycnometer after adding the particles and water was measured, and knowing the density of water (or ethanol), the volume of the added water/ethanol, and thus the loose packed bed voidage was then calculated. The minimum fluidization velocities were measured from pressure drop versus superficial gas velocity curves at the intersection of two straight-line portions, as recommended by Kunii and Levenspiel (1991). The physical surface structure such as roughness and sphericity of all particles were analyzed by Scanning Electron Microscopy (SEM). Typical images are shown in Figure 2.5. It is clearly evident from the images that glass beads are spherical and have smooth surfaces, whereas the polyethylene particles are non-spherical and have rough surfaces. The sphericity of the particles was approximated by the Riley sphericity (Riley, 1941):

$$\varphi = \sqrt{(D_s/D_L)} \tag{1}$$

where D_L is the diameter of the smallest circumscribing circle and D_s is the diameter of the largest inscribed circle of particles. D_s and D_L values were determined from the SEM images of the particles (Figure 2.5).

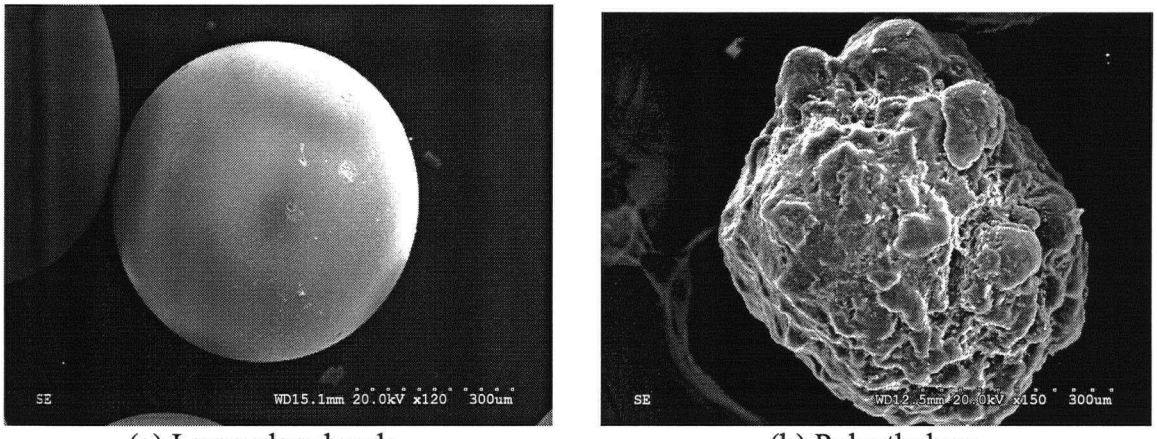

(a) Large glass beads (b) Polyethylene

Figure 2.5. SEM images of relatively large particles used in this study.

2.3.3. Added fines

The added fine particles employed in this study were Larostat 519, glass beads (GB), silver-coated glass beads (S-GB), silica and catalyst (with the same silica base). Key properties are provided in Table 2.3.

Table 2.3. Added fines used in the experiments and their properties.

Particles	**GB I**	**S-GB I**	**Larostat 519**	**GB II**	**S-GB II**	**Silica**	**Catalyst**
Particle density (kg/m^3)	2500	2700	520	1100*	1700*	NA**	NA**
Size range (μm)	10-80	18-49	6-20	8-25	8-20	12-85	10-77
Vol. weighted mean (μm)	30	32	13	11	14	44	40
Sphericity (-)	~1	~0.92	~0.70-0.90	~1	~0.92	NA**	NA**
Terminal velocity (m/s)	0.065	0.078	0.003	0.004	0.01	NA**	NA**

* Hollow glass; **NA = Not Available

Densities were provided by the suppliers, whereas the size ranges and the volume weighted means were again measured by using the Malvern Mastersizer 2000, as described in previous section (see Appendix B for size distribution graphs). All samples were suspended in distilled water for the measurements. The terminal velocities were

determined based on the dimensionless particles size and gas velocity method, as recommended by Kunii and Levenspiel (1991).

Larostat 519 is an antistatic agent commonly used in fluidization research and practice. It is a quaternary ammonium compound in white powder form. Its typical applications include the reduction of static explosion hazards in air-conveyed dust handling systems or in spray-on coatings to achieve uniform coverage,. This powder was provided by Chemcentral Corp., of New Berlin, WI, USA.

.

In order to study the charging between particles of the same material but different sizes, GB type I particles, made of soda lime, i.e. of similar composition to the large glass beads, were employed. It would have been preferable to have kept the surface area per unit mass of the different added fines alike to facilitate comparison of charges carried for different operating conditions. However, it was not possible to obtain GB I particles in the same size range as the Larostat 519. Therefore, GB type II particles were also employed. These are hollow glass (low density) spheres made of borosilicate. All fine glass beads were provided by Potter Industries Inc. in the desired size ranges.

In order to study the effect of conductance of the materials added to the fluidized bed on the charge generation inside the bed, both conductive and non-conductive fines were considered. Since glass bead particles are relatively non-conductive, silver-coated glass beads (S-GB I & II) were also utilized. S-GB I & II particles are silver coated GB I & II particles, again provided by Potter Industries Inc. They have powder resistivities of $1.6x10^{-3}$ and $2.0x10^{-3}$ ohm-cm, and silver metal proportions by mass of 13.4 and 31.8%, respectively.

In the polymer industry, one method of producing polyethylene (high and linear low-density) involves injecting very fine catalyst particles into fluidized bed reactors, with the polymer then growing around the catalyst kernels (Burdett et al., 2001). Therefore, it was considered appropriate here to employ deactivated catalyst particles and silica, which is the catalyst base, as additional fines. The catalyst is an industrial catalyst used in the

manufacturing of polyethylene and provided by a company. They have required that the properties of the catalyst not be divulged.

The physical surface structure, such as roughness and sphericity of all particles, were analyzed by Scanning Electron Microscopy (SEM). Typical images appear in Figure 2.6. These images show that the fine glass beads and silver-coated glass beads are closely spherical. However, the silver-coated glass beads have moderately rough surfaces compared to the uncoated and smooth regular pure glass beads. The silica and catalyst particles appear to be quite different by being non-spherical and having uneven surfaces with peaks and valleys. The Larostat 519 particles, on the other hand, look like clusters of smaller granules. The Larostat 519 particles are the most non-spherical and have the most uneven surfaces, followed by the silica and catalyst particles, and then the silver-coated glass beads.

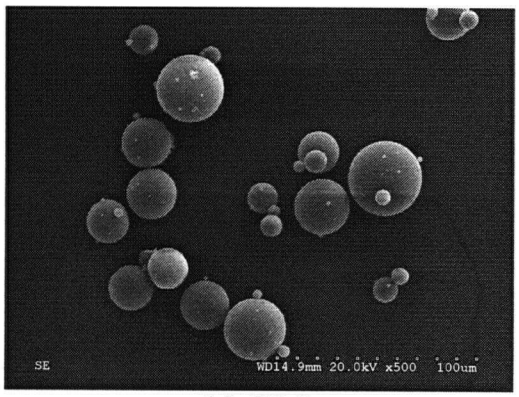

(a) GB I

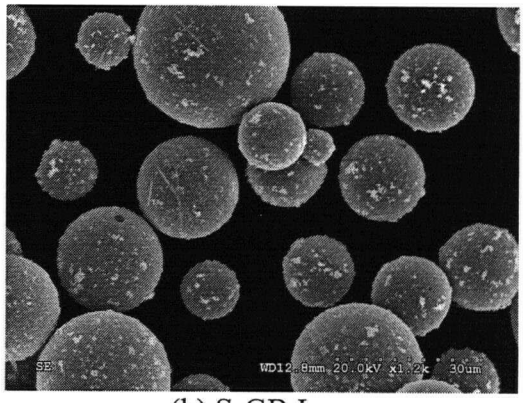

(b) S-GB I

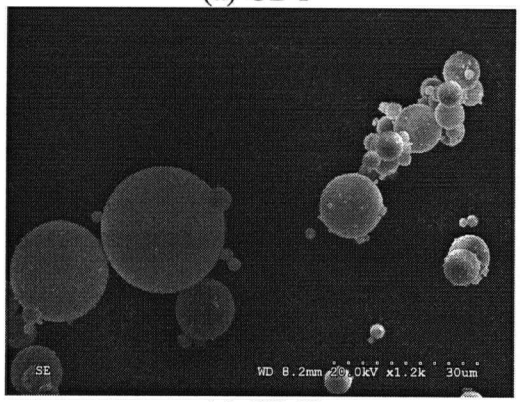

(c) GB II

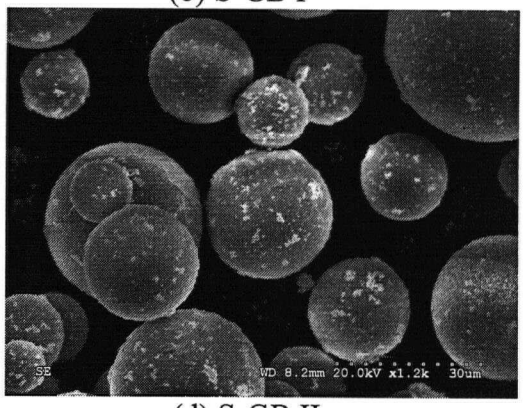

(d) S-GB II

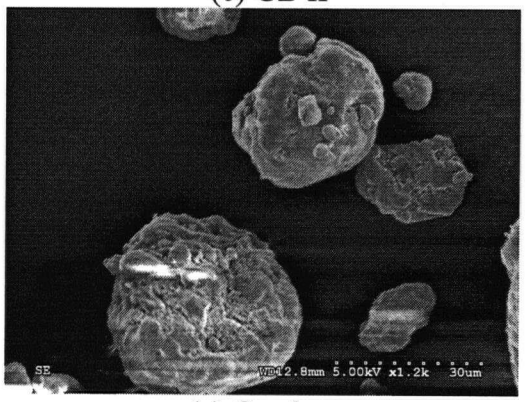

(e) Catalyst

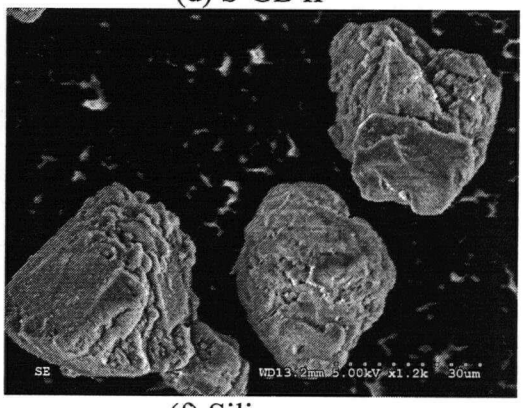

(f) Silica

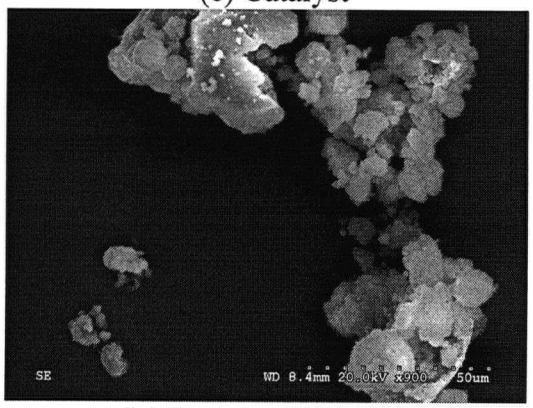

(g) Larostat 519

Figure 2.6. SEM images of added fine particles in this study.

2.4. Experimental Method

Experimental procedures include single and multiple bubble injection and free bubbling experiments. Free bubbling experiments include preliminary tests where triboelectrification due to particle-gas contacting was studied, and tests conducted with different fines added to the fluidized bed.

2.4.1. Bubble injection

In order to investigate the effect of particle-gas contacting on the net charge generation inside the fluidized bed Faraday cup system, bubble injection experiments were conducted with mono-sized relatively large glass beads. Prior to each run, glass beads were washed with ethanol (95%) and distilled water to clean any dirt from their surfaces, and then dried in an oven. The electrometer was connected to the column and set to the charge (Coulomb) mode, after which charge measurement was started. After 60 s, the glass beads were poured into the column. As they entered the column, their initial charges were measured by the electrometer. On average, it took 30 s to pour the particles into the column. The charge measurement continued for 5 minutes.

The static bed height was maintained at 0.2 m for all experiments. The background superficial velocity of dry air through the Teflon distributor was maintained at 0.19 m/s for the bubble injection experiments to facilitate stable bubbles.

The bubble injection vessel was filled with air through a needle valve. A relief valve was used to bleed air to adjust the excess gas pressure in the injector. A computer-controlled solenoid valve controlled the bubble injection. The volume of injected air was controlled by adjusting the duration of the voltage pulse and the pressure in the vessel prior to opening the solenoid valve. A pressure gauge measured the pressures in the vessel before and after bubble injection, permitting the volume of the injected air to be calculated. Single and multiple gas bubbles of volume 1.2×10^5 mm^3 were injected into the bed of large glass beads, while the charges induced on the inner column were measured by the

electrometer. For multiple bubble experiments, the injection frequency was 0.33 s^{-1}. All experiments were performed at room temperature.

2.4.2. Free bubbling

In order to determine the effect of fines entrained from the fluidization column on the net charge generated inside the fluidized bed Faraday cup system, preliminary free bubbling experiments were performed with mono-sized and binary mixtures of particles. The static bed height was maintained at 0.2 m for all experiments. The large glass beads were used as the mono-sized particles. These particles were again first washed with ethanol and distilled water and then dried in an oven to remove dirt from their surfaces and to eliminate as many of the fines as possible. The electrometer was connected to the column and was set to the charge (Coulomb) mode, and charge measurement then began. After 60 s, the glass beads were poured into the column (pouring taking ~ 30 s). As they entered the column, their initial charges were determined by the electrometer, with the measurement continuing for 5 minutes.

For free bubbling tests, the charge measurement was first started with no air flow. After 30 s, the particles were fluidized with extra dry air from a cylinder at a superficial gas velocity of 0.22 m/s while electrical charges were measured on the inner column. The bed was operated at this velocity to ensure that it was operating in the bubbling regime (above minimum fluidization velocity) with vigorous bubbling, which results in good interaction between the particles and the particles and the column wall. The charge measurement stopped when the charges reached a steady state value so that there were no more fines or dust left in the system that might affect the charge measurement when fines were added. The particles were next emptied from the column and mixed with 0.5 vol.% of GB I particles. The binary mixture of particles was then poured back into the column, and the experiment was repeated.

In order to determine the effect of the addition of fine glass beads on the charge measurements, the mono-disperse and binary experiments were repeated, except that a

dust lock filter (provided by BC Air Filter with 26-30% dust capture efficiency of 1 μm particulates) was placed inside the inner column, about 0.02 m below the top of the copper section before fluidizing the binary mixture. The filter was added to keep the fine particles within the inner Faraday cup. All experiments were performed at room temperature.

2.4.3. Free bubbling with added fines

To investigate the changes in the electrostatic charges of various fine particles after their addition to gas-solid fluidized beds, free bubbling experiments were conducted with different fines. The free bubbling experiments, similar to those in section 2.4.2, involved mono-sized and binary mixtures of particles. The large glass beads and polyethylene particles were used as the mono-sized particles, with different particulate fines, as presented in Table 2.3, added to provide binary mixtures. The static bed height was maintained at 0.2 m. Extra dry air from a cylinder was the fluidizing gas for all experiments. All experiments were again performed at room temperature.

The procedure was similar to that described above. When large glass beads were the mono-sized particles, the particles were first washed with distilled water and ethanol (95%) and then dried in an oven to clean any dirt from the surfaces and eliminate fines. The electrometer was connected to the column and set to charge (Coulomb) mode. Charge measurement was then initiated. After 60 s, the glass beads were poured into the column over a period of ~ 30 s, and as they entered the column, their initial charges were measured by the electrometer for a period of 5 minutes. The charge measurements then started again, and after 30 s, particles were fluidized at a superficial air velocity of 0.22 m/s, while charges were measured on the inner column. The mono-sized particles were fluidized to generate some charges inside the bed before the addition of fines. Even though the large mono-sized glass beads had been washed to eliminate fines, there could still be some residual fines. Therefore, the charges were measured during the fluidization to determine whether any fines remained in the system so that they would not affect the charge measurements when different fines were added to the column. The fluidization

was stopped when the measured charges reached a steady state value. Fine particles (0.2 wt%) were then injected into the fluidization column close to the distributor by the injection unit shown in Figure 2.7 (a).

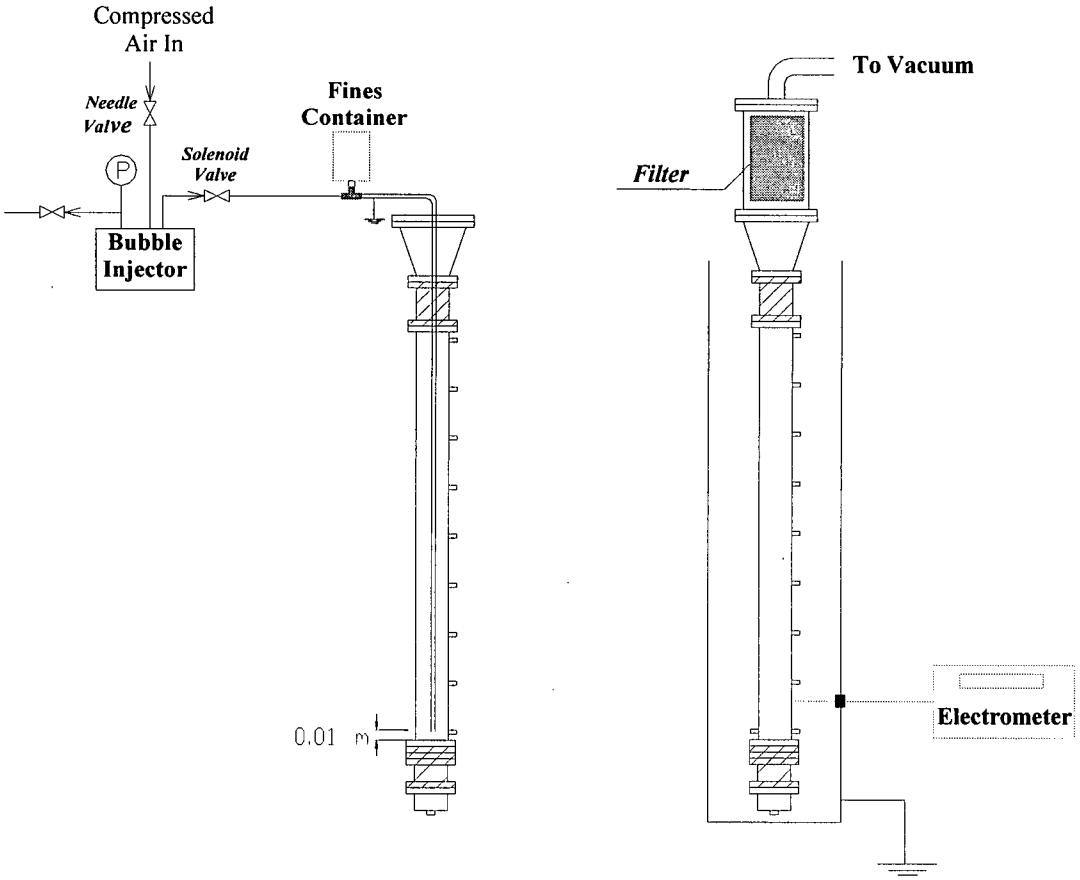

Figure 2.7. Schematic diagram of (a) fines injection unit, and (b) fluidization column with filter bag to capture entrained fines.

The injection unit consisted of a container to hold the fines connected to a grounded stainless steel tube of 0.003175 m internal diameter by a three-way adaptor. The adaptor was connected to the bubble injection unit on the other side. The container was first filled with the desired amount of fines and sealed. As the fines dropped into the adaptor, they were injected into the bed through the tube by injecting extra dry air bubbles with the bubble injection unit set at a pressure of 2 psig (13.8 kPa). The injection frequency was 0.1 s^{-1}. As each bubble was injected, the location of the tube inside the bed was varied

radially to distribute the fines as evenly as possible at the bottom of the bed. The tube was grounded to minimize extra charging of the fine particles as they traveled through the tube. Then, the top Plexiglas section of the column was replaced by a dust luck filter (provided by BC Air Filter with 26-30% dust capture efficiency of 1 μm particulates) contained in a box connected to a source of vacuum to capture all entrained fines (see Figure 2.7 (b)).

Charge measurement then started, and after 30 s the binary particle mixtures were fluidized with the same operating conditions as for the mono-sized system. As the fluidization continued, since the operating gas velocity was much greater than the terminal velocity of the fines, fines were entrained from the bed inducing charges on the inner column measured by the electrometer. Fluidization was terminated when the measured charges reached steady state, indicating that negligible detachable fines remained in the bed to be entrained. The total charges carried by the entrained fines corresponded in magnitude to the final steady state value of the measured charge. The mass of fine particles entrained was determined by weighing the filter before and after each run by an A&D Weighing model GR-200 analytical balance with a capacity of 0.01 to 210 ± 0.0002 g.

In each run, the procedure of injection of the fines into the bed took 2-4 minutes with the top of bed exposed to the atmosphere. As soon as the fines had been added, the cover was reinstalled and the flow of air re-established. Therefore, it was not anticipated that the ambient relative humidity would have had a significant effect on the fluidizing gas relative humidity when the free bubbling fluidization of binary mixture was performed.

At a later stage, it was suggested (Castle, 2004) that the Teflon piece at the top of the copper section of the inner column might have affected the charges measured by the copper section by inducing a field downward into the copper section of the bed. Therefore, this piece was removed and two of the previous runs were repeated to test the accuracy of the results. The results turned out to be virtually the same as for the previous runs (see Appendix C). Since the inner column had to be repositioned to extract the

Teflon piece and also this piece was clearly unnecessary, it was not replaced for the next set of experiments.

The results presented in Appendix C, Figures C1 and C2, were performed at the same operating conditions. These results also represent the degree of reproducibility of the measurements. As shown in Figure C4, where the two measurements are plotted in one graph, there is a maximum of about 10% difference between the measurements.

Next, polyethylene particles were utilized as the mono-sized particles. The mono-sized and binary mixture experiments were conducted with exactly the same operating procedure as explained previously, except that the particles were fluidized with a superficial air velocity of 0.27 m/s. This velocity again ensured that the bed was operating in a similar manner to the bed of relatively large glass beads so that the bed behaviour was in the bubbling regime when viewed from the top of the fluidization column.

The free bubbling experiments were repeated for different relative humidities (RH) of the fluidizing gas as indicated in Table 2.4.

Table 2.4. Relative humidities tested.

Mono-sized Particles	**Fluidization Runs**	**RH %**			
Large Glass Beads	***Mono-sized***	0%	15%	35%	60%
	Binary	0%	15%	35%	60%
Polyethylene	***Mono-sized***	0%	5%	60%	
	Binary	0%	5%	60%	

In order to determine the initial charges of fines upon their injection into the fluidized bed, as well as ensuring that fines did not gain significant charges while traveling through the injection tube, the same fines were injected into a small Faraday cup instead of the fluidization column. These fines were injected with the same procedure as described

above. The small Faraday cup used was the same as in Figure 2.3. The initial charge-to-mass ratios, Q/m, for different fines are presented in Table 2.5. The m values are the total masses of fines (0.2 wt% of the bed material) injected into the bed for the free bubbling fluidization of the binary mixture systems.

Table 2.5. Initial charge/mass ratios, Q/m, for different fines.

	GB I	**S-GB I**	**GB II**	**S-GB II**	**Larostat 519**	**Catalyst**	**Silica**
Q/m (μC/kg)	-0.75	-0.64	-1.20	-0.95	-0.13	-0.68	-1.20

In each run, after the free bubbling fluidization of the binary mixture, the particles left inside the column were discharged and the inner walls of the fluidization column were cleaned (vacuum plus wet cloth) to ensure that no fines left behind in the column that would affect the measurements for the subsequent experiments.

Chapter 3. Results and Discussion

The novel on-line fluidized bed Faraday cup measurement technique portrayed in the previous chapter was used to measure the net charges generated inside the fluidized bed, due to either charges leaving the system or being neutralized, thereby resulting in a net charge. Consequently, net charges generated inside the fluidized bed caused by charges leaving the system either with entrained fines or carried by the gas leaving the top of the column were measured. The effect of fluidizing gas on charging mechanism, either by particle charge neutralization due to gas ionization, or by triboelectrification due to particle-gas contact was investigated. This chapter presents the experimental results obtained by the Faraday cup fluidized bed system.

3.1. Triboelectrification Due to Particle-Gas Charging

If particle-gas charging occurs inside a fluidized bed with no particles entrained, the gas leaving the column could carry some charges with it, leaving a net charge behind that could be detected by the Faraday cup system. This possibility was examined by means of bubble injection experiments. The background gas velocity was maintained at 0.19 m/s (91% of U_{mf}) for these measurements, and each of the single injected bubbles had a volume of 1.2×10^5 mm^3. No particles were entrained from the column under these conditions. The charges measured were very small, ~ 2×10^{-12} C, due to the single bubble injection, well within the background noise of the Keithley Electrometer ($\pm 10^{-11}$ C, see Section 2.2). Therefore, many bubbles were next injected in succession to provide more charge generation. Charges were measured after every 400 bubble injections. As shown in Figure 3.1, the cumulative measured charges stayed nearly constant after the first series of injections. Note that all of the measured values are below the threshold of where significance can be affected for the readings as stated previously. This is an indication that the air leaving the column did not carry any appreciable charges. We can therefore infer that particle-gas contact had negligible effect on the particle charging mechanism, at least for the conditions studied in this work.

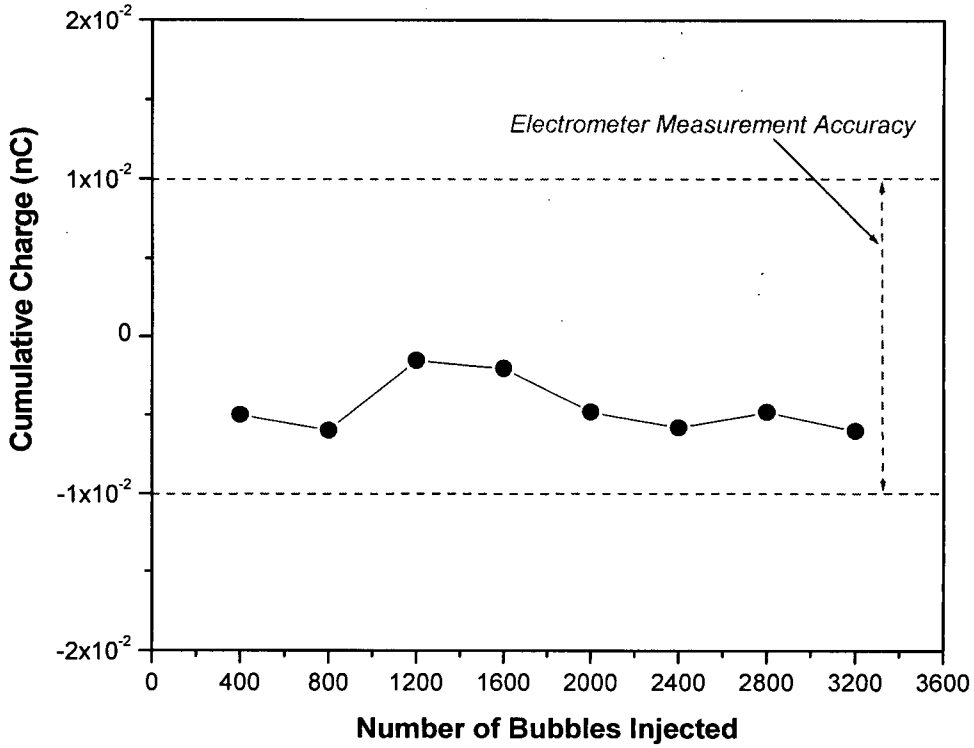

Figure 3.1. Cumulative charge measured for multiple bubble injections. Background superficial air velocity: 0.19 m/s; bed depth: 0.20 m; volume of gas pulses: 1.2×10^5 mm^3; frequency of bubble injection: 0.33 s^{-1}.

3.2. Triboelectrification Due to Gas Ionization

The possibility of gas ionization due to frictional charging was also considered. When frictional charging between particles occurs in air, the high electrical field between the surfaces as they separate can cause the air to ionize, and the ions then neutralize the surface charges (Cross, 1987). Chen et al. (2003) compared all available literature data on directly measured specific particle charges in gas-solid fluidized beds at steady state conditions with the maximum surface charge build-up on particles that can cause air breakdown (air ionization). The results indicate that all measured charges were much less than the maximum specific charge required for ionization. Thus it is highly improbable that the fields generated by particle separation are high enough to initiate discharges. Therefore, air ionization is not expected to have a significant effect on particle charge dissipation.

3.3. Net Charge Due to the Fines Leaving the Column

In order to determine whether the net charge generated inside the fluidized bed Faraday cup system when the bed was freely fluidized are due to fines carried over and leaving through the exit of the column, the following experiments were performed: (a) The charge was first measured while fluidizing the relatively large glass bead particles (see Table 2.2 for particle properties). (b) The net charge was then determined after adding 0.5 vol.% of fine GB I particles (see Table 2.3 for properties) to create a binary system with the much larger glass beads. (c) The measurements were next repeated for the same binary system of large and small glass beads, with a fine filter added to the top of the copper section of the column to capture all entrained fines.

The cumulative charges measured due to the free bubbling fluidization of the mono-sized and binary system are presented in Figure 3.2.

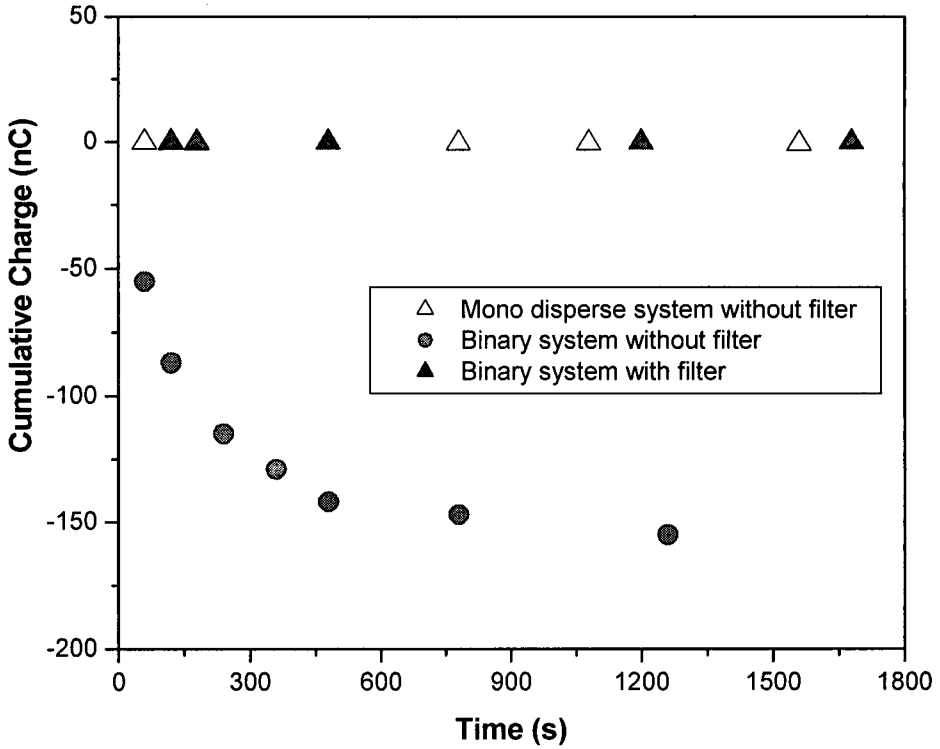

Figure 3.2. Charges due to fines leaving freely bubbling fluidized bed for mono-disperse and binary glass bead systems. Superficial air velocity: 0.22 m/s; bed depth: 0.20 m; fines proportion: 0.5 vol.%.

As shown, the charges measured for the mono-dispersed system were significantly smaller (in magnitude) than those measured in the binary system without the filter. For the binary system without the filter, it is also apparent that the rate of generation of charges decreased as the fluidization continued. This presumably occurs because the operating gas velocity is much higher than the terminal velocity of fine particles so that immediately after the fluidization starts, fine particles begin to be entrained from the bed; as fluidization continued, most of the fines escaped from the column leaving few fines to be entrained. The results also indicate that the fines leaving the system were positively charged. Figure 3.2 also presents the corresponding net cumulative charges generated inside the bed. It can be seen that in the case studied, a net charge of -1.5×10^{-7} C was generated inside the bed due to the fines entrained from the system.

The results also show that for the case studied (large glass beads and GB I), since the smaller particles were charged positively, the larger particles left behind should have been charged either more positively if charge transfer occurred from larger to smaller particles, or less positively or even negatively if bipolar charging had occurred, as has been proposed to explain contact charging between particles of the same material but different sizes (Ali et al., 1998; Zhao et al., 2000).

During the experiments, fine particles were observed visually to be carried out from the top of the column, with some settling on the conical wall of the expanded top section of the vessel. A small sample of these fines was collected and their size distribution analyzed by a Malvern Mastersizer 2000. The size distribution (20-80 μm) is narrower and their average particle size (38 μm), larger than for the original added fines of 10-80 μm with an average particle size of 30 μm, indicating that most of the finer particles had been entrained from the bed.

For the binary mixture with the filter present within the Faraday cup, the measured charges were almost zero. This confirms that the gas does not carry appreciable charges and shows that the net charge measured by the Faraday cup fluidization column system when there was no filter resulted from net charges carried by fines entrained from the

fluidized bed. This finding is of significant practical importance, since fines are always carried over to a greater or lesser extent in fluidized bed processes. Even when entrained particles are efficiently captured by cyclones and returned to the bed, the capture efficiency is always less than 100%, so that some relatively fine particles are continuously lost from practical fluidized bed systems.

3.4. Changes in Electrostatic Charges of Fine Particles after Addition to Gas-Solid Fluidized Beds

Some previous research has been performed to find ways of preventing and reducing electrostatic charges in gas-solid fluidized beds. One of the methods investigated is the addition of antistatic agents or fines, but efforts have generally been confined to minimizing the influence of electrostatics, rather than understanding the phenomena involved. Wolny et al. (1983) added conductive, semi-conductive and dielectric fine materials and concluded that the addition of fines to fluidized beds decreases the electrostatic effects, independent of the electrical nature of the fines. They determined the effect of adding fines by measuring the charge on single particles discharged from the bed during the experiments into a Faraday cage. Wolny et al. (1989) studied the effect of adding fines such as aluminum powder on bed behaviour due to electrostatic charge generation by withdrawing particles from the bed and placing them in an electric field. By measuring the electric field inside the bed by a wall-mounted ball probe, Park et al. (2002) found that Larostat 519 reduces the electrostatic charge build-up in the bed. Good et al. (1989) and Song et al. (1995) used a spherical electrode to monitor changes in bed voltage due to the addition of different chemical additives to reduce sheeting in polymerization processes. Previous works have all focused on measuring the change in the bed charge due to the addition of fines. However, in order to gain a better understanding of the effect of addition of fines on electrostatic charge generation/dissipation inside the bed and especially its mechanism, it is also necessary to study the changes of the electrostatic behaviour of fines after their addition to the bed.

Free bubbling experiments, as described in section 2.4.3, were carried out to examine changes in electrostatic charges of different fines after they were injected into beds of relatively large glass beads and polyethylene particles.

3.4.1. Bed material: large glass beads

Experiments were conducted utilizing relatively large glass beads as the mono-sized particles and Larostat 519, GB and S-GB I & II as added fines for the binary mixtures (see Tables 2.2 and 2.3 for particles properties). These experiments were performed at various relative humidities (RH) of the fluidizing gas (0%, 15%, 35% and 60%). Figures 3.3-3.7 show the cumulative net charges measured over time, during fluidization of mono-sized and binary mixtures of particles, with different added fines. Each plot presents the results for a different relative humidity of the fluidizing gas.

In order to ensure that the fluidizing gas alone does not carry any charges that would influence the results of the mono-sized and binary systems, the charges were measured while passing air alone through the fluidization column at the same superficial gas velocity as for the freely bubbling fluidization runs. As can be seen, the measured charges for air alone are close to zero (magnitude < 5×10^{-11} C). At the beginning of each run, the initial charge-to-mass ratio of the mono-sized relatively large glass beads, Q_o/m, was measured, and the values are indicated on each graph. It can be seen that the large glass beads initially carry relatively large negative charges, -2.1×10^{-8} to -6.0×10^{-7} C/kg.

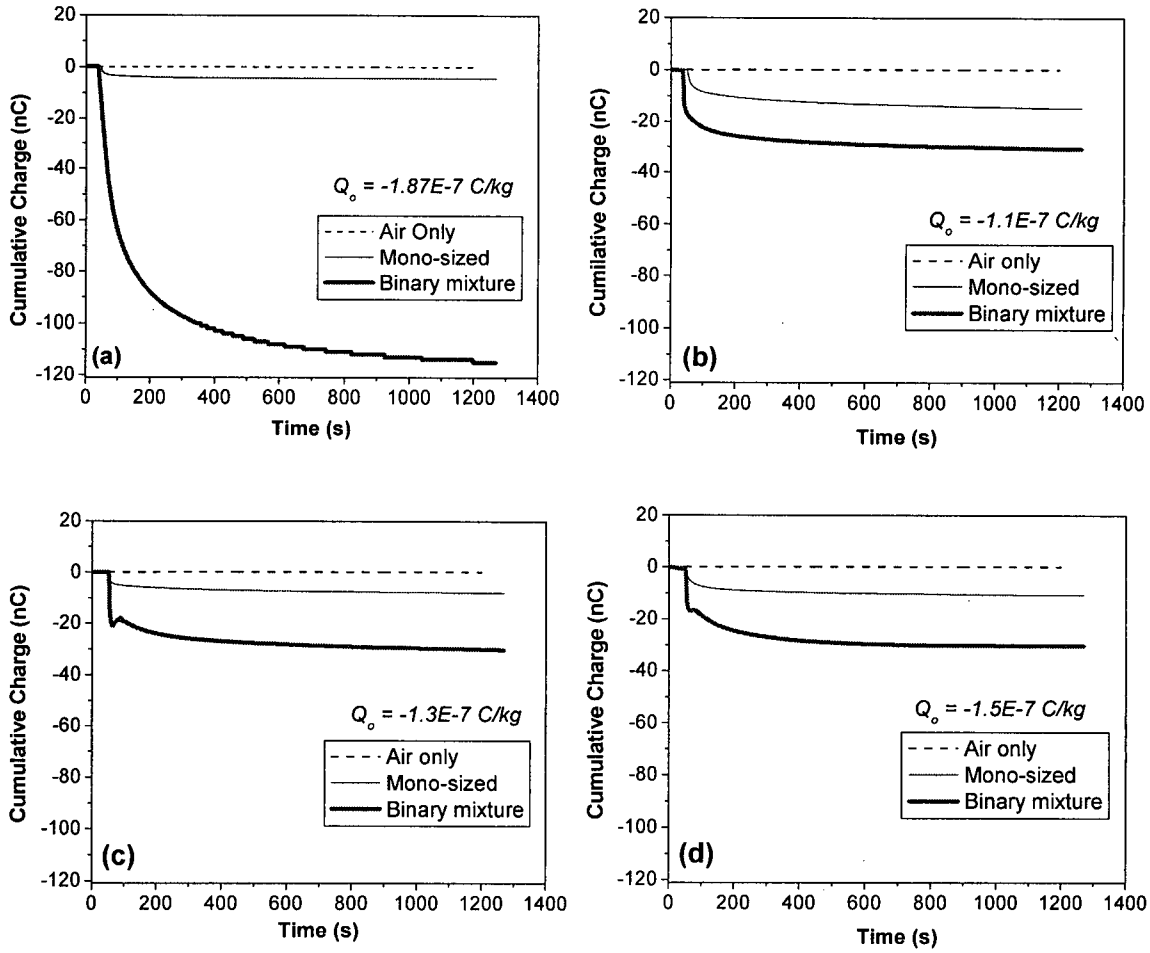

Figure 3.3. Charges measured while fluidizing mono-sized and binary mixture glass beads with GB I added as fines. (a) RH=0%, (b) RH=15%, (c) RH=35%, (d) RH=60%; Superficial air velocity: 0.22 m/s; bed depth: 0.20 m; fines proportion: 0.2 wt%.

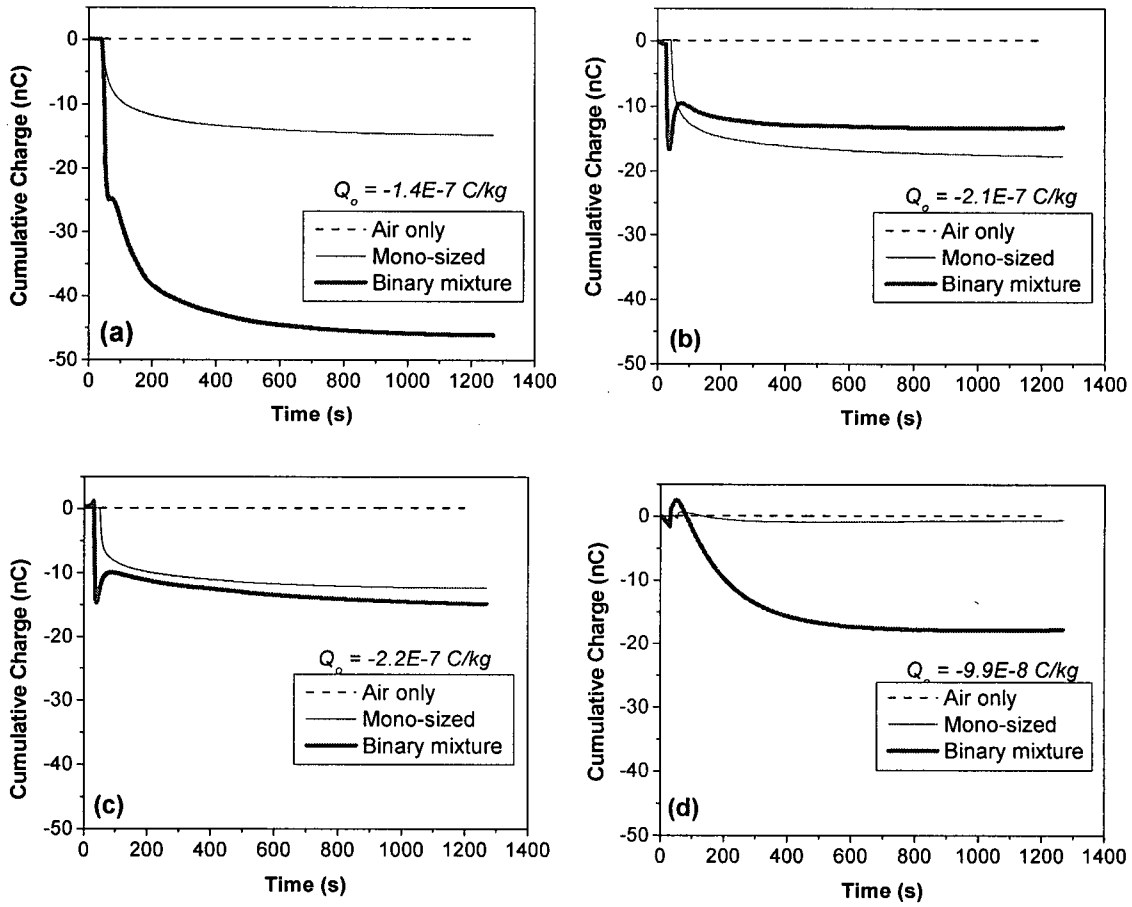

Figure 3.4. Charges measured while fluidizing mono-sized and binary mixture glass beads with S-GB I added as fines. (a) RH=0%, (b) RH=15%, (c) RH=35%, (d) RH=60%; Superficial air velocity: 0.22 m/s; bed depth: 0.20 m; fines proportion: 0.2 wt%.

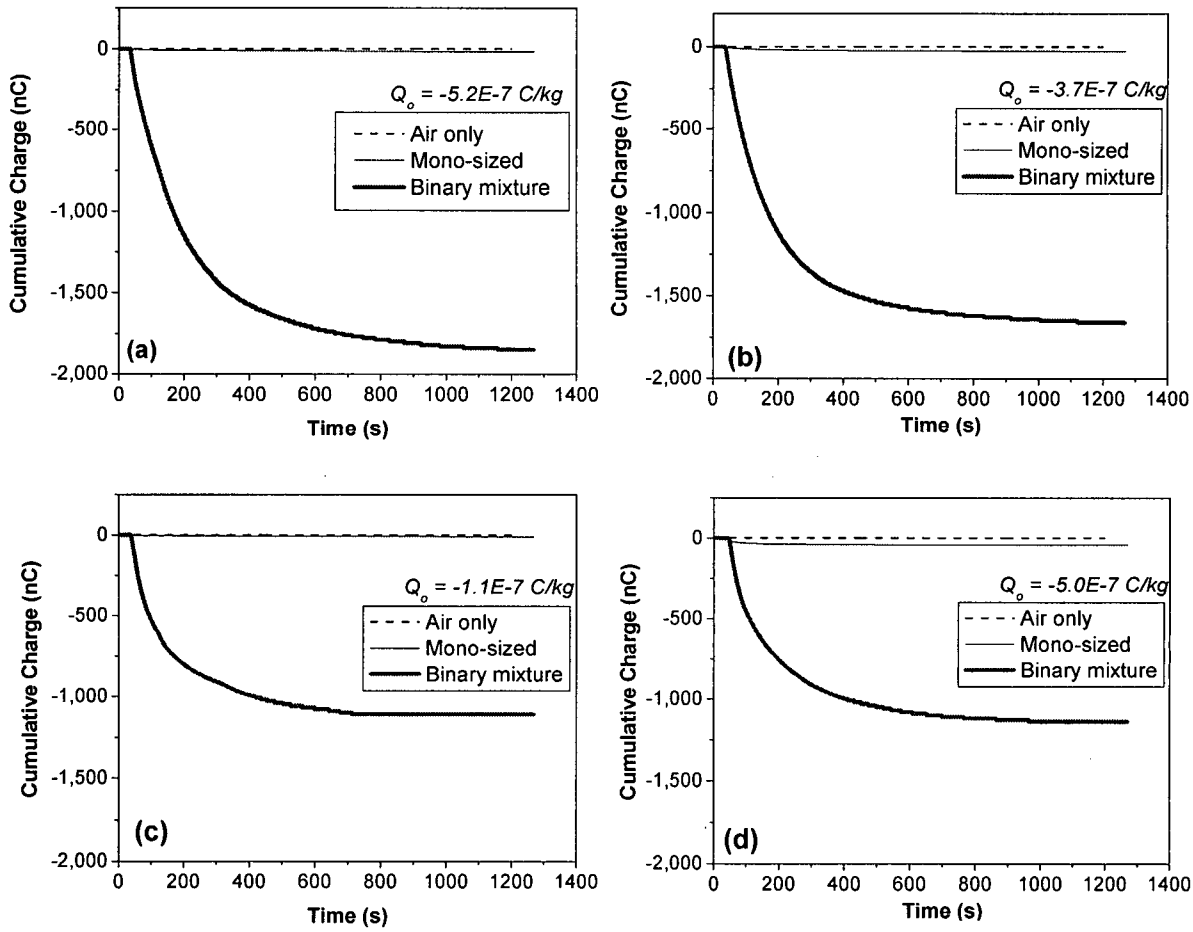

Figure 3.5. Charges measured while fluidizing mono-sized and binary mixture glass beads with GB II added as fines. (a) RH=0%, (b) RH=15%, (c) RH=35%, (d) RH=60%; Superficial air velocity: 0.22 m/s; bed depth: 0.20 m; fines proportion: 0.2 wt%.

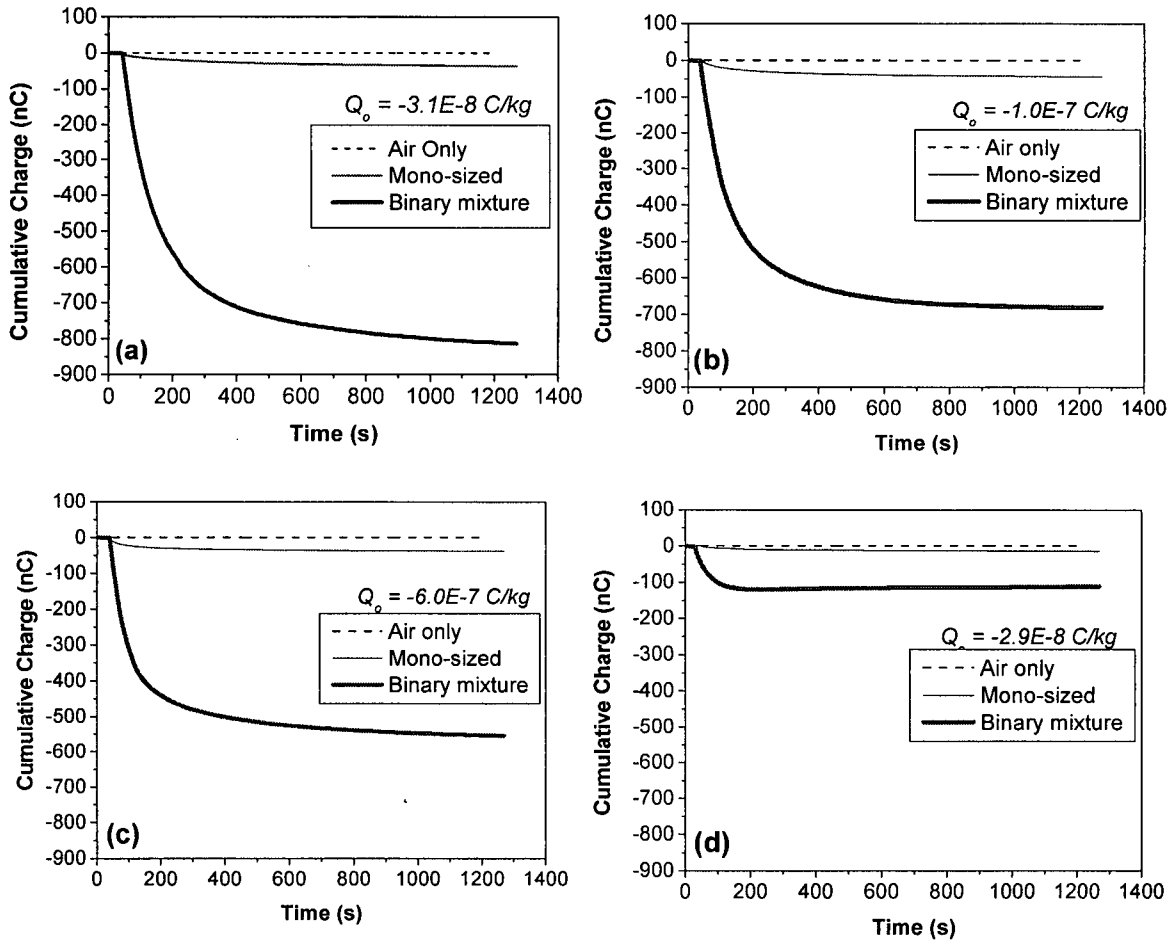

Figure 3.6. Charges measured while fluidizing mono-sized and binary mixture glass beads with S-GB II added as fines. (a) RH=0%, (b) RH=15%, (c) RH=35%, (d) RH=60%; Superficial air velocity: 0.22 m/s; bed depth: 0.20 m; fines proportion: 0.2 wt%.

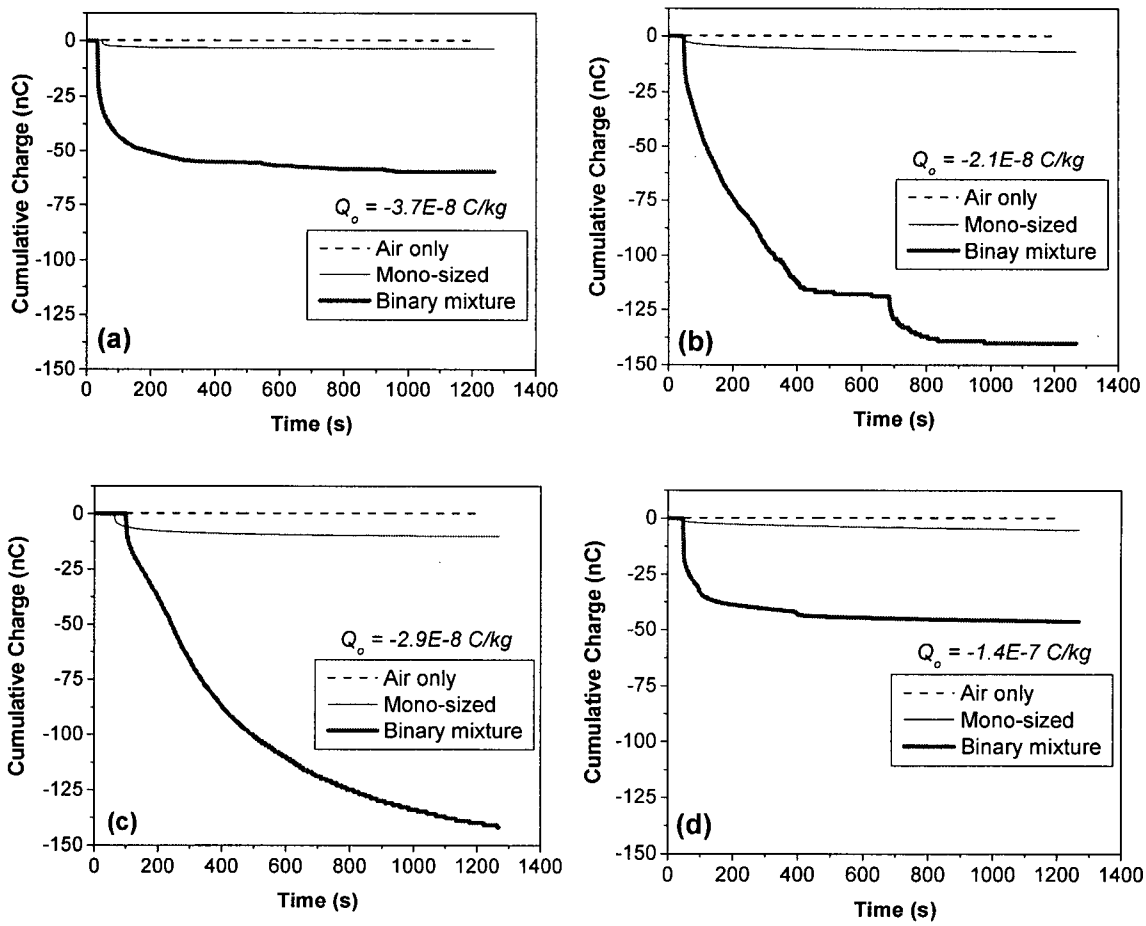

Figure 3.7. Charges measured while fluidizing mono-sized and binary mixture glass beads with Larostat added as fines. (a) RH=0%, (b) RH=15%, (c) RH=35%, (d) RH=60%; Superficial air velocity: 0.22 m/s; bed depth: 0.20 m; fines proportion: 0.2 wt%.

For all the runs, charges measured due to freely bubbling fluidization of the mono-sized large glass beads show a small negative change before approaching a steady state value. This indicates that some fines which had remained in the system have been entrained from the bed. The corresponding charges were too small to affect the charge measurements for the binary system appreciably. It can also be seen that for all runs, charges measured due to free bubbling of binary systems with different added fines show a relatively large negative deviation upon the start of the fluidization and then approach a steady state value. Even though all the measured charges are negative, since the particles leave the Faraday cup fluidized bed system, they induce charges of opposite polarity on the cup. Hence the actual charges on the entrained fines are positive. The same quantity of charges, but with opposite polarity (negative), must have been left behind in the bed which then could have reduced or neutralized the original net charge of the bed, if the bed is initially positively charged. Otherwise, fines entrainment can lead to further charge build-up inside the fluidized bed.

Results for the binary system of S-GB I fines for relative humidities of 15 and 35% (Figure 3.4 b and c) show a negative dip followed by a positive peak at the beginning of the measurements, before reaching steady state. This indicates that fines entrained from the fluidization column upon the start of the fluidization were positively charged, whereas those entrained just a few seconds later were negatively charged. One possibility could be that as the fluidization continues, the moisture in the system affects the silver coated fines by changing their electrical behaviour as they come in contact with large glass beads.

After completing the fluidization of the mono-sized and binary mixture particles, no large glass beads were observed to be attached to the column walls. However, thin layers of fines were observed clinging to the walls. This indicates that not all the fines injected into the fluidized bed were entrained from the fluidization column. The initial mass of fines injected into the bed before fluidization, and the overall masses of captured entrained fines, determined by weighing the filter before and after the period of fluidization, are presented in Table 3.1.

Table 3.1. Initial and overall captured masses for different fines and different gas relative humidities, with large glass beads as the major bed component.

Particles	***Initial Mass (g)***	***Overall Captured Mass (g)***			
		RH = 0%	***RH = 15%***	***RH = 35%***	***RH = 60%***
Larostat 519	6.0	3.52	2.96	1.84	1.87
S-GB I	6.0	5.05	5.12	4.7	3.92
GB I	6.0	2.00	1.82	4.47	4.50
S-GB II	6.0	4.52	4.52	4.67	5.27
GB II	6.0	3.37	3.87	3.75	3.83

In comparison, the mass of entrained Larostat 519 particles from the fluidized bed was less than those of the other injected fines. This could be because Larostat 519 particles tend to attach to the surfaces of the large glass beads as shown in Figure 3.8. The results also show that the mass of entrained Larostat particles decreased as a results of increasing the relative humidity of the fluidizing gas. This is due to the high tendency of Larostat particles to readily adsorb water and therefore, as the relative humidity increases, Larostat particles agglomerate and stick more to the bed material. Overall, the results show that between 30-80% of the fines injected into the fluidized bed were entrained from the fluidization column, thereby leaving the rest behind. As mentioned above, at the end of each run, thin layers of fines were observed sticking to the column walls. In addition, some fines might have settled in the holes of the pressure ports along the side of the inner walls of the column and some fines may have adhered to the bed particles.

In order to better analyze and compare the results for different added fines, the initial (at the point of injection, see Section 2.4.3 and Table 2.5) and final (steady state) charge-to-mass ratio, Q/m, was determined, where the m values are the final masses of captured entrained fines as shown in Table 3.1. The results are presented in Table 3.2. Comparison of Q/m for glass beads (GB I & II) and silver-coated glass beads (S-GB I & II) of different sizes shows that the finer the particles, the higher the charges carried per unit mass. This occurs because smaller particles have higher surface areas per unit mass and therefore are able to generate and retain more charges per unit mass.

Table 3.2. Initial and final charge/mass ratios, Q/m [μC/kg], for different fines and different gas relative humidities, with large glass beads as the major bed component.

Particles	***Initial Q/m***	***Final Q/m***			
		RH = 0%	***RH = 15%***	***RH = 35%***	***RH = 60%***
Larostat 519	-0.13	42	47	32	25
S-GB I	-0.64	9.1	3.1	2.6	4.6
GB I	-0.75	58	17	6.7	6.7
S-GB II	-0.95	179	150	118	23
GB II	-1.20	548	430	270	300

The results show that Q/m is lower for Larostat 519 than for GB II and S-GB II, even though all three species had very similar average particle sizes. This could be due to their physical surface structure as shown in Figure 2.6 in Chapter 2. SEM images of added fines show that Larostat particles are non-spherical and have uneven surfaces, whereas both glass beads II and silver-coated glass beads II are nearly spherical and have smooth or somewhat rough surfaces, respectively. Since the bed materials (large glass beads) are smooth and nearly spherical, there will be fewer contacts between them and Larostat 519 than for the fine glass beads II and the silver-coated glass beads II. Therefore, there is likely to be less charge generation or transfer between the large glass beads and Larostat 519. On the other hand, the SEM images of samples taken after each binary mixture run (Figure 3.8) show that Larostat 519 particles tend to attach to the surfaces of the large glass beads, whereas glass beads II and silver-coated glass beads II fines do not. This indicates that Larostat 519 particles remaining in the bed may have helped to dissipate the initial bed charges, leading to lower measured Q/m values.

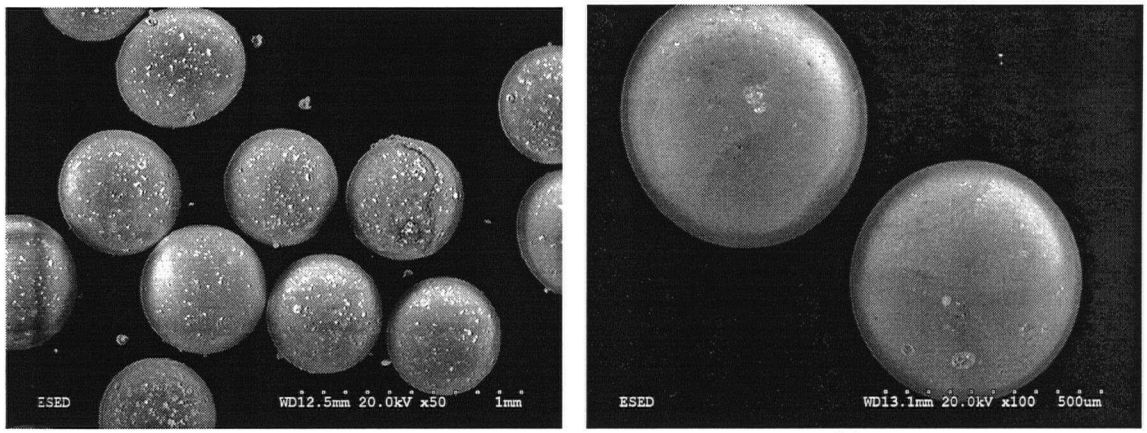

(a) (b)

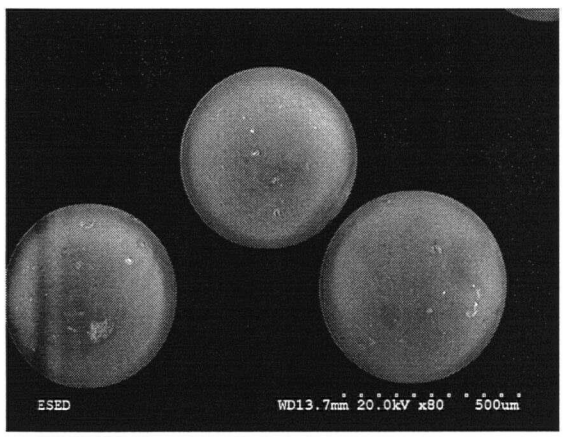

(c)

Figure 3.8. SEM images of samples taken after binary mixture runs at superficial air velocity: 0.22 m/s and bed depth: 0.20. (a) Large glass beads with Larostat 519 adhering to surface, (b) Large glass beads with GB II, (c) Large glass beads with S-GB II.

For the same size of fine particles, silver-coated glass beads carried less charge than the pure glass beads. This could be because the silver-coated glass beads are highly conductive and, therefore, can easily lose their charges to the column walls. They may also help to dissipate initial bed charges.

The charge-to-mass ratios are highest for the runs with extra dry air (RH=0%). As the relative humidity increases the Q/m ratios decrease. This was anticipated since it has long been reported that increasing the relative humidity of a fluidizing gas helps to dissipate charges and to reduce generation of electrostatic charges inside the bed. The results show

that for most fines, except for S-GB II, the measured Q/m values do not vary much with RH for relative humidities greater than 35%.

GB type I particles, which are of similar composition to the large glass beads, were utilized to study bi-polar charging. The results show that entrained GB I fines are positively charged. The initial net charges of large glass beads, measured at the beginning of each mono-sized fluidization run, were negative, but the final net charges are unknown. If the final net charges are assumed to have similar polarity to those of the initial ones, and if particle-particle charging is the dominant charging mechanism, then the results confirm that bi-polar charging occurs. However, in this case, where smaller particles are charged positively and larger particles negatively, the results appear to differ from the findings of Zhao et al. (2000) who claimed that when small particles contact larger particles, electrons should transfer from larger particles to smaller particles so that smaller particles become negatively charged, whereas larger particles become positively charged. This difference in findings could be due to surface impurities of the particles that affect their work function at the point of contact. Even though both the large and fine glass beads are made of the same material, they are not from the same batch. And since the fine particles were not washed prior to the experiment, they might contain some impurities.

Since the added fines have different particle sizes and densities, the charge-to-total surface area ratio, Q/A_s, was determined to better analyze the results presented previously. The total surface area of fines was estimated as

$$A_s = N (\pi d_P^2) / \varphi \tag{1}$$

where N is the number of particles, d_P is the particle diameter and φ is the sphericity. The number of particles, N, was estimated from

$$N = m / (\pi d_P^3 \rho_p / 6) \tag{2}$$

where m is the mass of particles entrained from the fluidization column and ρ_p is the particle density. The sphericities of the particles are given in Table 2.2.

As seen in Figure 2.5, Larostat particles look like clusters of small granules, and therefore it is difficult to find their sphericity in the same manner as it was determined for the other fines (see Section 2.3.2). Thus, Q/A_s ratios were determined for the two extreme values of sphericity, 0.7 and 0.9, for the Larostat particles. Table 3.3 presents the results of charge-to-total surface area.

Table 3.3. Initial and final charge/surface area ratios, Q/A_s [$\mu C/m^2$], for different fines and different gas relative humidities with large glass beads as the major bed component.

Particles	***Initial Q/A_s***	***Final Q/A_s***			
		RH = 0%	***RH = 15%***	***RH = 35%***	***RH = 60%***
Larostat 519[a]	-0.00010	0.033	0.037	0.025	0.020
Larostat 519[b]	-0.00013	0.043	0.048	0.032	0.025
S-GB I	-0.008	0.121	0.041	0.034	0.061
GB I	-0.009	0.725	0.213	0.084	0.084
S-GB II	-0.003	0.438	0.474	0.438	0.084
GB II	-0.002	1.105	0.867	0.545	0.605

Larostat 519[a] and 519[b] represent the results for 0.7 and 0.9 sphericity, respectively.

The results are consistent with the conclusions above based on the charge-to-mass ratios. Since the effect of particles size is incorporated in the charge-to-surface area ratios, the comparison of the results for GB I and II particles suggest that the difference between their chemical compositions also has an effect on the charges carried. However, for S-GB I and II particles, assumed to have similar chemical surface properties, the charge-to-surface areas are quite different perhaps due to surface contamination. The results for Larostat 519 particles indicate that the sphericity does not appear to play a significant role in determining charge-to-surface area ratios.

3.4.2. Bed material: polyethylene

Polyethylene particles, which are more typical industrial particulates than the glass beads, were next examined as the mono-sized relatively coarse particles, with Larostat 519, S-

GB I, catalyst and silica particles as added fines for the binary mixtures. Experiments were performed at various relative humidities of the fluidizing gas (0%, 5% and 60%). The results of the measured cumulative net charges due to free bubbling of mono-sized and binary mixtures are presented in Figures 3.9-3.12.

To verify that the fluidizing gas alone is free of any charges, air was passed through the fluidization column while charges induced on the column were measured. As can be seen in Figures 3.9-3.12, air alone carries negligible charges.

Initial charge-to-mass ratios of polyethylene mono-sized particles, Q_o, for different runs were determined to be in the range of $-9x10^{-8}$ to $-4x10^{-7}$ C/kg. The charges measured during the fluidization of mono-sized polyethylene particles for different runs show that a small amount of fines carrying positive charges were entrained from the fluidized bed. These fines could have adhered to the larger polyethylene particles during sieving. They could also have been generated due to attrition during the free bubbling fluidization of mono-sized particles.

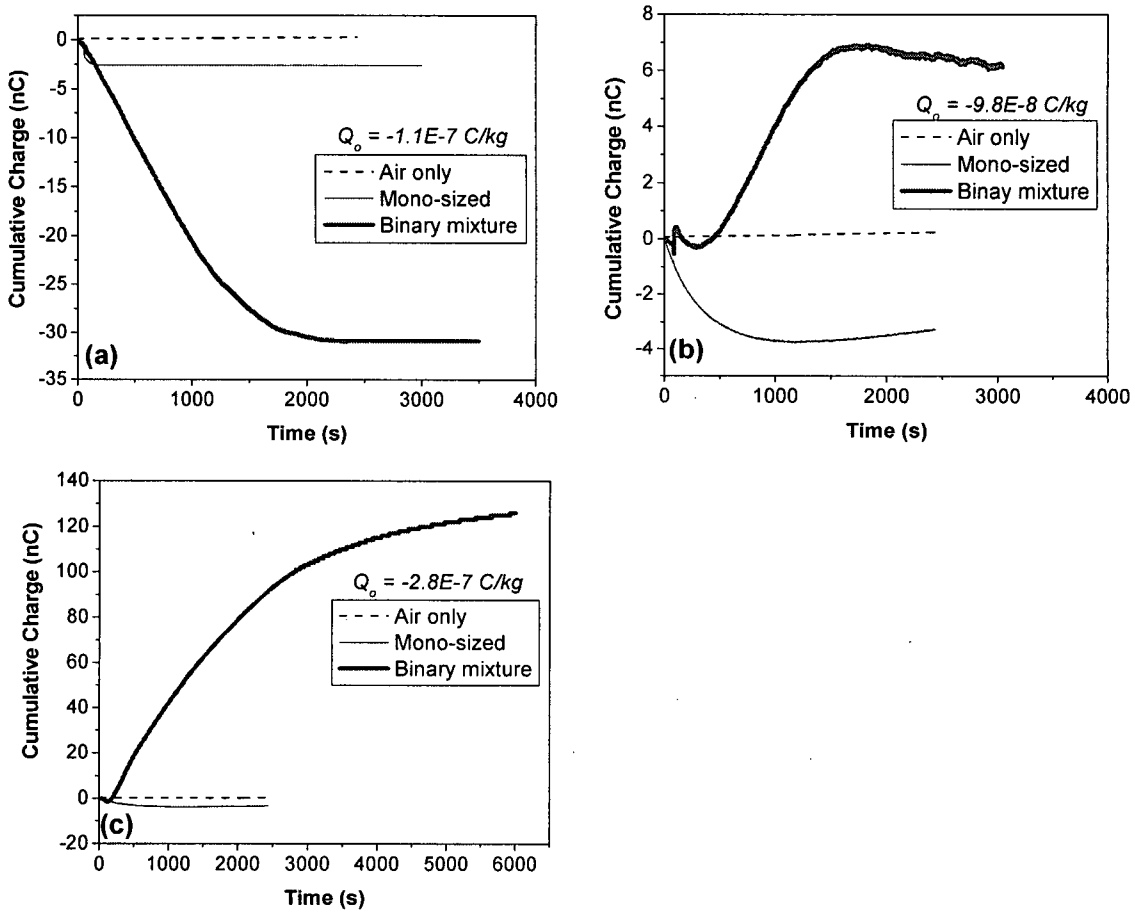

Figure 3.9. Charges due to catalyst particles leaving the fluidized bed of polyethylene particles. (a) RH=0%, (b) RH=5%, (c) RH=60%. Superficial air velocity: 0.27 m/s; bed depth: 0.20 m; fines proportion: 0.2 wt%.

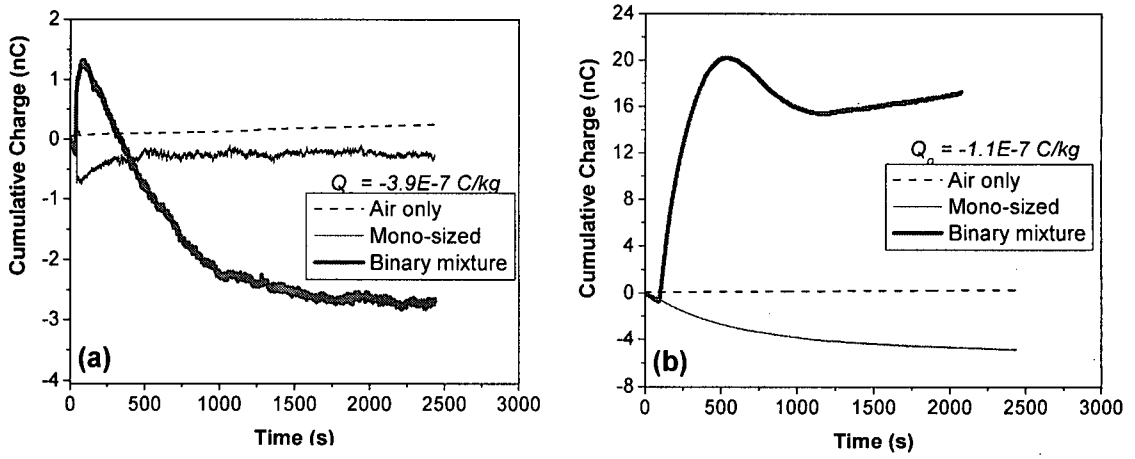

Figure 3.10. Charges due to S-GB I particles leaving the fluidized bed of polyethylene particles. (a) RH=0%, (b) RH=60%. Superficial air velocity: 0.27 m/s; bed depth: 0.20 m; fines proportion: 0.2 wt%.

The charges measured while fluidizing binary mixtures show that, except for fine silica particles, the added fines carried different polarity of charges out of the bed depending on the relative humidity of the fluidizing gas. This variable impact could be due to the effect of relative humidity of the fluidizing gas on the bed material (polyethylene particles) and/or on the electrical behavior of added fines. It has long been known (see section 1.4.1) that increasing the relative humidity of the fluidizing gas helps to reduce or dissipate charges inside beds of polyethylene particles. On the other hand, Larostat 519 is known as a hygroscopic material meaning that it readily adsorbs water, which then could affect its electrical behaviour as it comes in contact with polyethylene particles. Even though catalyst particles are mainly composed of silica, and therefore both might be expected to adsorb water in similar manner, they behaved differently. The reason could be that catalyst particles contain metal oxides such as titanium and magnesium oxide, causing their surface composition to differ from that of the silica particles. When silica is subjected to moisture, water molecules chemically and physically adsorb on the surface to form Si-OH groups and Si-O----H-O-H, respectively. On the other hand, interaction between moisture and catalyst particles results not only in reaction of silica with water molecules, but also in formation of Ti-OH and Mg-OH. Therefore, it is possible that in comparison, catalyst, silica, S-GB I and Larostat 519 particles behave differently when exposed to moisture which then affects their chemical and physical properties.

The catalyst and silver-coated glass beads behaved in a similar matter by being positively charged at 0% RH and negatively charged at 60% RH (see Figures 3.9 and 3.10). This could be because of their similar surface electrical conductivities. Catalyst particles contain magnesium which is highly conductive, with an electrical conductivity of $2.33 \times 10^{7}\ \Omega^{-1}m^{-1}$ (Kittle, 1996) and silver-coated glass beads are also conductive with electrical conductivity of $6.2 \times 10^{5}\ \Omega^{-1}m^{-1}$ (value obtained from supplier). As a result, at 0% RH when these fines come in contact with polyethylene particles, which are good insulators, they become positively charged due to contact charging. However, when exposed to higher moisture content, either existing in the bed from fluidization of mono-sized particles or due to the higher relative humidity of the fluidizing gas, they help to

dissipate bed charges by becoming more conductive due to the existence of the water molecules, and thus become negatively charged.

Results for the binary system of S-GB I fines for relative humidity of 0% (Figure 3.10 a) show a positive peak followed by a negative dip at the beginning of the measurements, before reaching steady state. This indicates that fines entrained from the fluidization column upon the start of the fluidization were negatively charged, whereas those entrained just a few seconds later were positively charged. One possibility could be that the silver coated fines are charged due to different charging mechanisms.

In order to verify that humidity affects the polarity of the charges on these fines, the humidity of the gas was increased by a small increment of 5%, and the run with catalyst as the added fines repeated (see Figure 3.9). Results confirmed that as the relative humidity of the fluidizing gas increased, catalyst particles became more positively charged. This finding could also explain the fact that in industrial polymer reactors it has been found that addition of even a few ppm of water helps to dissipate electrostatic charges (Goode et al., 2000).

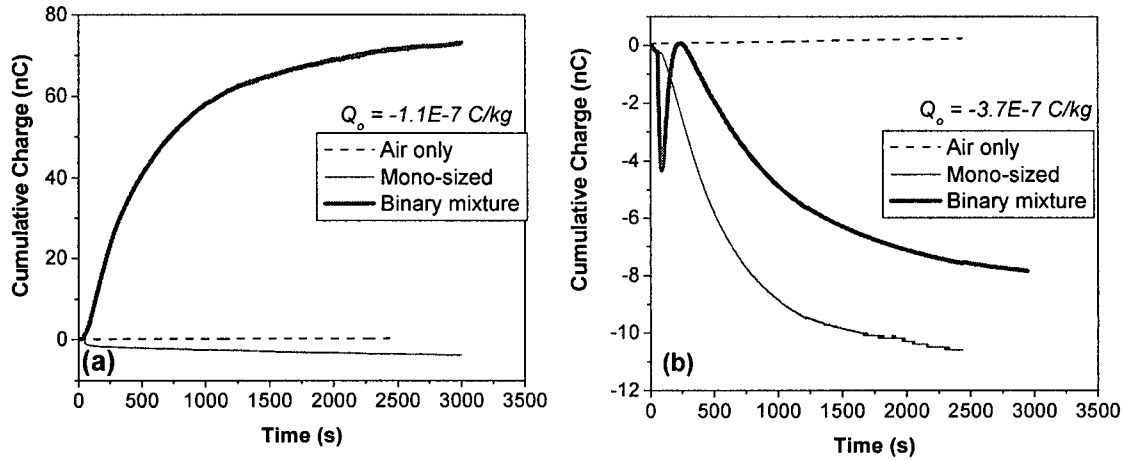

Figure 3.11. Charges due to Larostat 519 particles leaving the fluidized bed of polyethylene particles. (a) RH=0%, (b) RH=60%. Superficial air velocity: 0.27 m/s; bed depth: 0.20 m; fines proportion: 0.2 wt%.

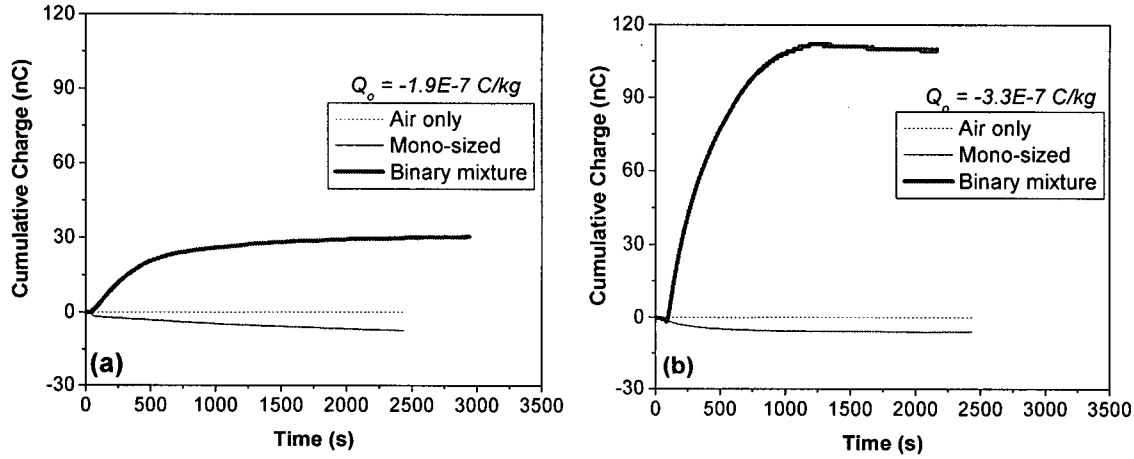

Figure 3.12. Charges due to silica particles leaving the fluidized bed of polyethylene particles. (a) RH=0%, (b) RH=60%. Superficial air velocity: 0.27 m/s; bed depth: 0.20 m; fines proportion: 0.2 wt%.

The initial mass of fines injected into the bed before fluidization, and the overall masses of captured entrained fines, determined by weighing the filter before and after the period of fluidization, are presented in Table 3.4.

Table 3.4. Initial and overall captured masses for different fines and different gas relative humidities, with polyethylene particles as the major bed component.

Particles	***Initial Mass (g)***	***Overall Captured Mass (g)***		
		RH = 0%	***RH = 5%***	***RH = 60%***
Larostat 519	1.40	0.559	-	0.379
Catalyst	1.40	0.0466	0.121	0.774
Silica	1.40	0.830	-	0.620
S-GB I	1.40	0.300	-	0.725

The results show that the mass of entrained Larostat and silica particles decreased as a result of increasing the relative humidity of the fluidizing gas. This is due to the high tendency of these particles to readily adsorb water, and therefore as the relative humidity increases, they agglomerate. Therefore, their entrainment rates decrease. On the other hand, the entrainment rate of catalyst and S-GB I fines increased when the relative humidity increased. This could be because increasing the relative humidity helps the

dissipation of charges, and therefore fewer particles would cling to the column walls or to the bed material. Overall, the results show that between 3.3-60% of the fines injected into the fluidized bed were entrained from the fluidization column, thereby leaving the rest behind. As mentioned above, at the end of each run, thin layers of fines were observed sticking to the column walls. In addition, some fines might have settled in the pressure ports along the side of the inner walls of the column or been adhered to the bed particles.

To make the results for different added fines comparable, the charge-to-mass ratio, Q/m, was again determined. The results are presented in Table 3.5. The initial (see Section 2.4.3 and Table 2.5) and final (steady state) charge-to-mass ratio, Q/m, were determined, where the m values are the initial mass of fines injected and the final masses of captured entrained fines, as presented in Table 3.4.

Table 3.5. Initial and final charge/mass ratios, Q/m [μC/kg], for different fines and different gas relative humidities with polyethylene particles as the major bed component.

Particles	***Initial Q/m***	***Final Q/m***		
		RH = 0%	***RH = 5%***	***RH = 60%***
Larostat 519	-0.75	-131	-	21
Catalyst	-0.68	647	-65	-161
Silica	-1.20	-370	-	-176
S-GB I	-0.64	131	-	-29

Comparison of Q/m for catalyst, silica and S-GB I fines, all of which have similar average particle sizes, shows that, as was the case for the glass bead experiments in section 3.4.1, the S-GB I particles carried the least charges on a per unit mass basis. This could again be because the silver-coated glass beads are the most conductive, and thus they can more readily lose their charges to the column walls, while also helping to dissipate initial bed charges. In addition, the SEM images of these fines (see Figure 2.6) show that silver-coated glass beads are relatively smooth and spherical compared to catalyst and silica particles which are non-spherical and have extremely uneven surfaces.

Since the bed materials, polyethylene particles (see Figure 2.4), appear to have surface structures similar to the catalyst and silica fines, it is expected that there will be fewer contacts between the polyethylene particles and silver-coated glass beads than for either the catalyst or the silica particles.

The results show that Larostat 519 particles carried less Q/m compared to catalyst and silica particles. Even though they seem to have somewhat similar physical surface structures, catalyst and silica particles are more similar to polyethylene particles than to the Larostat. Therefore, there are likely to be more points of contact between the polyethylene particles and the silica and catalyst fines than for the Larostat particles.

The effect of the relative humidity of the fluidizing gas on charge generation or dissipation inside the fluidized bed can also be seen from the experimental results. The higher the relative humidity, the lower are the charge-to-mass ratios, as expected. For the relative humidity of 60%, the measured Q/m values are very similar for the catalyst and silica particles. This likely occurs because catalyst particles also contain silica, so that they would likely behave in a similar manner when exposed to humidity by being highly water adsorbent, affecting their charge generation/dissipation behaviour.

After completing the free bubbling fluidization of mono-sized particles, it was observed that a thick layer of polyethylene particles was attached to the inside of the column walls for the runs where the relative humidity was 0%. On the other hand, for the experiments at 60% relative humidity, there were very few particles adhering to the fluidization column. Observations after fluidizing the binary mixtures indicate that at 0% relative humidity, there were fewer particles clinging to the column walls when Larostat 519 and silver-coated glass beads were utilized. For the 60% humidity runs, there were almost no polyethylene particles on the column walls when Larostat 519 and S-GB I particles were present, whereas with the catalyst and silica particles, some polyethylene particles were attached to the fluidized bed walls. Overall, the observations show that increasing the relative humidity of the fluidizing gas and utilizing fines such as Larostat 519 and silver-

coated glass beads helped to dissipate (or reduce the generation of) electrostatic charges inside the fluidized bed.

The charge-to-surface area ratios could not be determined for catalyst and silica fines since their densities are unknown.

In order to study bi-polar charging in the polyethylene system, the original polyethylene particles that had not been sieved, and therefore which contained some finer particles, were fluidized with air having relative humidities of 0% and 60%. The particle size distribution of these particles is given in Table 2.2 and in Appendix B. Figure 3.14 presents charges measured due to entrainment of the fine polyethylene particles from the fluidization column.

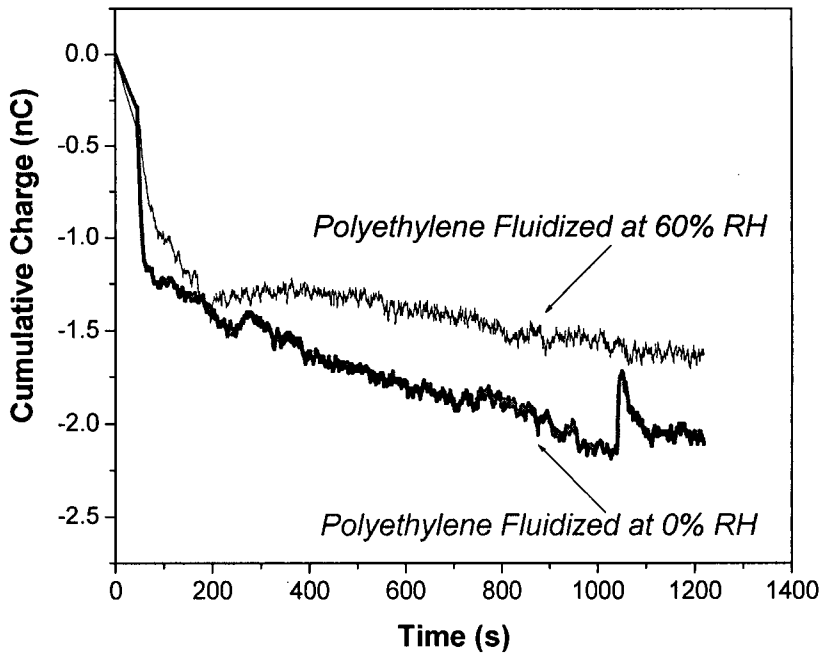

Figure 3.13. Original polyethylene particles fluidized at 0% and 60% relative humidity. Superficial air velocity: 0.27 m/s; bed depth: 0.20 m.

Since the density of polyethylene is relatively low and the amount of fines entrained from the column was small, the weight of the fines captured by the filter was too small to be

measured accurately. However, from Figure 3.13 it can be seen that the fine polyethylene particles are positively charged. Even though the net charge on the particles before the start of the fluidization was measured to be -3.0×10^{-8} C/kg, it is difficult to conclude that bi-polar charging occurred since the net charge and/or the large particle charges due to the fluidization are not known. However, if the net charge of particles at the beginning of the fluidization, where most of the fines were entrained, would have been similar, in polarity, to the measured initial net charges, then it can be concluded that bi-polar charging has occurred. In that case, these results would be opposite to those reported by Zhao et al, (2000). For the polymer particles in their study, larger particles were positively charged, whereas smaller particles were negatively charged. On the other hand, one of the powders studied by Ali et al, (1994), a polyamide powder, resulted in large particles being charged negatively while the small particles charged positively. The disagreement in results found by different researchers for different polymers indicates that bi-polar charging in polymer particles needs further investigation.

3.4.3. Summary

Fines added to an initially charged fluidized bed carry significant, but different amounts of charges out of the column depending on their sizes, physical and chemical structure of particle surfaces, and the moisture content of the fluidizing gas, therefore leaving a net charge behind. This is an important finding since fines are always elutriated in fluidized bed processes and considerable work has been undertaken by other researchers to develop entrainment models to calculate the flux of entrained particles. Wolny et al. (1989) observed that an increase of the relative humidity made fines elutriation from a fluidized bed easier, suggesting that the attraction between the fines and bed particles are mainly due to electrostatic forces. Briens et al. (1992) measured the flux of entrained fines from a bed of polyethylene particles and found that neutralizing the particle charges inside the bed increased elutriation losses, indicating that electrostatic charges affected the bed charges. The results obtained in the present work are consistent with these earlier findings by showing that entrained fines carry significant amount of charges out of the fluidization column. They also suggest that since electrostatic forces play a role in determining the

fines entrainment flux, they should be incorporated into models developed to predict entrainment flux and, possibly also, transport disengagement height.

The next step is to determine the mechanisms underlying these charges and to study their significance. In order to do so, it is essential to know the initial and final charges of the fine and coarse particles. In the experiments reported in this chapter, the initial charges of both fine and coarse particles and the final charges of fines carried out of the fluidized bed were known. However, due to measurement limitations of the Faraday cup fluidized bed system, the final charges of the large particles and the column wall could not be separately determined. Therefore, further investigation was required to help understand the charging mechanisms in the fluidized bed Faraday cup system. These further experiments are presented in the next chapter.

Chapter 4. Bench-Scale Laboratory Experiments

In order to determine and study the dominant charging mechanism in the Faraday cup fluidized bed system, it is essential to know the charges on the large particles and fines before and after fluidizing their mixtures, and also to determine the charges accumulated on the column wall. In the experiments described in Chapter 3, the initial charges of both fines and coarse particles and the final charges of fines carried out of the fluidized bed were measured. However, due to limitations of the Faraday cup fluidized bed system, the final charges on the large particles and the column wall could not be determined. Therefore, a series of bench-scale experiments was conducted to help understand the charging mechanisms and to explain some of findings from the fluidized bed Faraday cup system. The experiments included bench-scale shaking experiments and particle-copper plate contacting tests. This chapter covers the experimental apparatus, procedure and results obtained.

4.1. Bench-Scale Shaking Experiments

Small samples of large and fine particles used in previous experiments were shaken in a small copper flask and in a glass flask for different periods of times, and the changes in their charges were measured by a bench-scale Faraday cup system. A copper container was chosen since the previous experiments had been performed in a copper fluidization column. The glass flask was tested to compare the electrostatic behaviour of particles in it to that in the copper flask. A bench-scale Faraday cup system consisting of two cups, placed one above the other was developed in the present work, with similar principles as the vertical array of Faraday pail sensor described by Zhao et al. (2000). The double Faraday cup system is able to separate and measure charges of the particles of two different sizes making up the binary mixture.

Two sets of experiments were conducted:

a) The large glass beads were shaken for a period of time; different fines were then added, and the binary mixture was shaken for different periods of time before the charges were measured.
b) The large glass beads and the fines were shaken together from the beginning for different periods of time, and then the charges were measured.

Case (a) is very similar to the previous experiments in the fluidized bed system where the large particles were fluidized for a certain period of time in order to generate some charges, after which fines were added, the binary mixture was fluidized again, and the charges on the entrained fines were measured. Since in case (b), large and fine particles were shaken together from the beginning, it was thought likely that case (b) would be more representative of charge separation, whereas case (a) would help to identify charge transfer. It was hoped that comparison of previous and new results would help to elucidate the charging mechanisms in the fluidized bed system.

4.1.1. Experimental apparatus

The experiments were performed in the double Faraday cup system shown in Figure 4.1. This system consisted of two Faraday cups, one above the other.

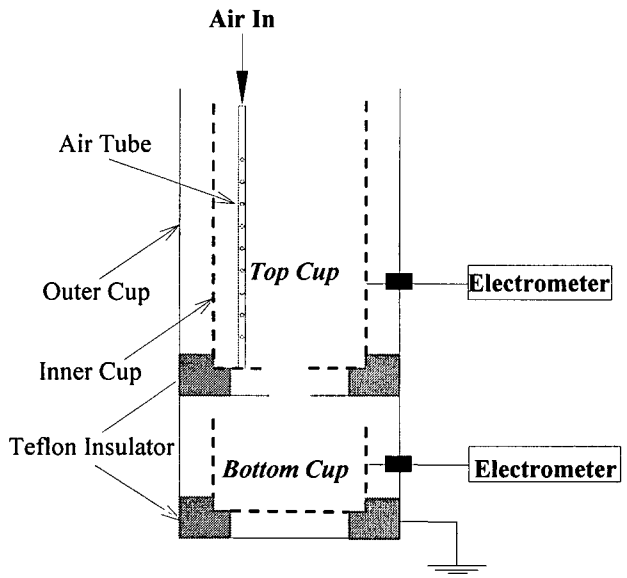

Figure 4.1. Schematic of double Faraday cup system.

The bottom cup was a normal Faraday cup, whereas the top cup had openings on the bottoms of both the inner and outer cups centered on the axis. All cups were made of 0.003 m thick copper sheet. The inner bottom cup was 0.127 m tall, whereas the outer bottom cup was 0.152 m high. The inner top cup was 0.279 m tall, whereas the outer top cup was 0.305 m high. The diameters of the inner and outer cups were 0.152 m and 0.203 m, respectively. The diameters of both holes on the bottoms of the top cup were 0.0508 m. The inner and outer cups were insulated from each other by Teflon pieces. Both cups were individually connected to Keithley Model 6514 digital electrometers. The outer cups were both grounded. A 0.00635 m stainless steel tube having an array of 0.003175 m holes on one side (see Figure 4.1) was used to blow air into the top cup to help separate fines from the binary mixture so that they would settle in the top cup. Appendix A provides photographs of the double Faraday cup system. The same large particles (glass beads) and fine particles (Larostat 519, GB I and S-GB I) that had been used in the fluidized bed Faraday cup experiments were employed in the bench-scale shaking experiments.

4.1.2. Experimental procedure

Two small 100 ml flasks, one made of copper and the other of glass, were used to shake the particles. In each run, 60 g of large glass beads and 0.12 g (0.2 wt%) of fines were utilized. Before each sample was shaken, charges on the walls of the empty flasks were measured by hanging them from a rubber thread inside a normal Faraday cup. The initial charges of the 60 g samples of large glass beads were also measured by the Faraday cup. A Burrell Wrisk-Action Model 75 shaker with a shaking radius of 0.133±0.004 m and an arc travel of 10 degrees at a frequency of 300±30 oscillations per minute, agitated both flasks simultaneously for different periods of time.

In case (a), large glass beads were first shaken for 10 minutes. Fines were then added, and shaking was resumed for different periods of time. In order to determine changes in the charges on the large glass beads after adding fines, it was necessary to know the charges acquired by the large glass beads after 10 minutes of shaking. However, this measurement could only be conducted by pouring these particles into a Faraday cup. This

could have resulted in charge dissipation. Consequently, the average charge of three samples of large glass beads shaken for ten minutes separately was measured and assumed as the initial charge on the glass beads before adding the fines. In case (b), a binary mixture of large glass beads and fines was shaken from the beginning for different periods of time. After each run, the binary mixtures of particles from each flask were poured into the double Faraday cup as shown in Figure 4.2. Great caution was exercised so that the large glass beads traveled straight down through the holes in the bottoms of the inner and outer top cups into the inner bottom cup. The fines settled in the top cup with the help of the air blown from the air tube. The charges on the particles as they settled in the top and bottom cups were measured by the two electrometers. The empty flasks were then inserted into a Faraday cup to measure the charges accumulated on their walls. All experiments were conducted at room temperature and relative humidity.

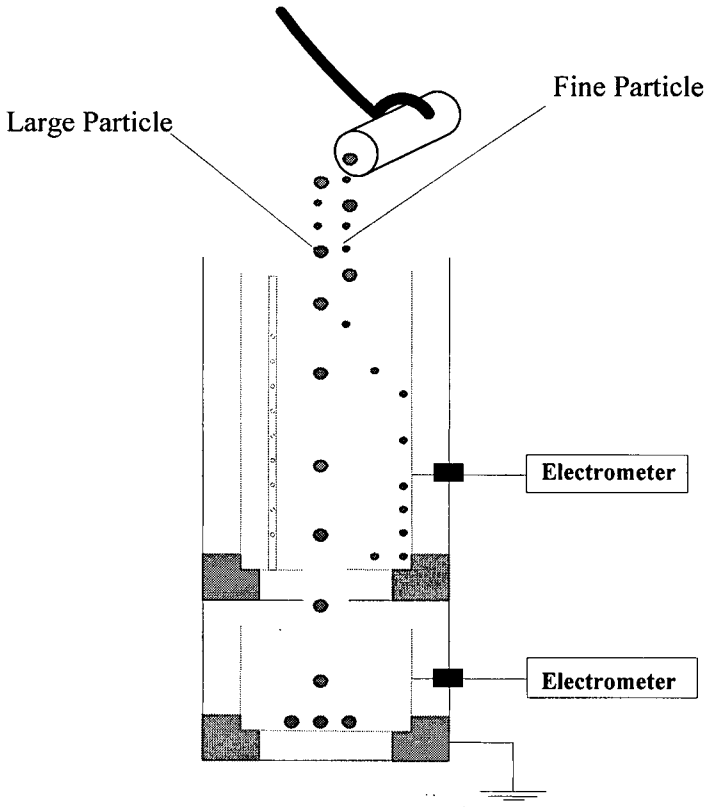

Figure 4.2. Illustration of pouring of binary mixtures of particles into the Faraday cup system and separation of the two species by the air flow.

4.1.3. Results and discussion

In case (a), the average charges gained by large glass beads after being shaken for 10 minutes were first determined. The results are presented in Table 4.1. Since the particles were narrowly-sized, the only plausible charging mechanism should be charge separation between the particles and the wall. The results show that for both flasks, glass beads were charged negatively while the walls were charged positively. The total charge acquired by the particles was almost an order of magnitude larger when the wall was made of glass rather than copper. This is likely due to the fact that copper is highly conductive so that charges can be dissipated much more quickly. This was also apparent from the average charges on the flasks walls. Negligible charges were measured on the walls of the copper flask.

Table 4.1. Charge measurements after 10 minutes of shaking, large glass beads alone.

	Glass Beads Charge (μC)				**Wall Charge (μC)**			
	Run #1	**Run #2**	**Run #3**	**Average**	**Run #1**	**Run #2**	**Run #3**	**Average**
Glass Flask	-0.01550	-0.01452	-0.01290	**-0.01431**	0.01680	0.02620	0.02220	**0.02173**
Copper Flask	-0.00114	-0.00152	-0.00224	**-0.00163**	0.00002	-0.00002	0.00000	**0.00000**

In order to examine the rate of charge dissipation of the copper and glass flasks, a simple experiment was performed. The walls of empty flasks were charged by rubbing with a piece of rubber. The charges on both walls were then measured by a Faraday cup over time. The results are shown in Figure 4.3.

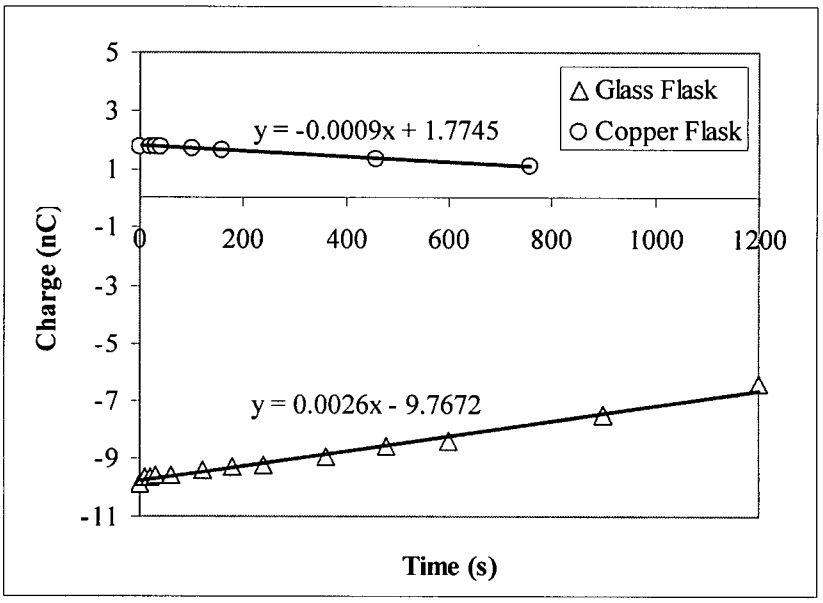

Figure 4.3. Dissipation rate of charges on the walls of glass and copper flasks.

As can be seen, the charge dissipation rate for both flasks was very similar. However, at the end of each experiment, both flasks were touched momentarily with the rubber clamp used throughout the present work to hold the flasks, and then the charges were measured again. It was observed that all the charges on the copper flask were dissipated, whereas the charge did not change for the glass flask. This demonstrates that since copper is highly conductive, it can easily lose its charges through any point of contact. Charges on the copper flask might even have been dissipated while the flasks were shaken by the shaker machine through the metal clamps with rubber covered tips holding the flasks.

Due to the conservation of charge, when the charge separation between particles and wall is the only charging source, then the net charge between the two surfaces should be zero. This is almost true in the case of the glass flask, but not for the copper flask, again probably due to rapid dissipation of charges from the copper surface.

The electrostatic charges of large glass beads and fines for two series of shaking experiments are shown in Figures 4.4 to 4.9. The dates of the experiments and their corresponding ambient relative humidities, determined based daily weather record, are presented for each run.

Overall, the results show that in both flasks and for the two different shaking procedures, different added fines became positively charged whereas large glass beads gained negative charges. It is again apparent from the results that the net charges were almost zero for the glass flask, but not for the copper flask. As above, this was likely due to quick charge dissipation by copper.

In the runs with Larostat 519, shaking was terminated after only one minute at most since further shaking would have resulted in particle agglomeration. This was because Larostat 519 readily adsorbs the moisture and thus results in particles agglomeration. The effects of addition of Larostat 519 are shown Figures 4.4 & 4.5. It can be seen that the charges measured on large glass beads for case (a) decreased to almost zero as the Larostat was added and the mixture was shaken for only 10 seconds. On the other hand, in case (b), the charges on the large glass beads remained close to zero for all shaking periods tested. These results indicate that for both glass and copper flasks, Larostat 519 reduced (case a) and prevented (case b) the charge generation on the large particles.

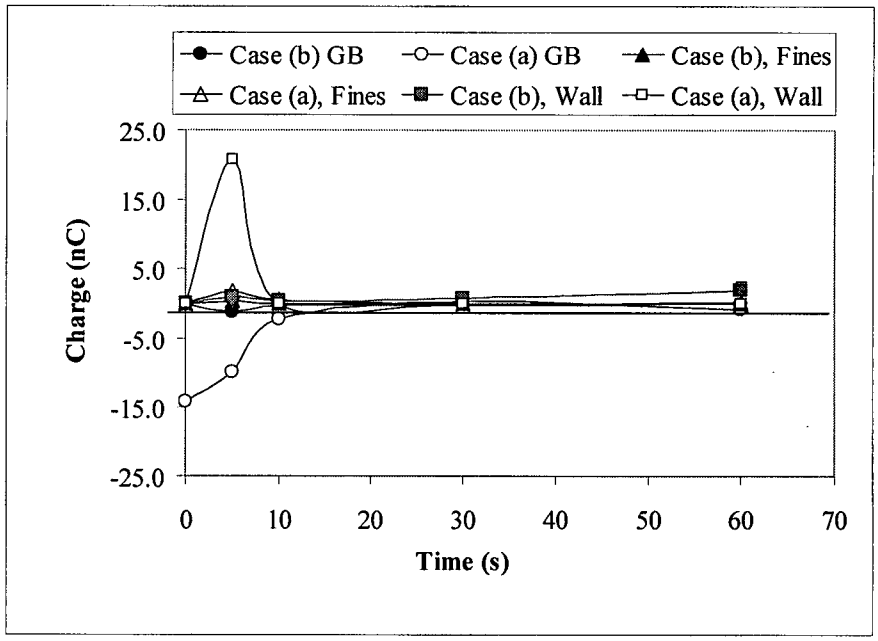

Figure 4.4. Effect of addition of Larostat 519 for cases (a) & (b) in glass flask. (Case (a): 09/09/05, Ambient RH ≈ 35%; Case (b): 09/03/04, Ambient RH ≈ 40%)

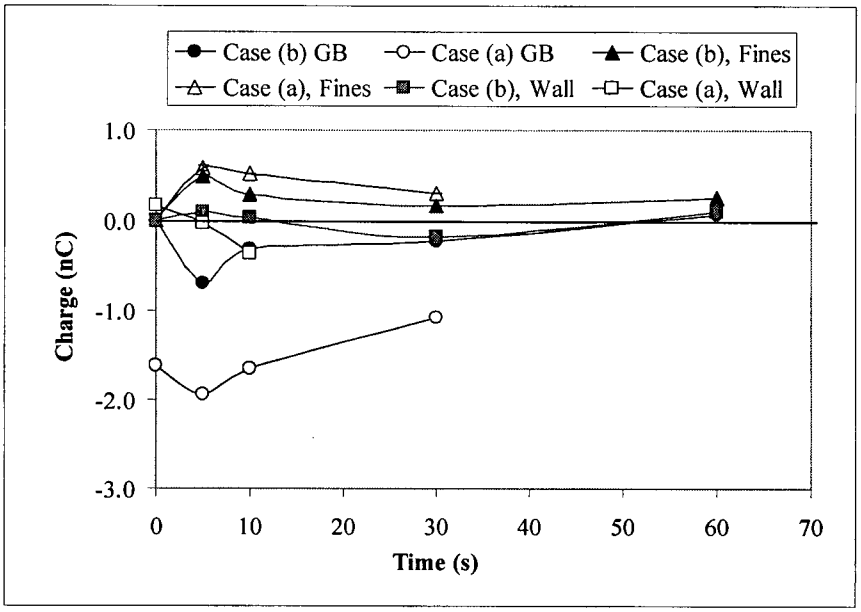

Figure 4.5. Effect of addition of Larostat 519 for cases (a) & (b) in copper flask. (Case (a): 09/09/05, Ambient RH ≈ 35%; Case (b): 09/03/04, Ambient RH ≈ 40%)

The effects of adding fine glass beads and silver-coated glass beads are presented in Figures 4.6-4.9. For both flasks, the charges on the large glass beads increased in both cases (a & b). Therefore, not only did these fines not result in charge reduction in case (a) or prevent charge generation in case (b), but they promoted further charge generation in both cases.

Overall, it can be seen that only Larostat 519 inhibited the charge separation while assisting the charge dissipation on large glass beads. Wolny et al. (1983) concluded that fines (independent of their nature) decrease the number of contacts between large particles and the wall, thereby reducing the charge generation. However, the present results contradict those findings.

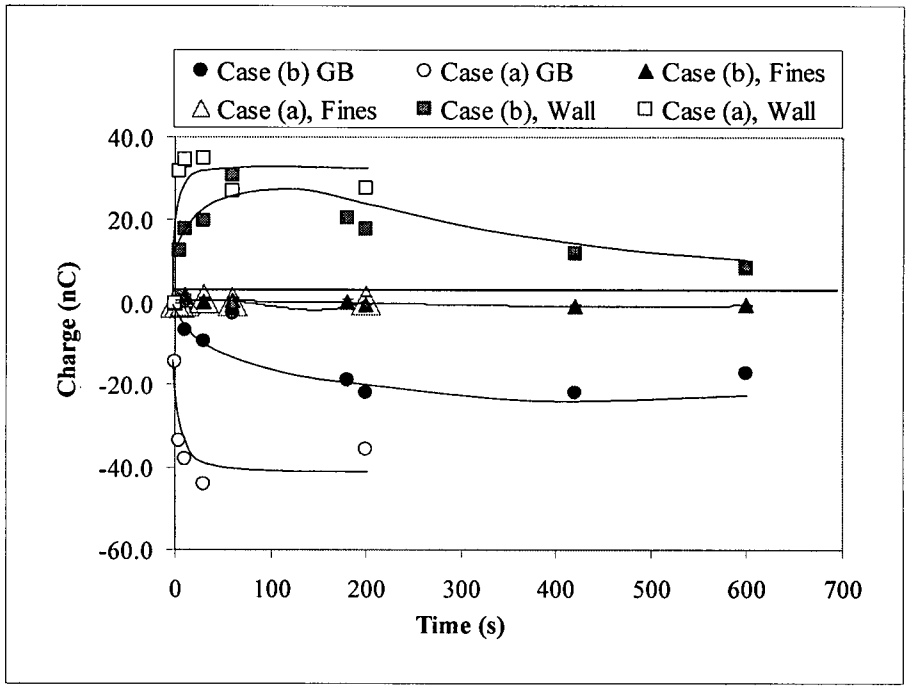

Figure 4.6. Effect of addition of glass bead fines for cases (a) & (b) in glass flask. (Case (a): 09/09/05, Ambient RH ≈ 35%; Case (b): 09/06/04, Ambient RH ≈ 55%)

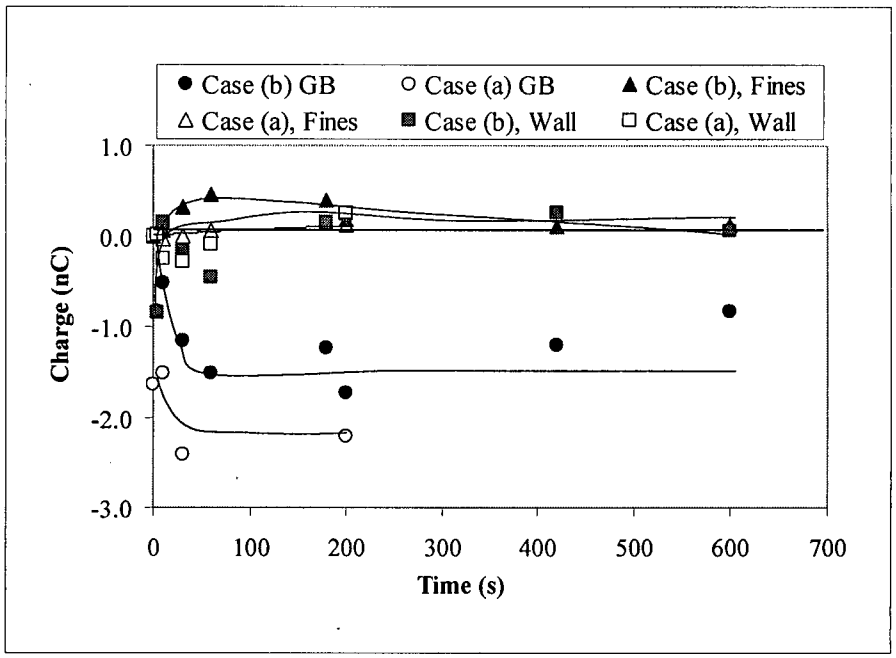

Figure 4.7. Effect of addition of glass bead fines for cases (a) & (b) in copper flask. (Case (a): 09/09/05, Ambient RH ≈ 35%; Case (b): 09/06/04, Ambient RH ≈ 55%)

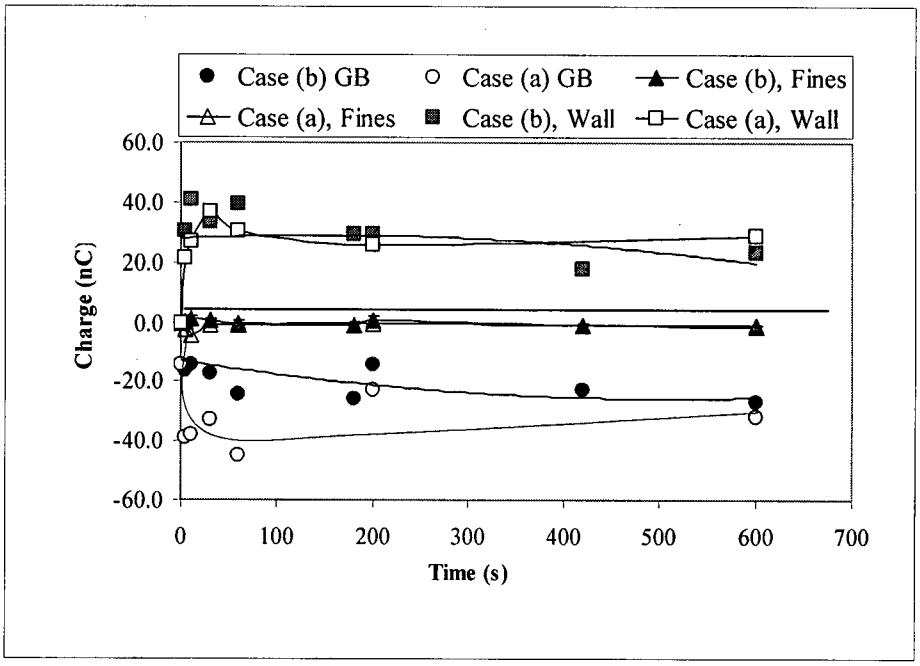

Figure 4.8. Effect of addition of silver-coated glass bead fines for cases (a) & (b) in glass flask. (Case (a): 09/09/05, Ambient RH ≈ 35%; Case (b): 09/07/04, Ambient RH ≈ 45%)

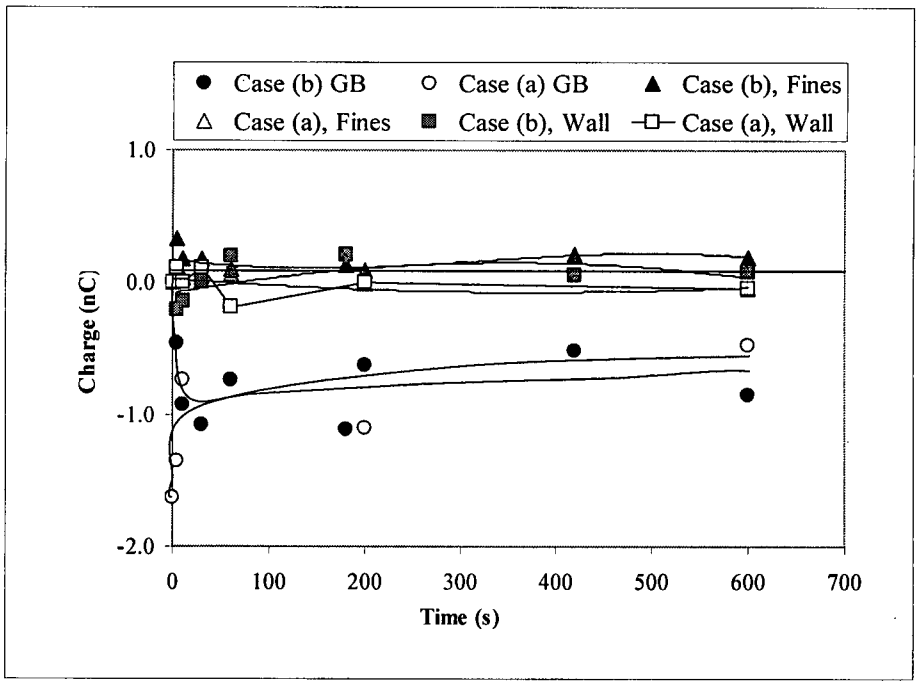

Figure 4.9. Effect of addition of silver-coated glass bead fines for cases (a) & (b) in copper flask. (Case (a): 09/09/04, Ambient RH ≈ 35%; Case (b): 09/07/04, Ambient RH ≈ 45%)

The charges carried by fines (Larostat 519, GB I and S-GB I), alone for cases (a) and (b) and when particles were shaken in copper flask, are presented in Figures 4.10 and 4.11. Since case (a) is very similar to the previous experiments performed in the fluidized bed Faraday cup system, the results obtained for this case can at least verify the polarity of charges obtained in the fluidized bed experiments. As shown in Figure 4.11, in all three cases, the fines carried positive charges after being mixed with large glass beads and shaken for different periods of times. This is consistent with the results in the fluidization system where the entrained fines carried positive charges out of the fluidization column in all cases.

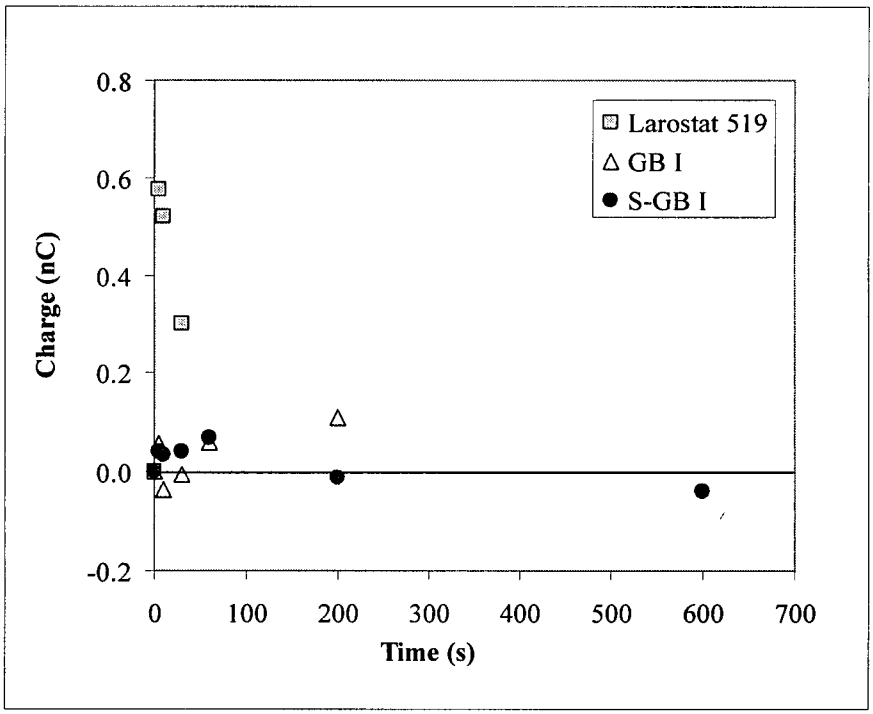

Figure 4.10. Charges carried by different fines for case (a) in copper flask.

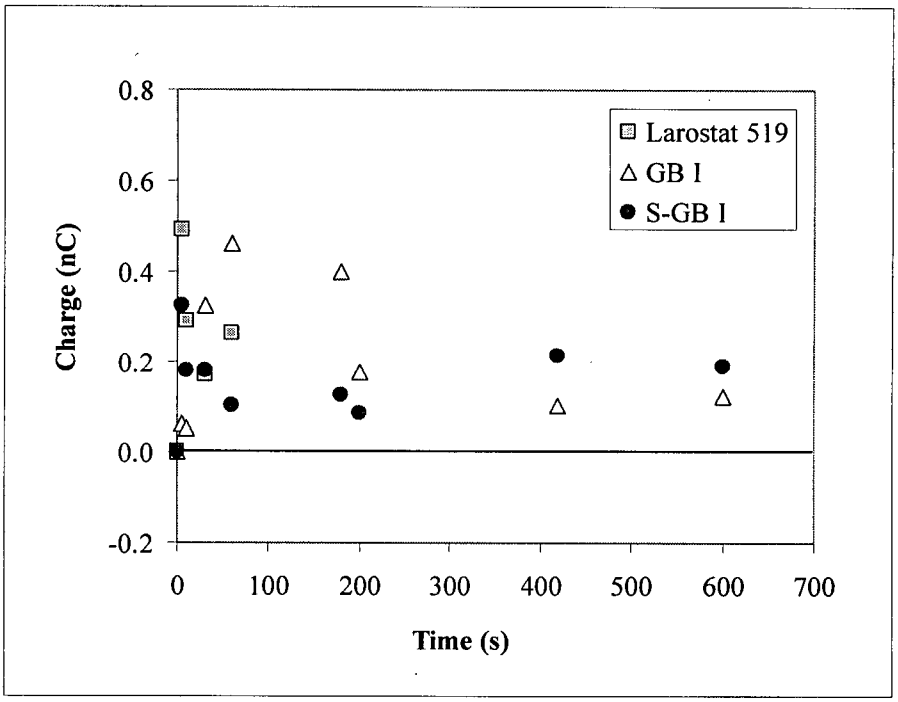

Figure 4.11. Charges carried by different fines for case (b) in copper flask.

In this work, the measured charges are all presented as absolute charges. However, since the particle sizes and densities differ, it would be more useful to present the results as charge per mass ratio, Q/m. However, it was very difficult to weigh the fines captured in the top cup, one reason being that the amount of fines in each run was very small (0.12 g), and another that a few large glass beads always ended up in the top cup, affecting the measured weight of the fines.

In order to get an idea of the differences between presenting the results as absolute charges or charge-to-mass ratios, it was assumed that all fines and large particles were separated from each other and settled on the top and bottom cups, respectively. The Q/m ratios were then calculated for both fine and coarse particles, where m values were initial masses of particles utilized. Results are presented in Figures 4.12-4.15 and Figures 4.16-19, respectively. Overall the results show that the fines were charged oppositely, with Q/m almost 10-100 times more than for the large glass beads. Figures 4.12-4.15 illustrate that the charges on the large glass beads decreased to almost zero when Larostat 519 was utilized in both cases. S-GB I particles helped to decrease the charges on the large glass beads in the copper flask only for case (a), whereas in all other cases they helped further

charge generation. Overall, GB I fines assisted charge generation rather than preventing it.

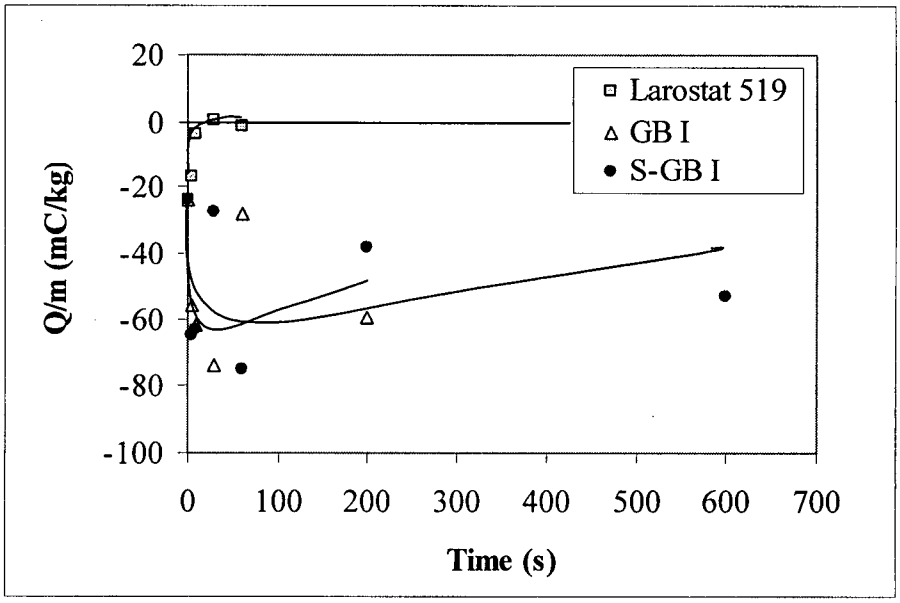

Figure 4.12. Effect of addition of different fines on large glass beads for case (a) in glass flask.

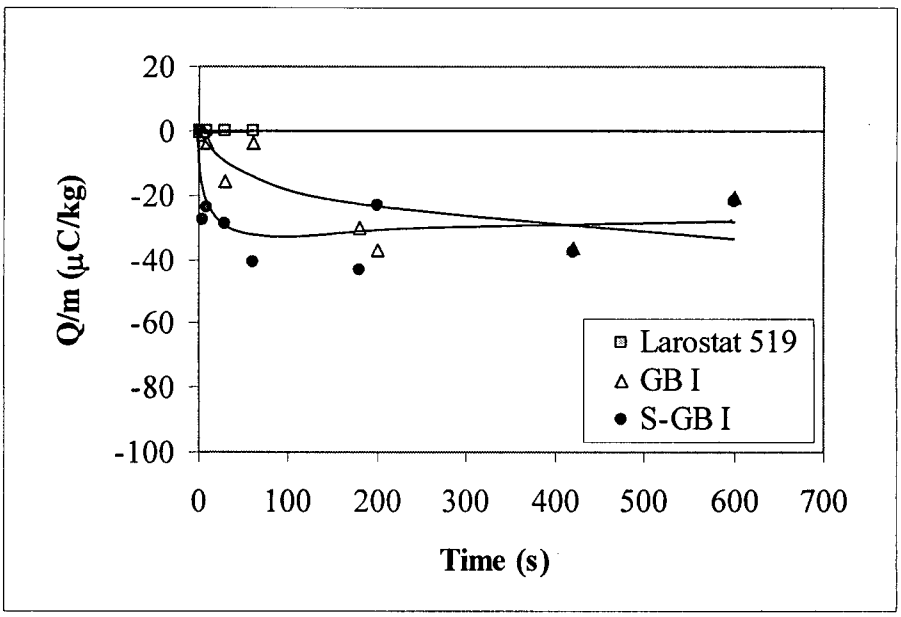

Figure 4.13. Effect of addition of different fines on large glass beads for case (b) in glass flask.

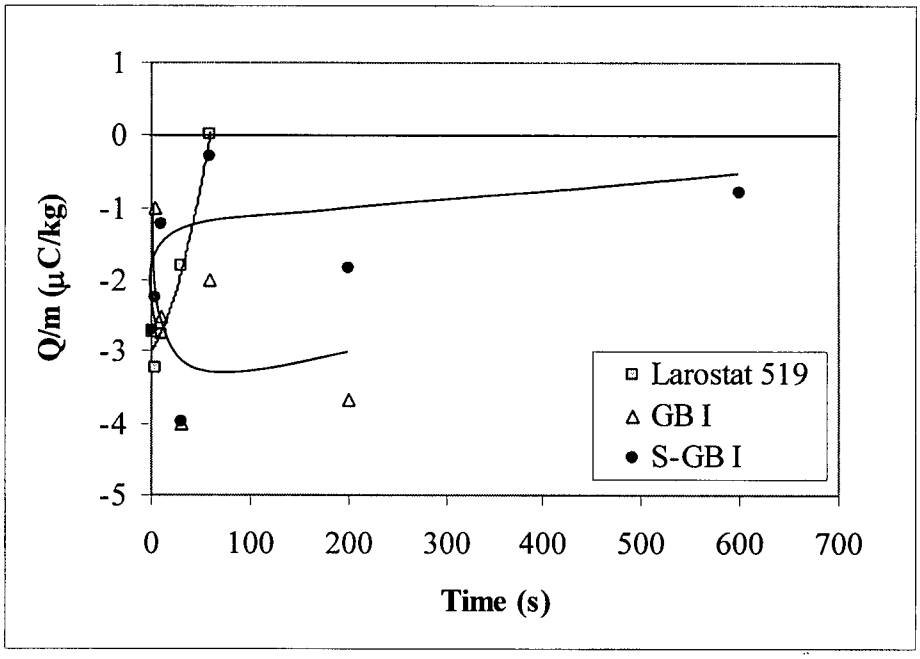

Figure 4.14. Effect of addition of different fines on large glass beads for case (a) in copper flask.

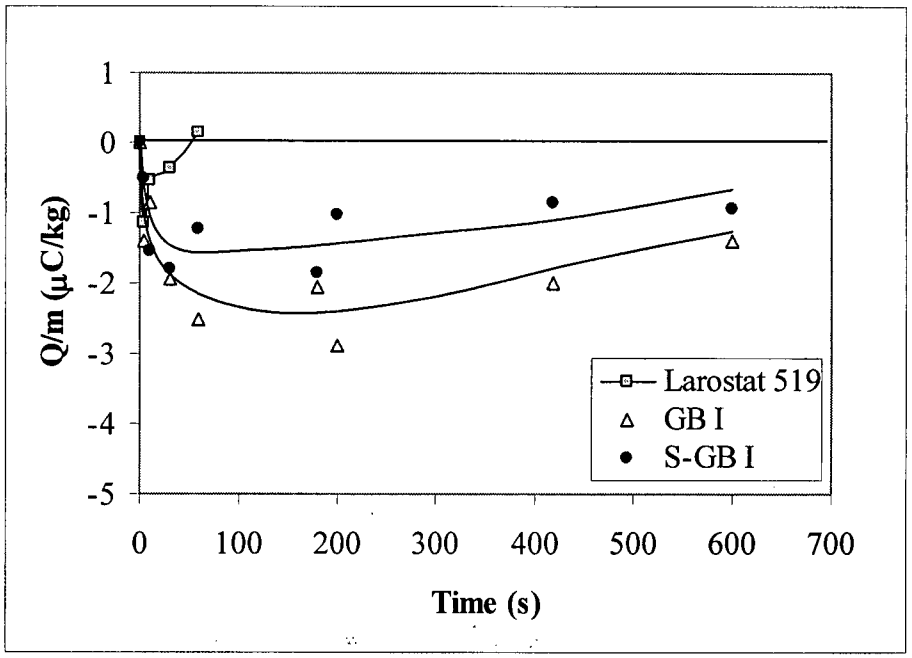

Figure 4.15. Effect of addition of different fines on large glass beads for case (b) in copper flask.

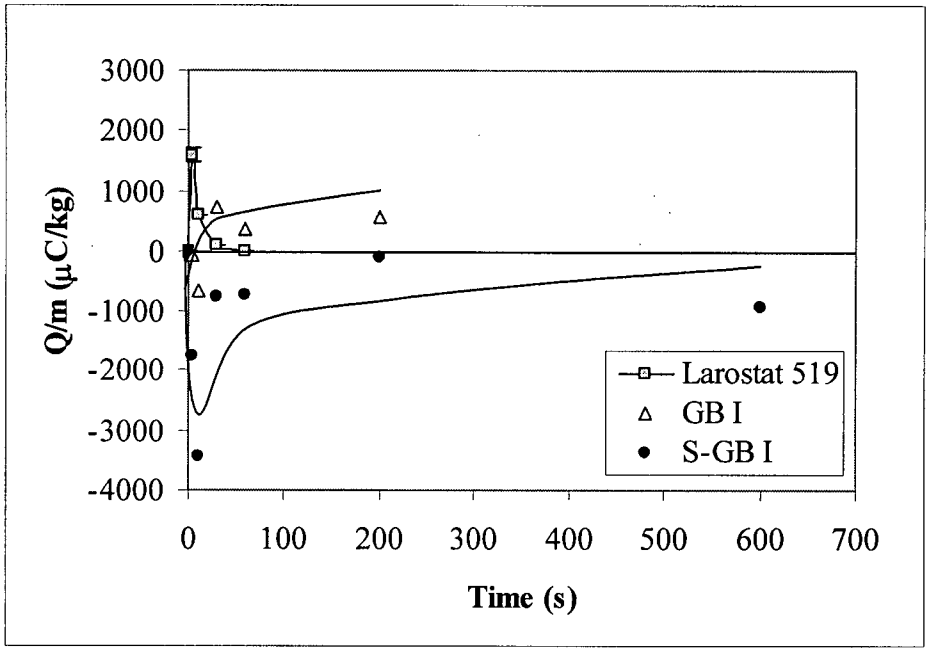

Figure 4.16. Charges carried by different fines for case (a) in glass flask.

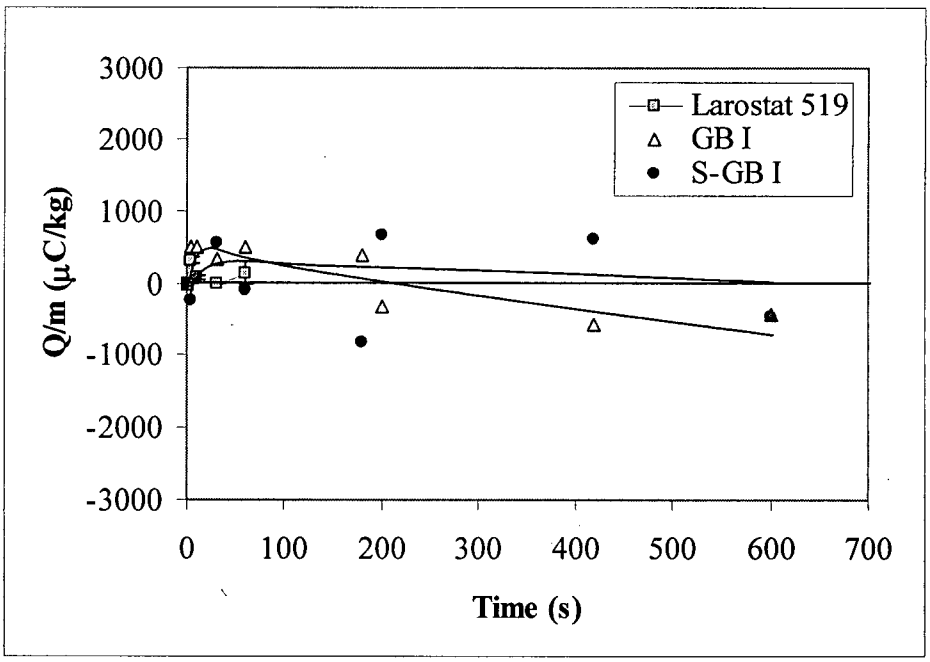

Figure 4.17. Charges carried by different fines for case (b) in glass flask.

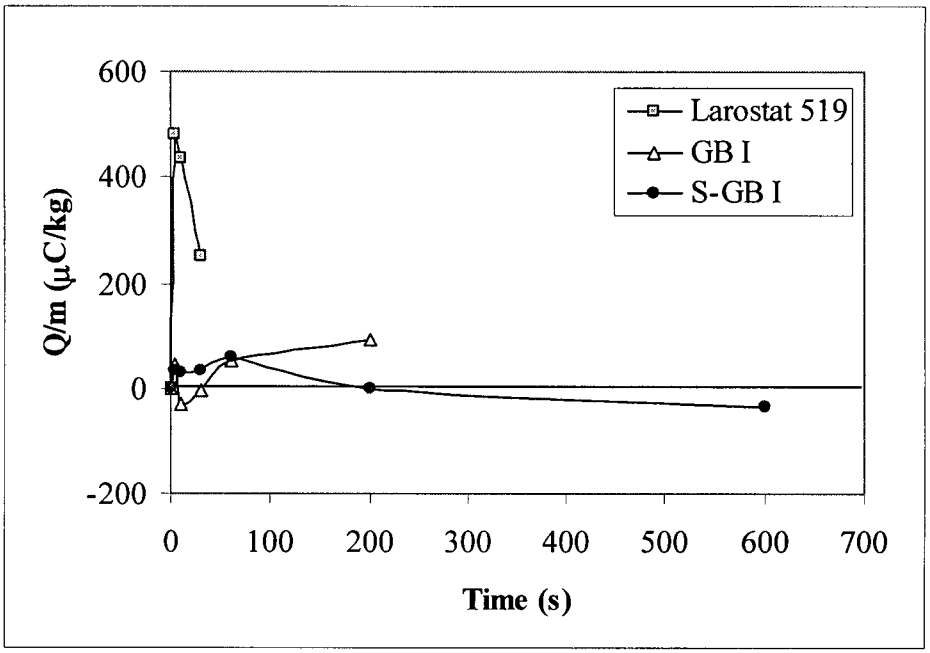

Figure 4.18. Charges carried by different fines for case (a) in copper flask.

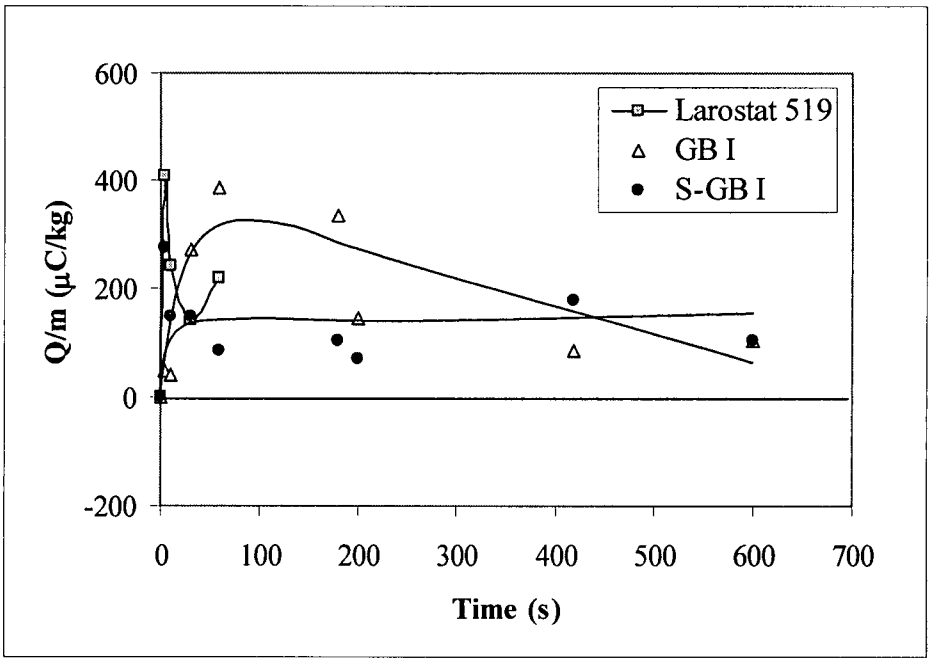

Figure 4.19. Charges carried by different fines for case (b) in copper flask.

One of the challenges involved in performing the experiments was pouring the particles into the Faraday cup system. It was important that no large particles settle in the top cup where they would affect the charges measured on the fines. Therefore, each run was

repeated three times and each data point presented in the above graphs is the average of three values. However, there were still large variations/scatter in the results, as shown by the error bars (see Appendix D). The average results suggest that the fines were charged positively, but by looking at the range of measured data presented by the error bars, it can be seen that the charges fluctuated between positive and negative. Therefore, it is very difficult to reach a definitive conclusion based on these measurements.

There were also significant variations in the charges measured for the same conditions, probably due in part to the humidity. All experiments were performed in the ambient environment where the humidity varied from day to day.

4.1.4. Summary

Bench-scale shaking experiments were performed to help understand the charging mechanisms in the experiments conducted in the Faraday cup fluidized bed system and to confirm some of the results. Although there were a number of uncertainties associated with the test results, the results confirmed that fines used in previous fluidization experiments gained positive charges as they came into contact with relatively large glass beads. Further, large glass beads became negatively charged as they came into contact with the copper walls, confirming that fluidization of mono-sized large glass beads results in particles being charged more negatively. Larostat 519 (of the three types of fines tested) acts as an antistatic agent by helping the charge dissipation and preventing further charge generation. It appears that the charges carried by fines are due to charge separation and not to charge transfer, since their polarity is opposite to that of the charges carried by the large glass beads. However, since the Q/m ratios could not be accurately determined, it was not possible to find whether fines-wall or fines-large particles charge separation is the dominant mechanism.

It is also very important to bear in mind that particle-wall contacting, or particle motion and mixing in the Faraday cup fluidization equipment, could differ significantly from the bench-scale shaking experiments. In particular, particle-wall contacts are likely to have been much stronger in the small flasks than in the fluidization column. Since electrostatic

charge generation is such a complex phenomenon, dependent on many different factors, caution is needed when applying the bench-scale experiments to the Faraday cup fluidized bed system.

4.2. Particle-Copper Plate Contacting Test

Bench-scale copper plate contacting tests were conducted to elucidate the charging mechanisms between the particles and column walls in the fluidized bed Faraday cup system.

Small samples of the same particles (fine and coarse) as were studied in the fluidized bed Faraday cup system were brought into contact with a copper plate and then collected in a bench scale Faraday cup. The Faraday cup is able to measure the charges acquired by the particles due to their contact with the copper plate. The initial and final charges of the copper plate are also measured by the Faraday cup. When the particles come into contact with the plate, if charge transfer occurs, then the particles should gain the same charge polarity as the plate. However, if charge separation is dominant, then it is anticipated that the particles should become negatively charged, whereas the copper plate should become positively charged. In order to determine whether charge transfer or charge separation occurs between the particles and the copper plate, the initial charge on the plate was varied from zero to positive. The likely charging mechanisms for different initial charges on the plate are portrayed in Figure 4.20.

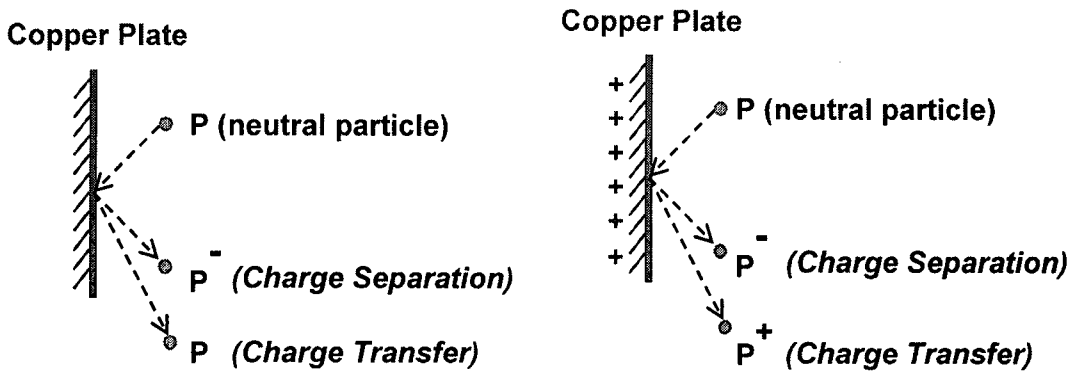

(a) (b)

Figure 4.20. Possible charging mechanisms between particles and a copper plate; a) Plate has zero initial charge; b) Plate has positive initial charge.

Figure 4.20a represents the case where an uncharged particle comes into contact with a copper plate with zero initial charges. Charge separation may occur, resulting in the particle becoming negatively charged. Alternatively, there may be charge transfer. In the latter case, since the plate carries no charge, the particle would leave the plate neutral.

Figure 4.20b shows a particle coming into contact with a positively charged copper plate. As in case (a), charge separation or charge transfer may occur. However, since the plate is positively charged, if there is charge transfer, then the plate would transfer some of its positive charge to the particle and therefore, the particle would acquire a positive charge. In both cases, if charge separation takes place, the plate will gain positive or negative charges, whereas if charge transfer occurs, the plate would stay neutral in case (a) or become less positively charged in case (b).

4.2.1. Experimental apparatus

The experimental setup assembled for this study is shown in Figure 4.21. The system included a Faraday cup and a copper plate. The Faraday cup was the bottom cup of the double Faraday cup system used in shaking bench-scale experiments (see Section 4.1.1 for details). The Faraday cup was connected to a Keithley Model 6514 digital electrometer. The copper plate was 0.051 m by 0.280 m, and 0.003 m thick. In order to measure the charges on the particles after their contact with the plate, the plate was mounted above the Faraday cup so that particles fell into the cup after contacting the plate (as illustrated in Figure 4.21).

The copper plate was held above the Faraday cup by a clamp and a stand at an angle of approximately 30 degrees to the vertical. Two small Teflon discs separated the copper plate from the clamp, at their point of contact, to eliminate any electrical discharges of the plate through the clamp.

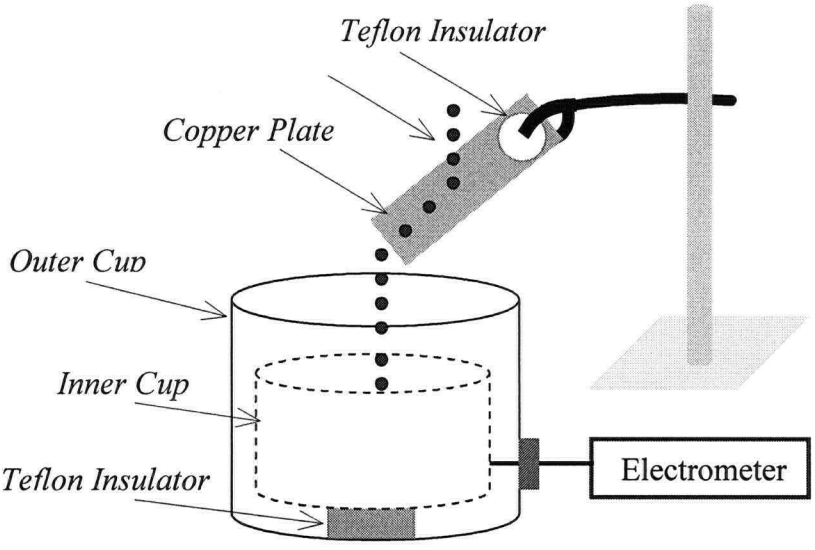

Figure 4.21. Schematic diagram of copper plate contacting apparatus.

The same large (large glass beads, polyethylene) and fine particles (Larostat 519, GB I, S-GB I, catalyst and silica) as had already been used in the fluidized bed Faraday cup experiments were employed in the particle-plate contacting experiments.

4.2.2. Experimental procedure

In each experiment, the initial charge of the copper plate was first measured by lowering it into the Faraday cup, after which the plate was mounted above the cup. Then, the charge measurement by the Faraday cup was started and after 60 s, Larostat 519, GB I, S-GB I and catalyst were poured over the plate at a rate of about 0.11 g/s and silica, polyethylene and large glass beads were poured at a rate of about 0.20 g/s. As the particles fell from the plate into the Faraday cup, their charges were measured, and this measurement was continued for nearly 2 minutes after all of the particles had settled in the cup. After completion of these charge measurements, the final charge on the plate was measured by again lowering the plate into the Faraday cup. In each run, 6 grams of particles were utilized, and the rate at which they were poured over the plate was maintained the same by ensuring that the time taken to pour the particles over the plate was constant. In order to measure the initial charges on the particles, 6 g samples of each type of particles were poured into the Faraday cup without the copper plate while their

charges were measured. All measurements were repeated three times to check the reproducibility. The resulting measurement data and errors associated with them are plotted in Appendix D.

The initial charge of the copper plate was varied from zero to approximately +2 nC and +5 nC for different runs. In order to charge the plate positively, the plate was rubbed with a piece of Teflon, and the plate charge was measured repeatedly by the Faraday cup until the desired values were obtained.

4.2.3. Results and discussion

Five types of fine particles (glass beads, silver-coated glass beads, Larostat 519, catalyst and silica), and large glass beads and polyethylene particles were brought into contact with a copper plate having approximately zero, +2 nC and +5 nC initial charges. The properties of the particles are provided in Chapter 2.

Since copper is highly conductive, it can easily lose its charge to any contacting devices such as the clamp which holds the plate. Therefore, in order to perform accurate measurements of charge transfer or charge separation between the plate and the particles, it is very important to fully electrically insulate the copper plate. To ensure proper insulation, the dissipation rate of charges on the copper plate was examined by a simple experiment. The copper plate was charged by rubbing with a piece of Teflon. The charges on the plate were then measured by inserting the plate into a Faraday cup twice every minute. The results shown in Figure 4.22 indicate negligible charge dissipation of the plate, confirming that the copper plate is very well insulated.

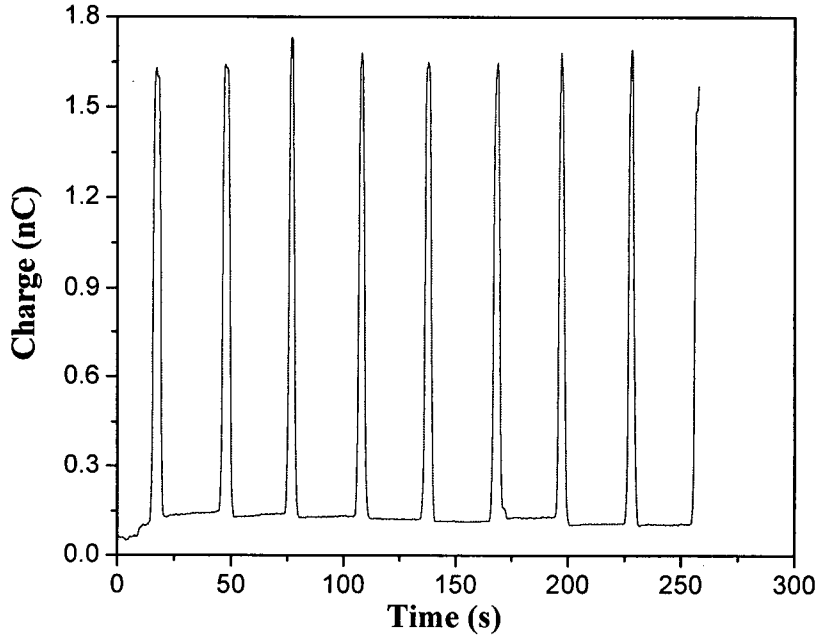

Figure 4.22. Charges measured when charged copper plate was repeatedly dipped into Faraday cup to test for charge dissipation.

The initial (Q_o) and final (Q_f) charges on the plate and the particles were measured by a Faraday cup. The results are summarized in Table 4.2. Overall, the results show that the plate transferred almost all of its charges to each of the four species of fine particles during their contact. However, charge transfer was negligible with the large glass beads and polyethylene particles.

Table 4.2. Initial and final charges, Q (nC), of particles and plate when 6 g of particles were poured over the copper plate.

Particles	$Q_{o,particles}$	$Q_{o,plate}$	$Q_{f,plate}$	$Q_{f,particles}$
Larostat 519	-0.16	0.026	-0.074	1.7
	-0.16	2.0	-0.090	4.3
	-0.16	5.3	-0.037	7.8
Glass Beads (GB I)	-6.6	0.21	0.30	-4.9
	-6.6	2.5	0.48	-0.56
	-6.6	5.3	0.24	6.7
Silver-Coated Glass Beads (S-GB II)	0.64	0.01	0.050	-3.5
	0.64	2.4	0.050	0.53
	0.64	5.3	0.011	5.0
Catalyst	1.45	-0.24	0.16	-0.59
	1.45	1.9	0.37	2.4
	1.45	5.3	0.25	9.2
Silica	0.57	-0.006	1.2	-4.8
	0.57	2.1	1.6	-2.0
	0.57	5.7	1.7	4.0
Large Glass Beads	0.12	-0.031	0.4	-1.5
	0.12	2.00	2.2	-4.2
	0.12	5.40	4.8	-7.8
Polyethylene	-1.17	-0.084	0.34	-1.9
	-1.17	2.2	2.5	-2.7
	-1.17	4.8	4.8	-2.3

The charges carried by the Larostat 519 particles with and without contacting the copper plate are shown in Figure 4.23. The Larostat particles are seem to have been initially slightly negatively charged. However, they carried positive charges after contact with a neutral or a positively charged copper plate. This shows that either charge transfer and/or charge separation occurs between the particles and the plate. As the particles come into

contact with a neutral plate, there were no charges to be transferred. Therefore, the positive charges gained by these particles must be caused by charge separation.

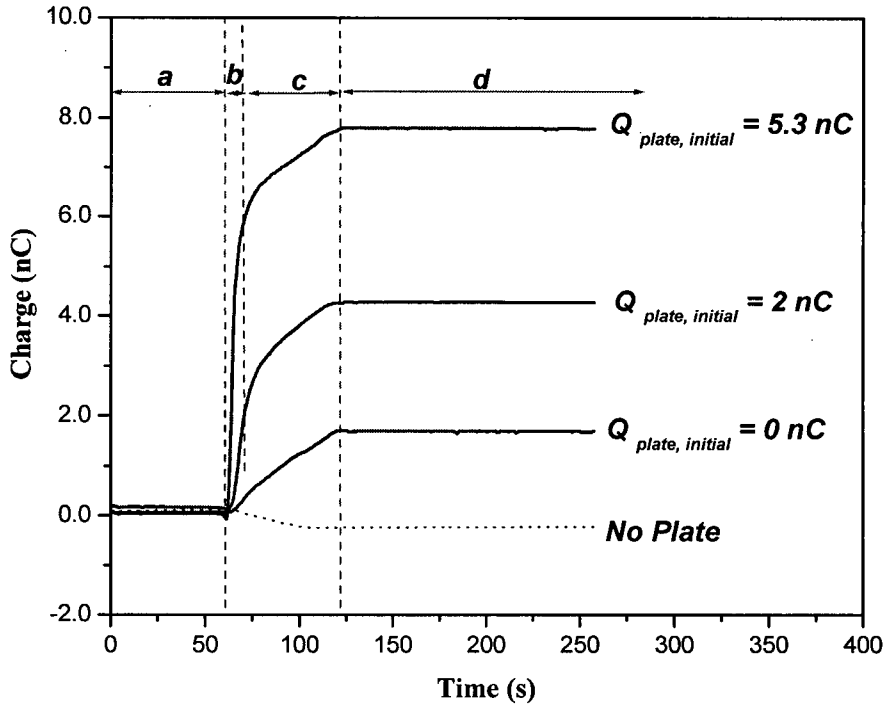

Figure 4.23. Charges carried by Larostat 519 particles due to contact with copper plate of different initial charges. (10/21/04, Ambient RH ≈ 60%)

The similarity of the charge curves in Figure 4.23, indicate that the charge plot can be divided into four intervals *a* to *d*. Interval *a* shows the charges before the particles were poured over the plate. Intervals *b* and *c* correspond to the period when the particles were contacting the plate and entering the cup. Section *d* shows the charges after all particles had been poured and had settled in the cup. In the cases where the plate was initially charged, either at +2 nC or at +5 nC, an initial sharp increase of charges is observed in interval *b*, followed by a more gradual increase in interval *c*. The total charges measured during interval *b* are almost equivalent to the initial charge of the copper plate, suggesting that charge transfer has occurred. On the other hand, the slope in interval *c*, with the plate initially charged, is very similar to that for the neutral plate. Therefore, it appears that charge separation occurred following the earlier charge transfer.

Figure 4.24 presents the measured charges for the fine glass beads. The results for the case where there was no plate indicate that the fine glass beads were initially negatively charged. Comparison of the charges measured on the fine glass beads as they came into contact with a neutral or initially charged plate clearly indicates that there was charge transfer between the particles and the plate when the plate was initially charged.

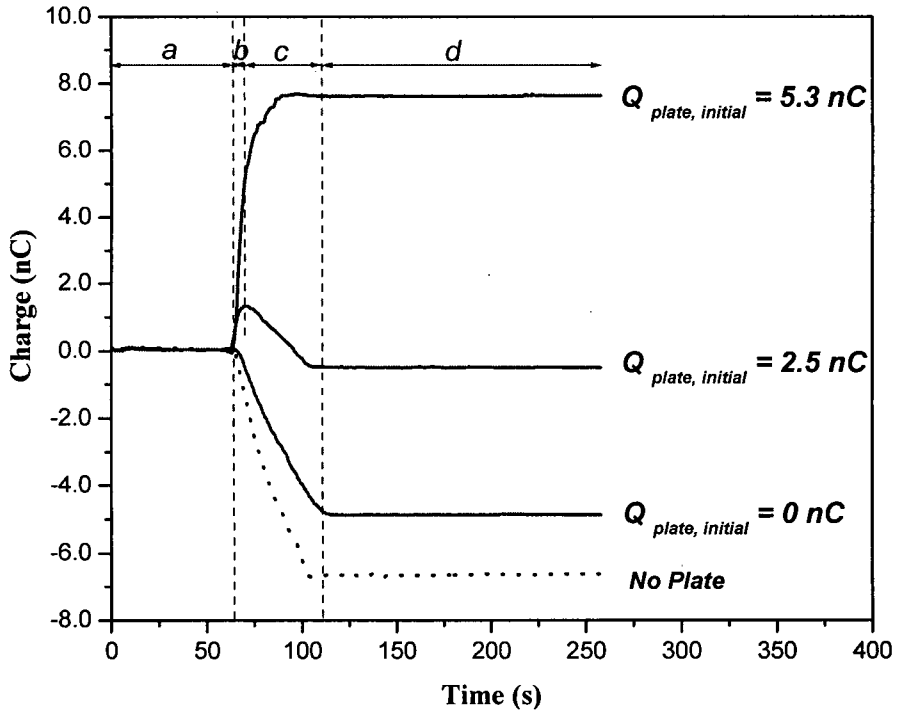

Figure 4.24. Charges gained by fine glass beads due to contact with a copper plate of different initial charges. (10/20/04, Ambient RH ≈ 55%)

When particles contacted a neutral plate, since there were no charges to be transferred from the plate, but because particles initially carried significant charges, charge transfer from the particles to the plate or charge separation were the only possible charging mechanisms. The results for this case show that the charges on the particles decreased by about 1.8 nC from their initial values, indicating that the particles transferred some of their charges to the plate. Therefore, it can be concluded that charge separation was not significant for this case. When the particles came into contact with the plate with an initial charge of +2.5 nC, positive charges were measured on the particles for some time,

after which the charges began to decrease at a similar rate to the case where the plate was initially uncharged.

The charge curves for the fine glass beads are divided into four intervals in Figure 4.24. In interval *b,* the charges were positive and increased (for $Q_{plate,\ initial}$ = 2.5 nC) to a maximum value of about 1.5 nC, almost half of the initial charge on the plate. This interval undoubtedly includes charge transfer between the particles and the plate. In interval *c*, charges initially decreased, with the slope being similar to that for the neutral plate, suggesting that no charge separation occurred after the plate had transferred all of its charges to the particles. When the initial charge on the copper plate was increased to +5.3nC, a sharp increase of positive charges on the particles was observed, to a maximum of about +5.5nC (interval *b*), indicating charge transfer. Then the charges further increased, but with a smaller slope (interval *c*). In this case, the initial charge on the plate was much higher than in the previous case. Therefore, charge transfer continued for almost all of the poured particles. Consequently, the few remaining particles were unable to significantly decrease the cumulative charge in interval *c*.

The electrostatic charges on silver-coated fine glass beads as they came into contact with the copper plate are shown in Figure 4.25. Without any plate, the initial charges on the particles were minimal and positive. The results show that the particles gained significant negative charges as they came into contact with the neutral plate. Since the particles were initially almost neutral and the plate did not have any initial charges, it can be concluded that the measured charges were due to charge separation between the particles and the plate. Comparison of the charges measured when the plate was initially neutral and when it was initially positively charged, clearly indicates that charges were transferred between the plate and the particles when the plate was initially charged. As shown in interval *b* of Figure 4.25, the particles became positively charged to a maximum cumulative charge of about +2 nC and +5.5 nC when the plates were initially charged to +2.5 nC and +5.3 nC, respectively. This shows that the copper plate transferred almost all of its charge to the fines. The slopes in interval *c* of Figure 4.25 are very similar for both the neutral plate

and the initially charged plates. Therefore, it can be concluded that charge separation occurred after the plate became neutral by transferring all of its charges to the fines.

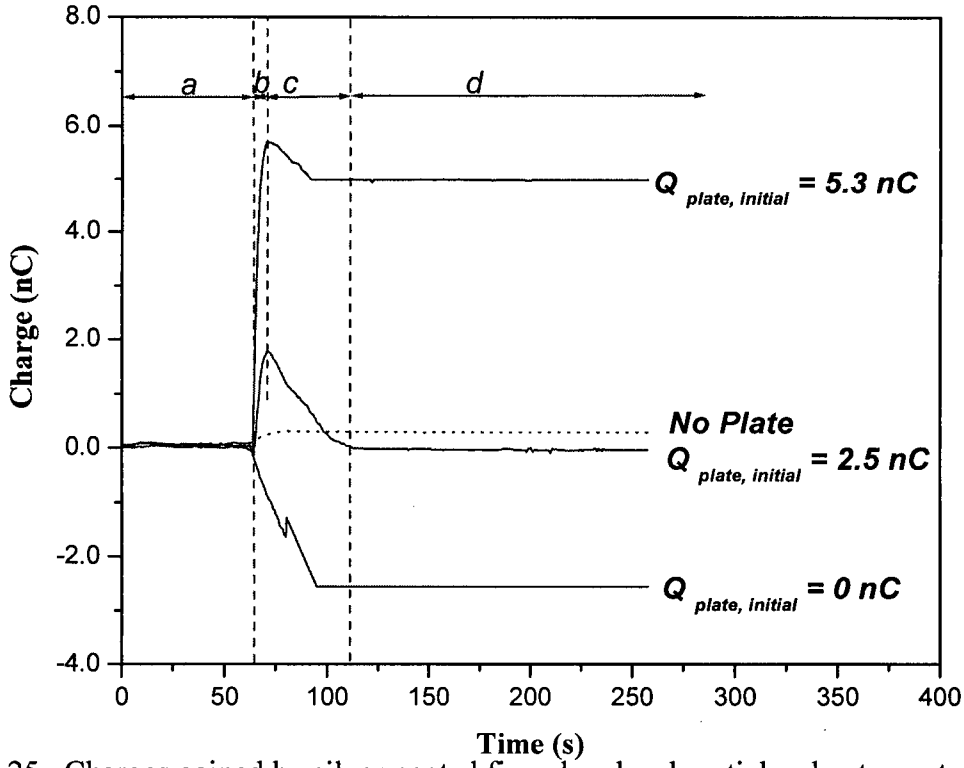

Figure 4.25. Charges gained by silver-coated fine glass bead particles due to contact with a copper plate of different initial charges. (10/19/04, Ambient RH ≈ 60%)

Figure 4.26 shows the charges measured for the catalyst particles. When no plate was present, particles were found to be positively charged (+1.5 nC). As the particles came into contact with a neutral plate, they became slightly negatively charged, indicating that charge separation occurred between the particles and the plate. In cases where the plate was initially charged, an initial increase of charges is observed in interval *b,* followed by a more gradual decrease in interval *c*. The slopes in interval *c* (once the plate was initially charged) are similar to those for the neutral plate. Therefore, it is apparent that charge separation again occurred following the charge transfer.

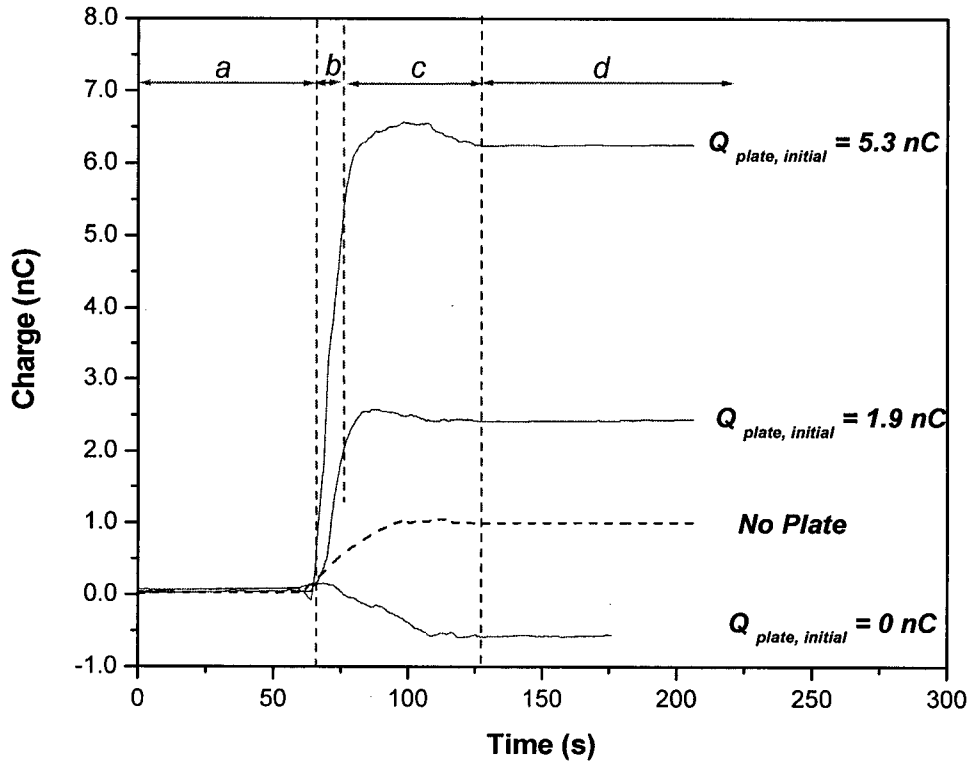

Figure 4.26. Charges gained by catalyst particles due to contact with a copper plate of different initial charges. (03/02/05, Ambient RH ≈ 60%)

The charges measured on fine silica particles with and without contacting the copper plate are shown in Figure 4.27. The results show that silica particles were initially charged slightly positive. However, as they came into contact with a neutral plate, they became significantly negatively charged, implying that charge separation had taken place. As the particles contacted the plate which was initially charged to +2.1 nC, they gained -2.0 nC of charges. This suggests that there was no charge transfer, but rather charge separation between the particles and the plate. As for the case where the plate was initially charged to +5.7 nC, the particles became positively charged to a maximum of +4.0 nC. This indicates that charge was transferred between the particles and the plate. As shown in interval *b*, there were no similarities between the slopes of charges measured on the particles while they contacted the plate with different initial charges.

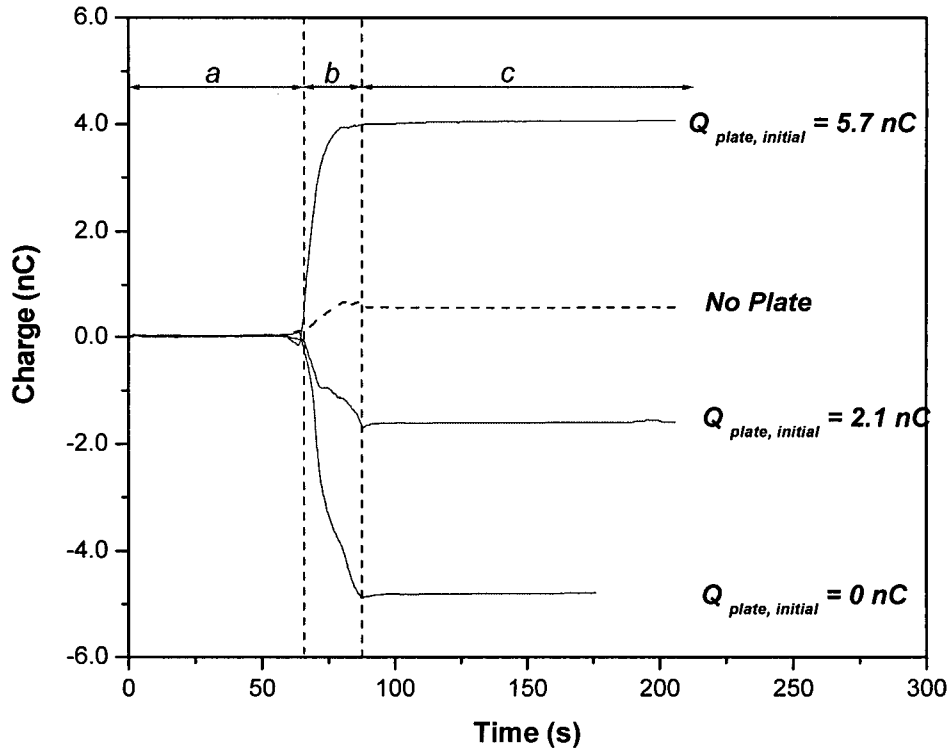

Figure 4.27. Charges gained by silica particles due to contact with a copper plate of different initial charges. (03/02/05, Ambient RH ≈ 60%)

The electrostatic charges on the (large) polyethylene particles as they came into contact with the copper plate are shown in Figure 4.28. The initial charges of the particles were approximately -1.17 nC when the copper plate was not present. When the particles contacted the neutral plate, they became further negatively charged, indicating charge separation. Comparison of the results for the neutral plate with those for initially charged plates shows that the charges measured were very similar in trend and polarity. In addition, as presented in Table 4.2, the charges on the plate before and after being contacted by the particles were essentially the same. Therefore, it is concluded that there was negligible transfer of charges between the polyethylene particles and the copper plate.

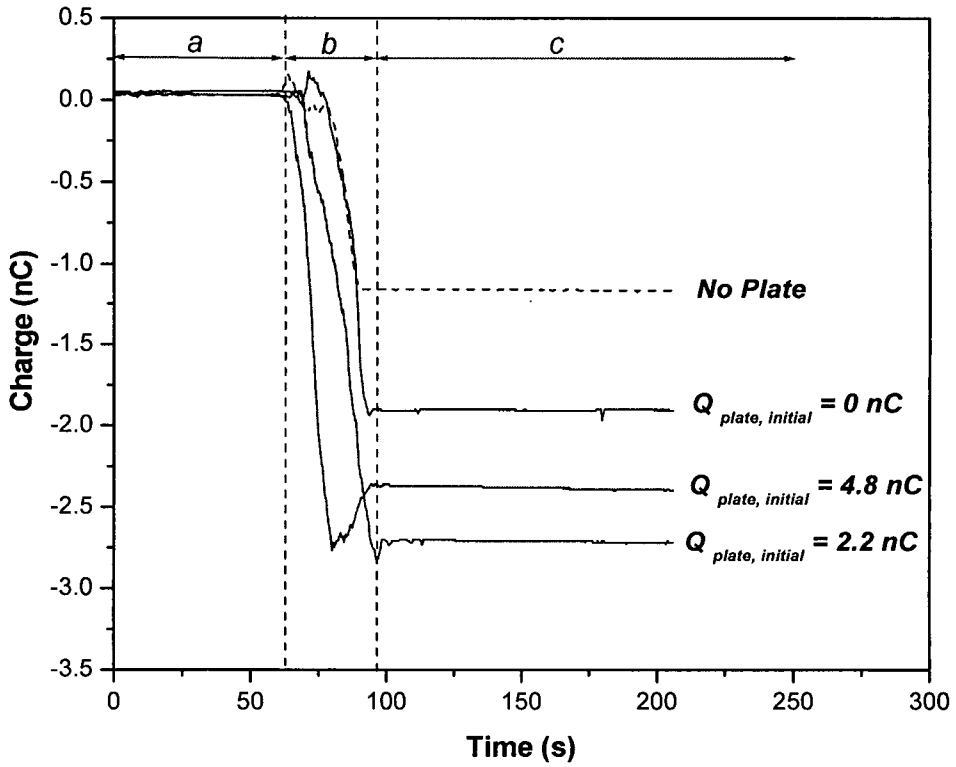

Figure 4.28. Charges gained by polyethylene particles due to contact with a copper plate of different initial charges. (17/01/05, Ambient RH ≈ 70%)

The electrostatic charges gained by the large glass beads as they contacted the copper plate appear in Figure 4.29 It can be seen that when there was no plate, almost zero charges were measured on the particles, i.e. the particles were initially neutral. As the particles came into contact with a neutral plate, they became negatively charged, indicating charge separation. Comparison of the results for the neutral plate with those for the initially charged plates shows that the results are very similar in trend and polarity. Also, as shown in Table 4.2, the charges on the plate before and after being contacted by the particles were nearly the same, indicating that as for the polyethylene particles, there was negligible transfer of charges between the large glass beads and the copper plate.

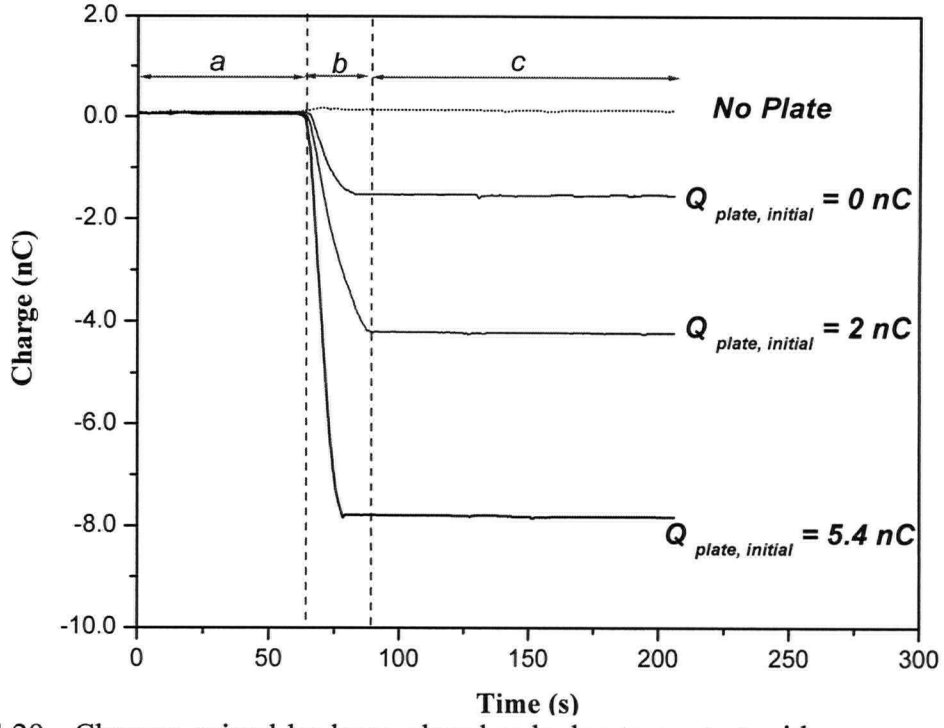

Figure 4.29. Charges gained by large glass beads due to contact with a copper plate of different initial charge. (10/25/04, Ambient RH ≈ 55%)

When the large glass bead particles were poured over the copper plate, it was observed that as they came into contact with the plate, they bounced off the plate and jumped into the cup as illustrated in Figure 4.30b. On the other hand, as the fines were poured over the plate, they slid along the plate until they slipped off into the cup as represented in Figure 4.30a. The polyethylene particles also bounced off the plate, but to a much lesser extent than the large glass beads.

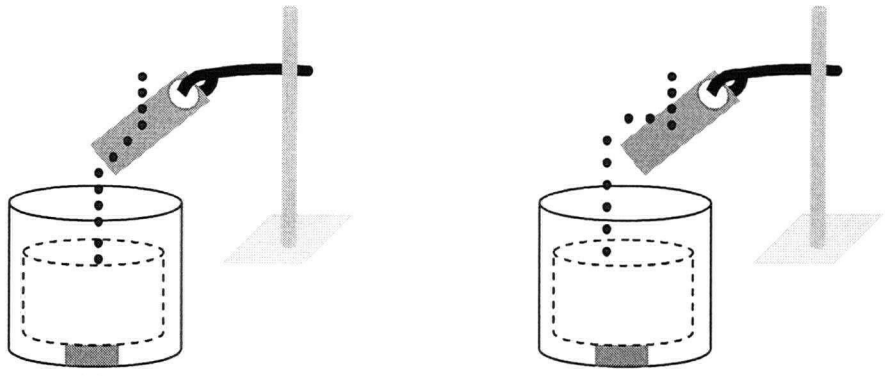

(a) (b)

Figure 4.30. Trajectories of particles as they were poured over the copper plate: (a) fine particles, (b) large glass beads.

These observations show that the polyethylene, and especially the large glass beads, had considerably less contact with the copper plate than the fines. This may well help to explain why there was negligible charge transfer between these particles and the plate.

When the plate was initially charged, given that there was negligible charge transfer between the plate and the large glass beads, charge separation must be the dominant charging mechanism. Therefore, it might be anticipated that the particles would become charged to the same extent, regardless of the initial charge on the copper plate. However, the results contradict with this. As shown in Figure 4.29, the negative charges on the particles increased as the initial positive charge on the plate increased.

Due to the conservation of net charge, when particles gain negative charges as they contact the plate, the plate should gain positive charges of the same magnitude. However, as mentioned above, the initial and final charges on the plate were the same for all runs with the large glass beads. Therefore, the generated positive charges must have dissipated by some other means. Possible charge dissipation methods in this system include discharging through the plate or some other mechanism such as air ionization at the point of contact. Since at the beginning of the experiments it was confirmed that the copper plate was electrically insulated and also that the initial charges on the plate remained constant for all experiments, the first possibility is rejected. To investigate the second possibility, the copper plate was placed inside the Faraday cup and large glass beads were poured over the plate as in the previous runs. When the plate was inside the Faraday cup, since all the charge generation and/or dissipation occurs within the measurement boundary of the Faraday cup, due to the conservation of charge, a zero net charge should be detected by the cup.

The experiments were performed for the neutral and +2 nC charged plate, and the results are presented in Table 4.3 and Figure 4.31. It can be seen that the initial and final charges on the plate were almost equal for both runs, similar to the previous results. However, negative charges were measured on the particles, but this time, the magnitudes of the charges for different initial charges on the plate were very close. Thus, the results indicate

a net charge much greater than zero for particles in both runs, which is contrary to what was expected.

Table 4.3. Charge measurement, Q (nC), results with the copper plate inside the Faraday cup.

Particles	$Q_{o,\ particles}$	$Q_{o,\ plate}$	$Q_{f,\ plate}$	$Q_{f,\ particles}$	$Q_{net,\ particles}$	$Q_{net,\ plate}$
Large Glass Beads	0.123	0.14	0.33	-1.78	-1.91	0.19
	0.123	2.12	2.16	-2.41	-2.45	0.04

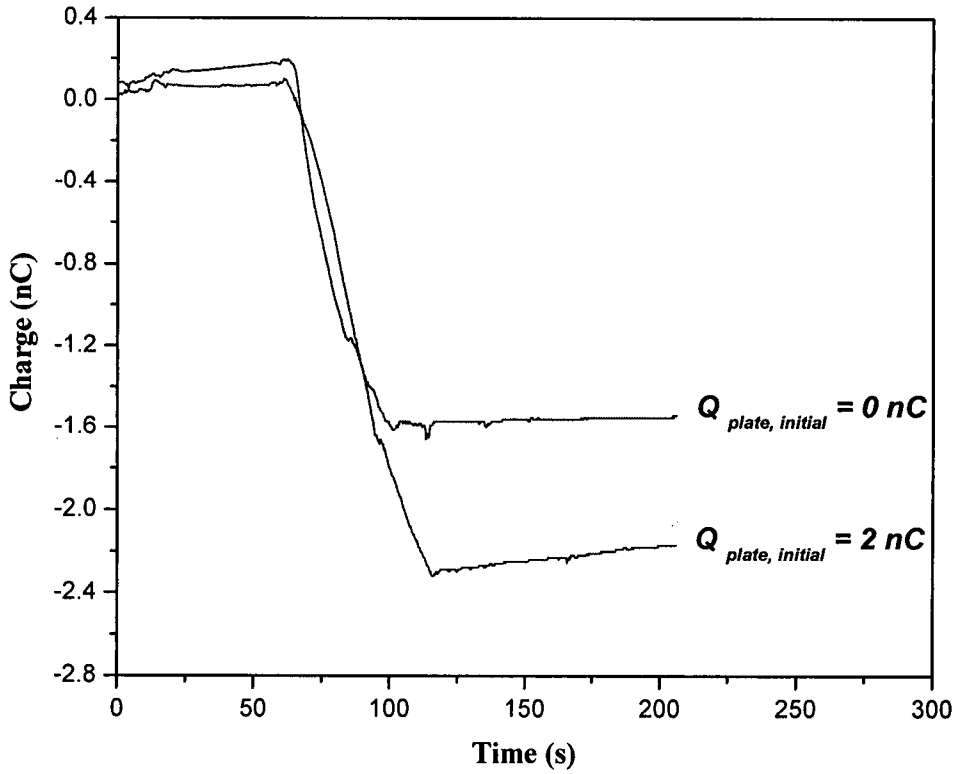

Figure 4.31. Charges gained by large glass beads due to contact with copper plate inside Faraday cup.

4.2.4. Overall charge balance

When particles contact a copper plate, if the system is electrically insulated so that there is no charge leakage, net charges should be conserved. An overall charge balance can be performed over the control volume consisting of the plate and particles in contact (Figure 4.32).

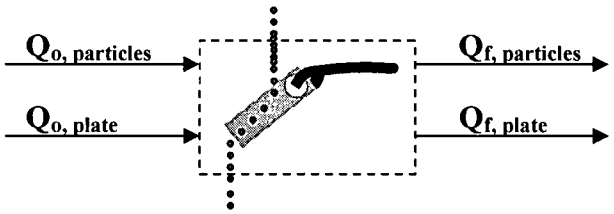

Figure 4.32. Control volume over the copper plate and particles in contact.

This gives,

$$\sum Q|_{t=0} = \sum Q|_{t=t,\ final} \quad (1)$$

$$Q_{o,\ particles} + Q_{o,\ plate} = Q_{f,\ particles} + Q_{f,\ plate} \quad (2)$$

$$\Delta Q_{particles} = Q_{f,\ particles} - Q_{o,\ particles} \quad (3)$$

$$\Delta Q_{plate} = Q_{f,\ plate} - Q_{o,\ plate} \quad (4)$$

Therefore,

$$\Delta Q_{particles} = \Delta Q_{plate} \quad (5)$$

Since the overall charging mechanism of the system involves both charge transfer and charge separation, equation (5) can also be presented as,

$$Q_{transfer,\ particles} = Q_{transfer,\ plate}$$

$$Q_{separation,\ particles} = Q_{separation,\ plate}$$

$$\Delta Q_{transfer} = \Delta Q_{separation} = 0 \quad (6)$$

Equation (6) indicates, based on the law of conservation of charge, that if charges are transferred from the plate to the particles, the particles should gain the same quantity of charges. The same results should apply to the charge separation; if particles gain charges due to charge separation, the plate should acquire the same net charges, but with opposite polarity. Charges measured due to the charge transfer and charge separation were calculated from results presented in Figures 4.23-4.29, where intervals b and c represent

charge transfer and charge separation, respectively, in Figures 4.23-4.26, and interval b represents the charge separation in Figures 4.27-4.29. Results are shown in Table 4.4. Charge transfer $\Delta Q_{transfer}$ is seen to be minimal. However, $\Delta Q_{separation}$ is higher than expected, i.e. non-zero, again suggesting that there must be charge dissipation from the plate throughout the process. It is also important to mention here that as shown in Appendix D, an average of ±1 nC error is associated with the charge measurements. This could also have contributed to high values of $\Delta Q_{separation}$.

Table 4.4. Overall charge, Q (nC), balance for particles and copper plate.

Particles	$Q_{transfer,\ particles}$	$Q_{separation,\ particles}$	$Q_{transfer,\ plate}$	$Q_{separation,\ plate}$	$\Delta Q_{transfer}$	$\Delta Q_{separation}$
Larostat 519	0	1.9	0	-0.10	**0**	**1.8**
	2.0	2.4	-2.1	0	**-0.089**	**2.4**
	5.3	2.7	-5.3	0	**-0.037**	**2.7**
Glass Beads (GB-I)	-1.8	0	0.087	0	**-1.7**	**0**
	1.3	-1.8	1.3	0	**2.7**	**-1.8**
	5.3	2.3	-5.1	0	**0.23**	**2.3**
Silver-Coated Glass Beads (S-GB I)	0	-2.4	0	0.04	**0**	**-2.4**
	1.9	-1.8	-2.3	0	**-0.55**	**-1.8**
	5.7	0.69	-5.2	0	**0.49**	**0.69**
Catalyst	0	-2.0	0	0.18	**0**	**-1.9**
	1.9	0.52	-1.5	0	**0.41**	**0.52**
	5.3	0.95	-5.1	0	**0.25**	**0.95**
Silica	0	-6.6	0	1.2	**0**	**-5.4**
	0	-3.8	0.55	0	**0.55**	**-3.8**
	2.2	0	-4.0	0	**-1.8**	**0**
Large Glass Beads	0	-1.5	0	0.43	**0**	**-1.1**
	0	-4.1	0	0.15	**0**	**-4.0**
	0	-7.7	0	-0.55	**0**	**-8.3**
Polyethylene	0	-0.74	0	0.42	**0**	**-0.32**
	0	-1.5	0	0.34	**0**	**-1.2**
	0	-1.1	0	0	**0**	**-1.1**

4.2.5. Summary

Bench-scale experiments were performed to help understand the charging mechanisms affecting the fluidized bed experiments, in particular the charging mechanisms between the column walls and the particles (fine and large). The results showed that as the fine particles used in this study came into contact with a copper plate, charge transfer occurred, with fines carrying away almost all of the charges initially on the plate, leaving the plate neutral. After that, Larostat 519, silver-coated glass beads and catalyst particles became further charged due to charge separation, whereas fine glass beads maintained their initial charges. Due to charge separation, silver-coated glass beads and catalyst fines became negatively charged, whereas Larostat 519 particles positively charged. Charge separation was determined to be the dominant charging mechanism between the large glass beads and polyethylene particles and the copper plate, with the particles becoming negatively charged. A charge balance over the system where charge separation was the dominant mechanism did not close, suggesting that charges generated on the copper plate dissipated in some unknown manner.

4.3. Conclusions

Comparison of the results from the shaking experiments and the copper plate contacting tests in regards to the fine particles clearly explains why the fine particles acquired significant positive charges in the shaking experiments. In the copper plate contacting tests, it was concluded that fines can gain almost all the charges initially on the plate by charge transfer. In the shaking experiments where the fines and large particles were shaken in a copper flask, the flasks walls became positively charged due to contact with large particles and thus when fines came into contact with the walls, they gained positive charges from the walls due to charge transfer. In addition, as the fines came into contact with the large particles, they became further positively charged due to charge separation. Therefore at the end of each run, the fines had gained considerable positive charges. The results from this study are compared in the next chapter with those from the Faraday cup fluidized bed system in an effort to better understand the charging mechanisms in the fluidization process.

Chapter 5. Discussion of Charge Generation Mechanisms

In the experiments described in Chapter 3, a gas-solid fluidized bed Faraday cup system was used to investigate the charges transported by fine particles of different composition from the fluidization column after their injection into an initially charged bed of relatively large and uniform particles. The results showed that the electrostatic behaviour of fines changed after their addition to the fluidized bed. The next step was to explore the mechanisms underlying these changes and to study their significance.

In order to determine and study the dominant charging mechanism, it is essential to know the charges on both the large particles and the fines before and after fluidizing their mixtures, and also to determine the charges accumulated on the column wall. In the experiments conducted in the Faraday cup fluidization column, the initial charges of both fines and coarse particles and the final charges of fines carried out of the fluidized bed were measured. However, due to limitations of the Faraday cup fluidized bed system, the final charges on the large particles and the column wall could not be determined. Therefore, bench-scale shaking experiments and particle-copper plate contacting tests were performed (Chapter 4) to help understand the charging mechanisms and to explain some of the findings of the fluidized bed Faraday cup system. This chapter links the bench-scale experimental findings to the fluidized bed experimental results to summarize and discuss possible charging mechanisms involved in the Faraday cup fluidization column in the present work, and thereby in gas-solid fluidized beds in general

5.1. Charges on Large Particles after Mono-Sized Free Bubbling Fluidization

In the experiments described in Chapter 3, mono-sized large glass beads and polyethylene particles were first fluidized to generate charges inside the bed before the addition of fines. For these experiments, the initial charge-to-mass ratio of the particles

was measured, though due to limitations of the Faraday cup fluidized bed system, the final charges on the particles could not be calculated. However, plausible explanations can now be given for these charges with the help of the experimental results from the bench-scale shaking and copper plate contacting tests presented in Chapter 4.

In case (a) of the shaking experiments (section 4.1.3), the average charges gained by large glass beads after being shaken for 10 minutes in a copper flask were determined (Table 4.1). The results showed that glass beads were charged negatively, whereas the walls were charged positively. In the particle-copper plate contacting tests (section 4.2.3), both large glass beads and polyethylene particles were brought into contact with a neutral copper plate. The results indicated that charge separation is the dominant charging mechanism between the large glass beads or polyethylene particles and the copper plate, with the particles becoming negatively charged (Figures 4.27 and 4.28). Since the Faraday cup fluidization column is made of copper, it is probable that, similar to the bench-scale experiments, when the large glass bead and polyethylene particles come into contact with the copper walls of the fluidized bed, they become negatively charged. If they initially carry negative charges, as in this study, they are then likely to become more negatively charged. This finding also indicates that for free bubbling fluidization of mixtures of binary particles with added fines, the relatively large particles initially carry negative charges.

5.2. Charging Mechanisms

The mechanism of charging by fines after their addition to a bed of initially charged particles could be due to charge transfer and/or to charge separation. Charge transfer could occur between the fines and the charged large mono-sized particles, and/or between particles and the column wall. Charge separation could be due to particle-particle (fines-large particles) interaction and/or to particle-wall (fines-wall) triboelectrification.

If charge transfer is the dominant mechanism, then the large particles and/or column walls would transfer some of their charges to fines that are initially neutral or carry

minimal charges as they come into contact. Therefore, the fines would acquire the same polarity of charges as the large particles and/or column walls. On the other hand, if charge separation is the dominant mechanism, then as the fines come into contact with the large particles and the column wall, they would gain positive or negative charges due to contact/frictional charging. If triboelectrification between the fines and the large particles is the dominant mechanism, then fines would gain charges of opposite sign to that of the large particles.

The possible charging mechanisms by fines in the Faraday cup fluidization column are summarized in Figure 5.1. In this diagram, Q_L, Q_W and Q_F correspond to charges on large particles, column wall and fines, respectively. The initial charges of large particles and the column wall before the addition of fines, are denoted as $Q_{o,L}$ and $Q_{o,W}$, respectively.

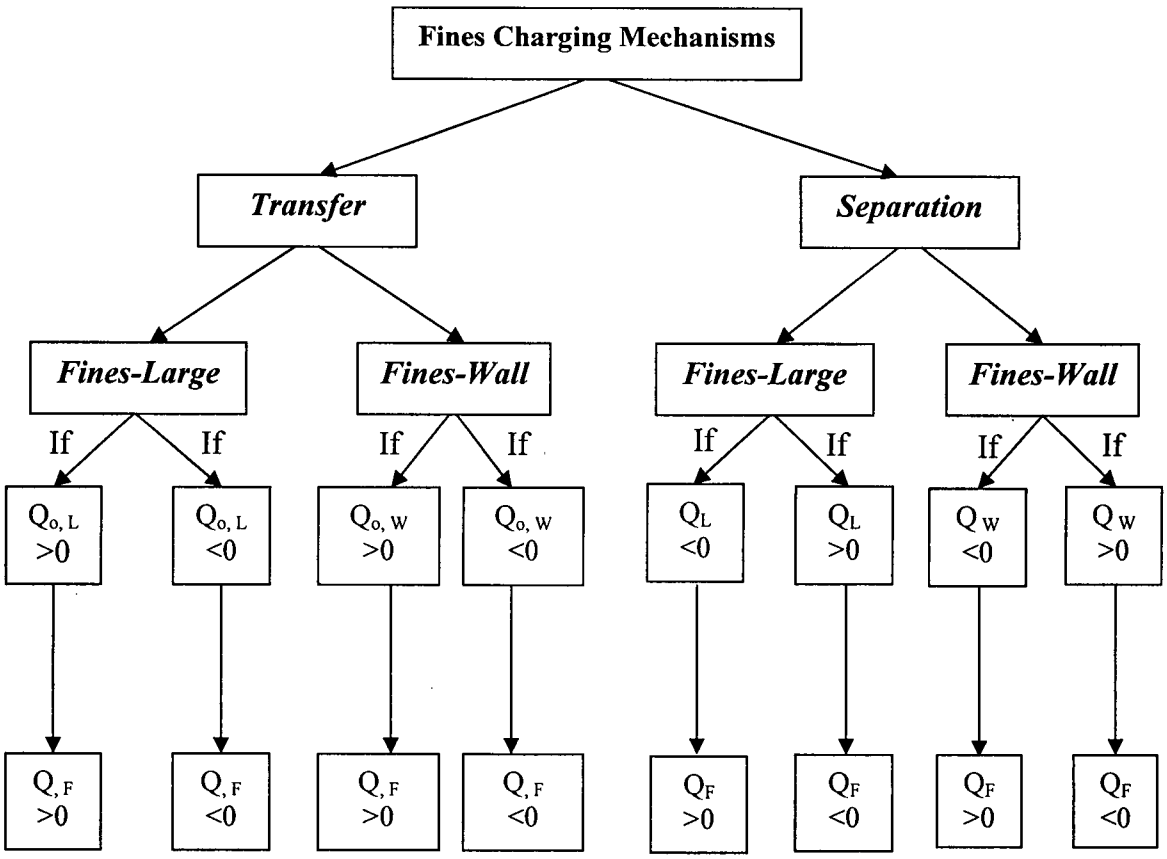

Figure 5.1. Charging flow chart of fines in Faraday cup fluidized bed.

As explained in Section 5.1, it was found that the large particles and column wall would have been negatively and positively charged, respectively, after mono-sized free bubbling fluidization. The column wall was grounded between runs, and therefore its charge would have been neutral at the start of the fluidization of the binary particle mixtures, and then it would have become positive as the fluidization continued ($Q_{o,W} \geq 0$). However, the charges on the large particles would have stayed the same ($Q_o < 0$) until initiation of fluidization of the binary mixtures. Therefore, the fines charging mechanism flow chart can be simplified as in Figure 5.2.

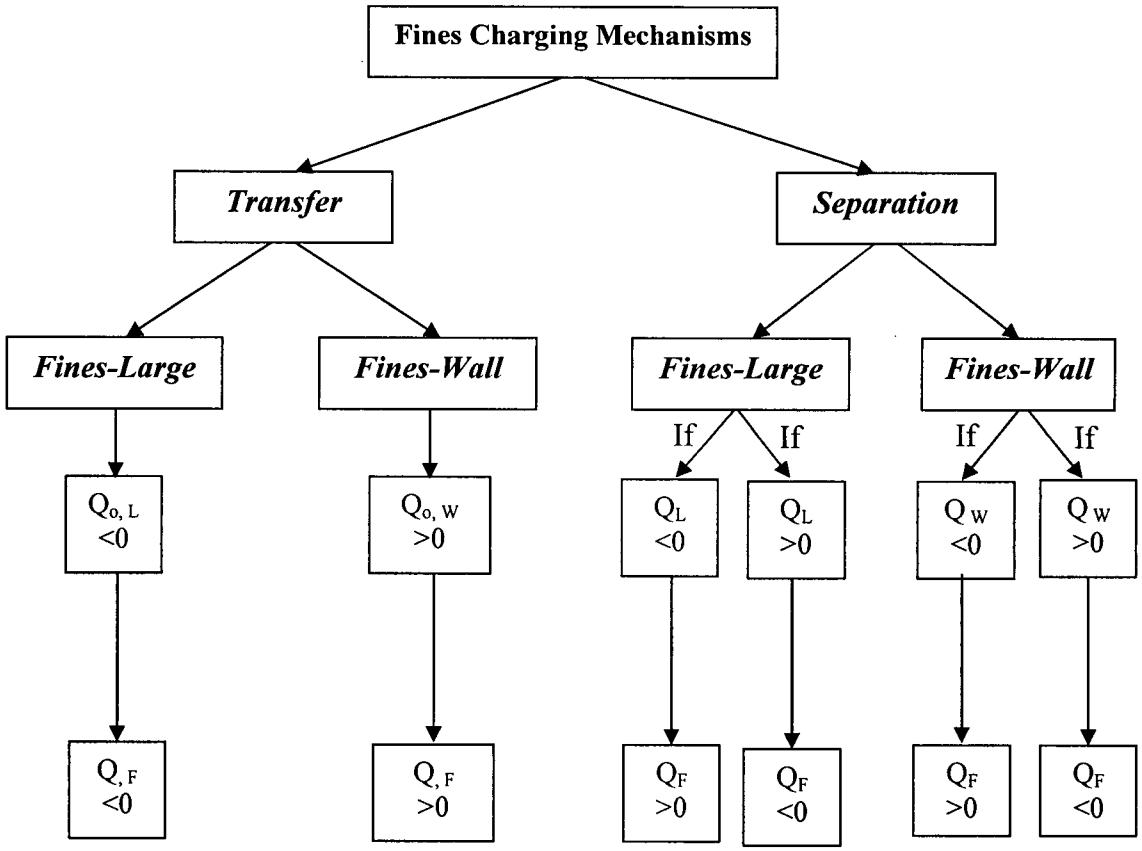

Figure 5.2. Simplified charging flow chart of fines in Faraday cup fluidized bed.

5.2.1. Charging mechanisms for large glass beads-fines binary systems

In the experiments described in Chapter 3, the charges carried by fines entrained from the fluidization column, after their addition to an initially charged bed of relatively large and uniform glass beads, were measured (see Table 5.1).

Table 5.1. Charge polarity of entrained fines for large glass beads-fines binary mixtures.

Fines	**Fines Charge Polarity (0%, 15%, 35% & 60% RH)**	
	+ ve	*-ve*
GB I	X	
S-GB I	X	
Larostat 519	X	
GB II	X	
S-GB II	X	

Overall, the results showed that all different added fines carried positive charges out of the fluidization column, even for different relative humidities of the fluidizing gas. Therefore, the fines charging mechanism flow chart can be further simplified to Figure 5.3.

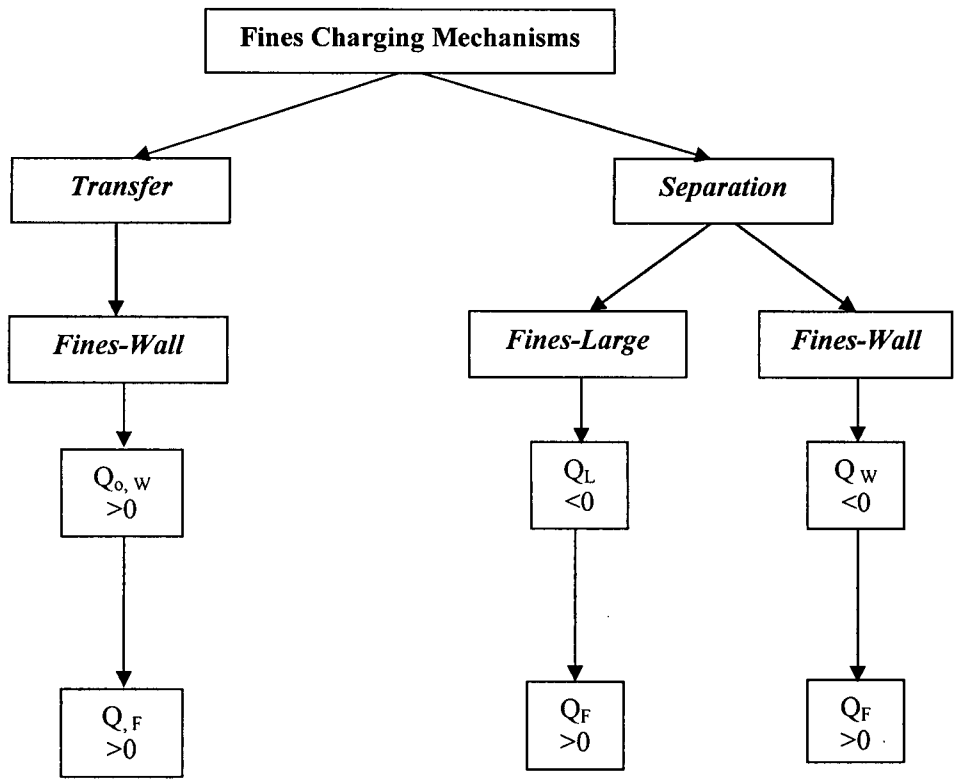

Figure 5.3. Charging flow chart of fines in Faraday cup fluidized bed of large glass beads.

As indicated in the fines charging mechanism flow chart (Figure 5.3), charge transfer between the fines and column wall, and charge separation between the fines and large glass beads, or between the fines and the column wall, could have caused the fines to become positively charged.

The results of the bench-scale fines-copper plate contacting tests, Table 5.2, showed that as the fines (Larostat 519, glass beads and silver-coated glass beads) came into contact with a copper plate, charge transfer occurred, with fines carrying away almost all of the plate's initial charges. Although the column wall was neutral at the start of the free bubbling fluidization, it could have gained positive charges during the fluidization period due to charge separation with the large glass beads. Therefore, it is possible that entrained fines could have gained some of their positive charges from the column wall due to charge transfer.

Table 5.2. Significant charging mechanisms of particles during copper plate contacting tests for large glass beads-fines binary systems and resulting charge polarities gained by the large and fine particles.

Particles	**Charge Transfer**		**Charge Separation**	
	Yes	*No*	*+ ve*	*-ve*
Large GB		X		X
Larostat 519	X		X	
GB I	X			X
S-GB I	X			X

* GB II and S-GB II fines were not utilized in the copper plate contacting tests.

In the experiments conducted in the Faraday cup fluidized bed system, the final charges on the large glass beads and column wall are not known. Therefore, if charge separation was the dominant mechanism, it is not possible to determine whether the positive charges acquired by the fines were due to charge separation between the fines and large glass beads or between the fines and the column wall. However, the copper plate contacting tests showed that charge separation between the fines and copper plate resulted in all

fines becoming charged negatively, except for Larostat 519 which charged positively. Therefore, it would appear that positive charges carried by the entrained GB I & II and S-GB I & II leaving the fluidization column were more likely due to charge separation between the fines and large glass beads, whereas the charges gained by the Larostat fines could have partly been due to charge separation between the fines and the column wall.

When Larostat 519 fines came into contact with a copper plate, charge separation occurred between the copper plate and the Larostat particles, resulting in the Larostat fines becoming positively charged. On the other hand, the results from the shaking experiments indicated that Larostat 519 reduced and prevented charge generation on the large glass beads. When the large glass beads and Larostat fines were shaken together from the beginning (case (b) in Chapter 4), since both types of particles initially carried minimal charges, it was thought likely that this case would be more representative of charge separation. The results showed that none of the large and fine particles gained any significant charges at the end of the shaking period. This therefore suggests that charge separation is not dominant when large glass beads and Larostat fines come into contact. For case (a), where Larostat particles were added to initially negatively charged glass beads, the results showed that the charges on the large glass beads decreased to almost zero, whereas Larostat particles gained minimal positive charges. This indicates either that charge transfer occurred, with the large glass beads approaching neutrality by transferring their charges to the Larostat particles, or that charge separation happened, resulting in the large glass beads becoming positively charged, neutralizing their initial negative charges. In both scenarios, the Larostat particles would then have become negatively charged. However, the results are opposite. If the Larostat particles had gained positive charges (by charge transfer or separation with the flask walls) just before contacting the large glass beads, then both charge separation and/or transfer could have reduced the charges on the large glass beads. In conclusion, the positive charges carried by entrained Larostat 519 particles as they were carried out of the Faraday cup fluidization column could have been due to charge separation and to charge transfer with the column wall, also resulting in reduction and prevention of net charge generation inside the bed. It is also important to mention that, as presented in Figure 3.9, Larostat

519 particles tend to become attached to the surfaces of the large glass beads, indicating that there will be less interaction between the large glass beads and the column walls, thereby preventing further charge generation in the bed. In addition, Larostat 519 particles are highly water adsorbent, which could have also helped further dissipate the charges on the large glass beads.

In conclusion, the fines charging mechanisms in the Faraday cup fluidization system could have included both charge transfer and charge separation, as summarized in Table 5.3. For the Larostat 519 fines, charge transfer and charge separation between the fines and the column walls appear to have been the dominant mechanisms. On the other hand, for the fine glass beads and silver-coated fine glass beads, charge separation between the fines and large glass beads, and also charge transfer between the fines and column walls were the leading mechanisms.

Table 5.3. Likely principal fines charging mechanisms with relatively coarse glass beads as the bed material.

Bed Material	**Charge Transfer**		**Charge Separation**	
	Fines-Wall	**Fines-Coarse**	**Fines-Wall**	**Fines-Coarse**
Larostat	X	-	X	-
GB I	X	-	-	X
S-GB I	X	-	-	X
GB II	X	-	-	X
S-GB II	X	-	-	X

It is important to consider that although charge transfer between fines and large glass beads was not found to be a source of charge generation on its own, it could have participated in the generation of net charges on the fines in combination with other mechanisms. The Q/m ratios of different added fines (Table 3.1) show that silver-coated glass beads carried less charges per unit mass than the pure glass beads, indicating that since the silver-coated glass beads are highly conductive, they can easily lose their charges to the column walls, and they can also help dissipate initial bed charges. Therefore, even though only two mechanisms were determined to be the leading sources

of charging of these fines, other mechanisms could also have participated in charge generation. However, since silver-coated glass beads are highly conductive, they can easily lose their charges, and therefore their net charges turned out be positive, but less than for pure glass beads. In Section 3.4.1, it was suggested that since the large glass beads are smooth and very nearly spherical, there is likely to have been more contacts between them and the fine glass beads and silver-coated glass beads than for the Larostat particles. This is consistent with the results presented in this section, in which charge separation between fines and large glass beads was found to be the leading mechanism for fine glass beads and silver-coated fine glass beads, but not for the Larostat particles.

5.2.2. Charging mechanisms for polyethylene-fines binary system

Chapter 3 reports measured charges carried by fines entrained from the fluidization column, after their addition to an initially charged bed of relatively large polyethylene particles. The polarities of charges carried by different fines leaving the column are summarized in Table 5.4. Overall, the results showed that different added fines carried charges of different polarities out of the fluidization column for various relative humidities of the fluidizing gas.

Table 5.4. Charge polarities of fines entrained from polyethylene-fines binary mixtures.

Fines	**Fines Charge Polarity (0% RH)**		**Fines Charge Polarity (5% RH)**		**Fines Charge Polarity (60% RH)**	
	+ve	*-ve*	*+ve*	*-ve*	*+ve*	*-ve*
Larostat 519		X	NA*		X	
S-GB I	X		NA			X
Catalyst	X			X		X
Silica		X	NA			X
Polyethylene	X		NA		X	

*NA= Not Available

In the case where the relative humidity of the fluidizing gas was 0%, catalyst, S-GB I and polyethylene fines carried positive charges as they were carried out of the fluidization column, whereas Larostat 519 and silica fines carried negative charges. Therefore, based on the fines charging mechanism flow chart (Figure 5.2), the possible charging mechanisms of catalyst, S-GB I and polyethylene fines are summarized in Figure 5.4, whereas those for Larostat 519 and silica fines are presented in Figure 5.5.

As illustrated in Figure 5.4, positive charges carried out of the fluidization column by catalyst, S-GB I and polyethylene fines could have been due to charge transfer between the fines and the column wall and charge separation between the fines and polyethylene particles, as well as the column wall.

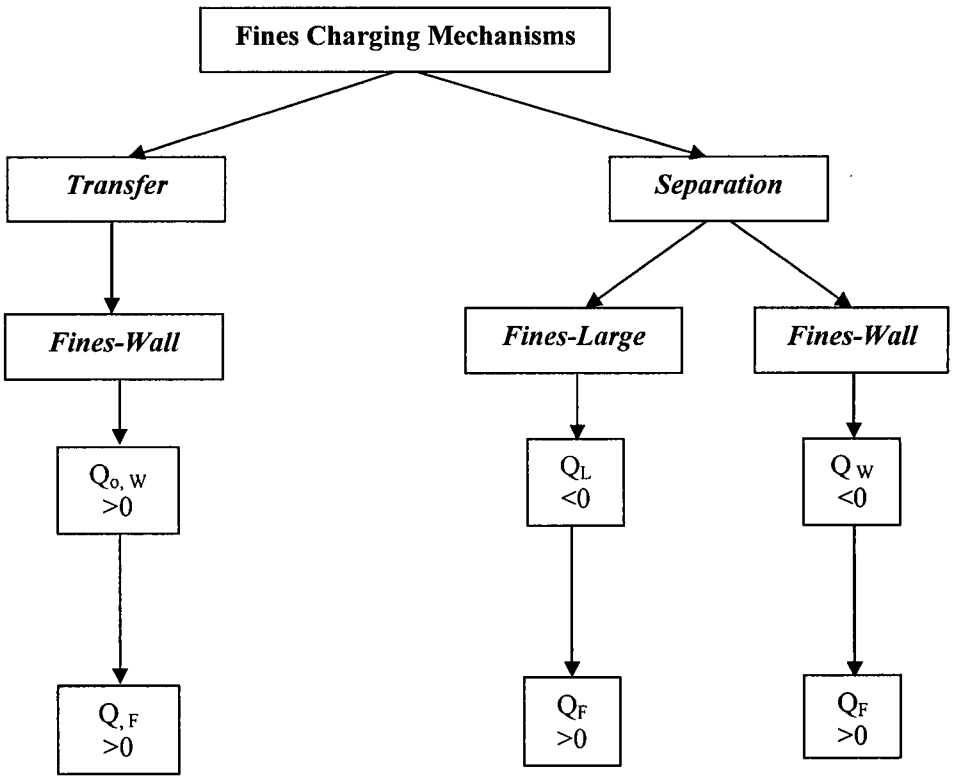

Figure 5.4. Charging flow chart of catalyst, S-GB I and polyethylene fines in Faraday cup fluidized bed of polyethylene particles at 0% RH.

The charging mechanisms of fines when they come into contact with the copper walls of the fluidization column were investigated in the copper plate contacting tests. The results are summarized in Table 5.5.

Table 5.5. Significant charging mechanisms of fines during the copper plate contacting tests for polyethylene-fines binary system.

Particles	**Charge Transfer**		**Charge Separation**	
	Yes	*No*	*+ve*	*-ve*
Polyethylene		X		X
Larostat 519	X		X	
S-GB I	X			X
Catalyst	X			X
Silica	X			X

As the fines came into contact with an initially charged plate, charge transfer occurred, with fines carrying away almost all of the initial charges on the plate. This indicates that charge transfer between the fines and the column wall could have happened. If charge transfer between the fines and column wall was the leading mechanism, two possibilities can be considered. In Section 5.1, it was determined that the column wall was neutral when fluidization of the binary particle mixture was initiated. If it is assumed that the column wall stayed relatively neutral while the added fines were being entrained from the bed, then charge transfer would not have occurred. On the other hand, if the wall acquired positive charges during the fluidization due to charge separation with the polyethylene particles, then the entrained fines would have carried positive charges out of the fluidized bed, consistent with the charge transfer mechanism between the fines and the column wall included in Figure 5.4.

Charge separation also occurred between the fines and the copper plate, resulting in the catalyst and S-GB I fines becoming negatively charged, which is opposite to the polarities found on entrained fines from fluidization column. This indicates that charge

separation between the fines and the column wall is not dominant. The possibility of charge separation between the fines and polyethylene particles is considered next. In that case, since shaking experiments were not performed for this binary system, the charge polarity on polyethylene particles after contacting the fines is unknown. However, since polyethylene is less conductive than the catalyst and S-GB I fines, it is anticipated that when they come into contact, polyethylene particles would gain negative charges, whereas the fines would gain positive charges. Since entrained catalyst and S-GB I fines leaving the fluidization column carried positive charges, it can be concluded that charge separation was the dominant mechanism for these fines. Since the polyethylene particles were initially charged negatively, the former case would have resulted in further charge generation inside the bed. This may have happened since the experimental observations showed that there were more polyethylene particles attached to the column walls when catalyst particles were utilized. In the case of the polyethylene fines, since the shaking and copper plate contacting tests were not conducted for these fines, it is difficult to determine their primary charging mechanism. However, if it is assumed that, since fine polyethylene particles are non-conductive compared to copper, they would become negatively charged, similar to large particles, as they come into contact with a copper plate. Hence, charge separation between them and the column wall is not dominant. Therefore, it can be assumed that they are charged due to charge separation between them and the large polyethylene particles. This supports the occurrence of bi-polar charging.

Figure 5.5 shows that negative charges carried by Larostat 519 and silica fines out of the fluidization column could have been due to the charge transfer between the fines and polyethylene particles and to charge separation between the fines and polyethylene particles, as well as between the fines and the column wall. Results presented in Table 5.6 indicate that charge separation between the fines and copper plate resulted in Larostat fines becoming positively charged, whereas silica fines gained negative charges. This suggests that charge separation between the fines and the column wall may only have been significant for the silica particles.

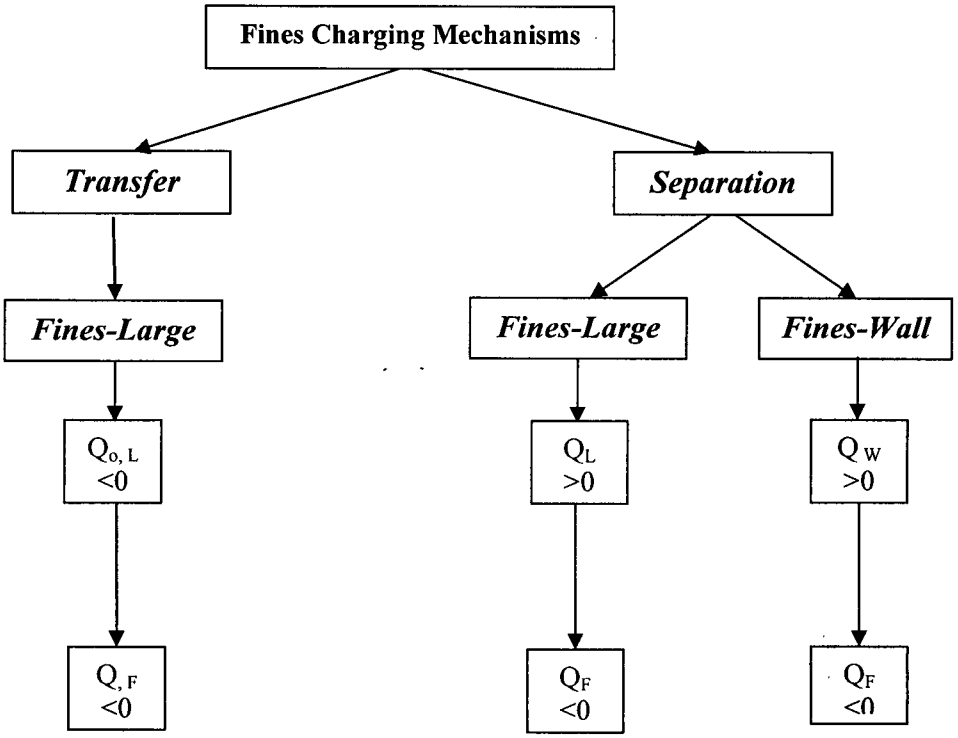

Figure 5.5. Charging flow chart of Larostat 519 and silica fines in Faraday cup fluidized bed of polyethylene particles at 0% RH.

Charge transfer between the fines and polyethylene particles could have also been the dominant charging mechanism. In that case, two scenarios can be considered. First it is assumed that fines contacted only the polyethylene particles and not the column walls. Therefore, since polyethylene particles were initially charged negatively, as fines came into contact with these particles, they would have transported the negative charges gained from the polyethylene out of the fluidization column. Second, it may be that fines were charged, due to charge separation with the column wall, before contacting the polyethylene particles. In this case, the Larostat particles would have become initially positively charged, whereas the silica particles would have become negatively charged. As these fines came into contact with the polyethylene particles, charge transfer would have occurred between them and, depending on which type of particles had the higher absolute charges, one type would have become less negatively charged while the other would have become more negatively charged. In either case, fines would have transported negative charges out of the fluidization column. Since polyethylene particles were initially charged negatively, charge transfer by Larostat 519 particles would have

resulted in charge dissipation on the polyethylene particles. This could be true as experimental observations indicated that fewer polyethylene particles clung to the column walls when Larostat 519 fines were utilized.

When the humidity of the fluidizing gas was increased to 60%, entrained fines carried opposite polarity of charges to those at 0% relative humidity, except for the silica and polyethylene fines (see Table 5.4). One reason could be that, since the larger mono-sized particles were also fluidized at 60% relative humidity, the final charges on polyethylene particles could have changed by being less negative or even neutral. It is expected that increasing the relative humidity of the fluidizing gas would help to reduce and prevent charge generation inside the fluidized bed. The possible charging mechanisms of Larostat 519, catalyst and S-GB I fines, based on the Figure 5.2 flow chart, are summarized in Figures 5.6 and 5.7. It can be seen that at higher humidity of the fluidizing gas, charge transfer between the Larostat fines and the column wall and charge separation between the fines and polyethylene particles, as well as column wall, appear to have been dominant.

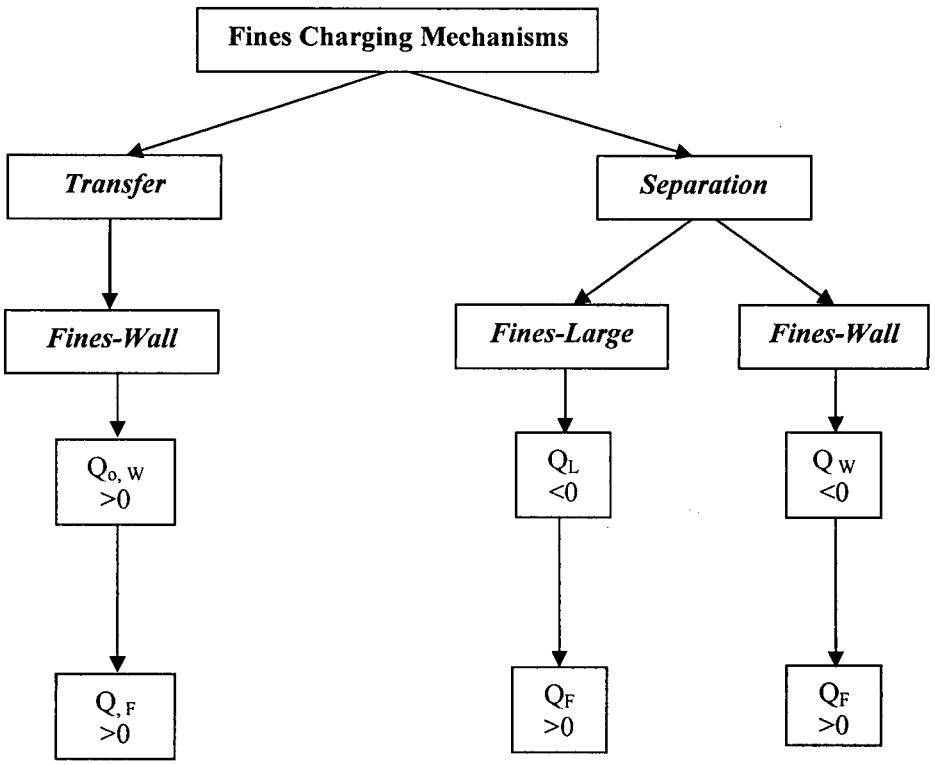

Figure 5.6. Charging mechanism flow chart for Larostat 519 fines in Faraday cup fluidized bed of polyethylene particles at 60% RH.

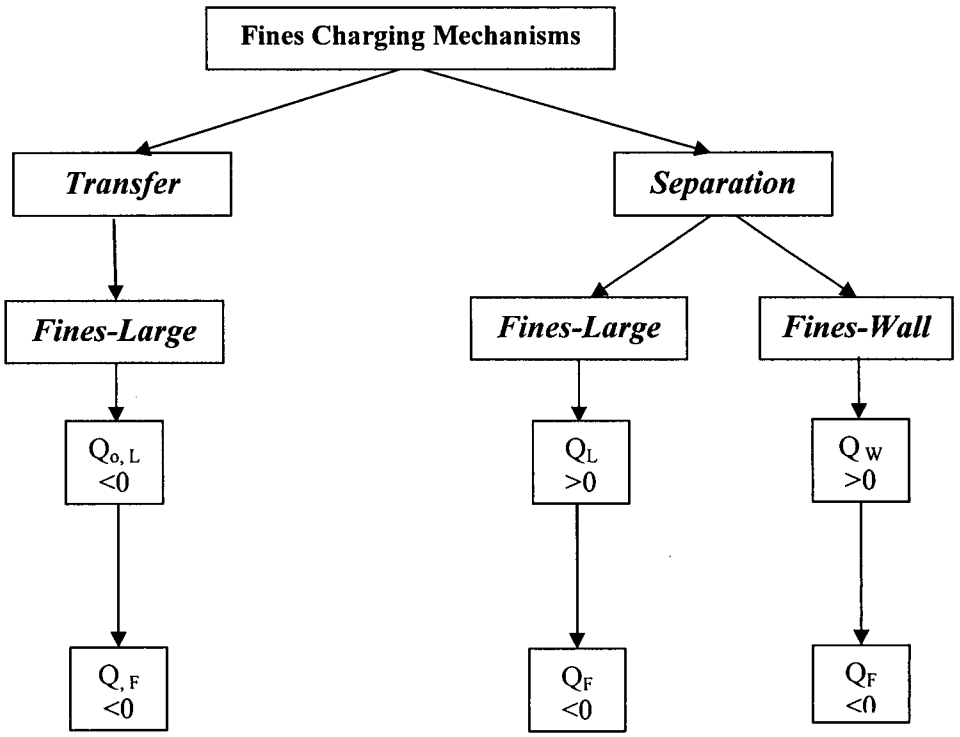

Figure 5.7. Charging mechanism flow chart for catalyst and S-GB I fines in Faraday cup fluidized bed of polyethylene particles at 60% RH.

When the binary particle mixture was fluidized at such a high relative humidity, a thin absorbed layer of water may have formed on the surface of the polyethylene particles, thereby preventing the fines from reaching the surfaces of the polyethylene particles. Charge separation between the fines and polyethylene particles would then have been less dominant than between the fines and the column walls. The polarity of charges carried by fines when leaving the fluidization column is consistent with this possibility. Furthermore, higher humidity could have helped to transfer charges between fines and polyethylene particles. Larsotat 519 fines readily adsorb water, which then could affect its electrical behaviour as it comes into contact with polyethylene particles. On the other hand, catalyst fines containing Ti and Mg chemically react with water, as well as physically adsorbing water. Therefore, in comparison, catalyst, S-GB I and Larostat 519 fines behave differently when exposed to moisture. Therefore, fines would have been able to carry more of the polyethylene negative charges out of the fluidization column, again reducing and preventing charge generation inside the bed.

In conclusion, as shown in Table 5.6, the fines charging mechanisms in the Faraday cup fluidization system of fines-polyethylene binary mixture probably included both charge transfer and charge separation. When the fluidizing gas relative humidity was 0%, principal charging mechanisms for the fines likely included charge transfer between fines and polyethylene particles for the Larostat 519 fines, charge separation between fines and polyethylene particles and also charge transfer between the fines and column walls for the catalyst and S-GB I fines, and charge separation between fines and column walls, as well as charge transfer between fines and polyethylene particles for the silica fines. When the relative humidity of the fluidizing air increased to 60%, charge separation between the fines and column walls and also charge transfer between fines (except for Larostat 519) and polyethylene particles appear to have been the dominant charging mechanisms. It is important to keep in mind that the major charging mechanisms found in this section are based on their individual effects on the entrained fines. However, they may have contributed to the net charges generated on the fines in combination with other mechanisms.

Table 5.6. Likely principal charging mechanisms for fines when the bed material was polyethylene.

Bed Material	**Charge Transfer**		**Charge Separation**	
	Fines-Wall	**Fines-Coarse**	**Fines-Wall**	**Fines-Coarse**
Larostat	-	X	-	-
S-GB I	X	-	-	-
Catalyst	X	-	-	X
Silica	-	X	X	-

In section 3.4.2, it was proposed that since polyethylene particles appear to have surface structures similar to those of the catalyst and silica fines, it is expected that there were more contacts between them than for the S-GB I fines. Therefore, based on the results in Table 5.6, it is speculated that for catalyst fines, charge separation between fines and polyethylene particles was more important than charge transfer between fines and column

walls. Also, for the silica fines, charge transfer between fines and coarse particles would be more important than charge separation between the fines and the column walls.

It is also important to consider the effect of relative humidity of the fluidizing gas on the bed material, as well as the added fines. Comparison of results for Larostat 519 fines at different relative humidities for both bed materials (large glass beads and polyethylene particles) shows that the moisture did not affect the charge polarity of these fines when added to the bed of large glass beads, whereas it did for the polyethylene particles. This is an indication that humidity must have also affected the electrical behaviour of polyethylene particles. One possibility could be that polyethylene particles might adsorb more water than the glass beads for some unknown reason. The influence of water on the surfaces of polymers and highly insulating materials on the particles electrical behaivour is less well understood (Cross, 1987), therefore this issue needs further investigation.

5.2.3. Summary

It has been long known that frictional and triboelectrification charging, and thus the charge polarity of contacting surfaces, are complex phenomena since they can be influenced by many factors such as surface finish, material purity, particle shape and moisture content (Cross, 1987; Johns, 1997). Therefore, it is very difficult to determine the sources of charge generation inside the Faraday cup fluidized bed system. Different charging mechanisms and their significance are considered in this chapter. Although the role of each charging mechanism (charge transfer and charge separation) on electrical behavior of fines was investigated individually, the net charges carried by entrained fines likely resulted from a combination of the two mechanisms. Therefore, it is not easy to generalize the charging mechanism results in this project so that they can be applied to other fluidization systems consisting of different materials of construction in combination with different types of fine and coarse particles.

The fines charging mechanisms considered in this study resulted from particle-particle and particle-wall interactions. The latter may have been more significant in this work than in industrial equipment since the fluidization unit utilized in this study was a lab-

scale column in which particle-wall contacts are relatively important. However, in large industrial units (with lower surface-to-volume ratios), particle-particle interactions are likely to be the leading charging mechanisms. Therefore, it can be concluded that, although similar charge generation mechanisms exist in all fluidized beds, the relative significance of the mechanisms depends on such factors as the scale and the material of the column, physical and chemical surface properties of the solid phases, as well as the humidity of the fluidizing gas.

Chapter 6. Conclusions and Recommendations

Electrostatic charges tend to build up in gas-solid fluidized beds due to repeated contact and separation among particles, and between particles and the column wall. These charges may cause problems such as particle agglomeration, particle-wall adhesion, as well as fires and explosions. In order to find ways of reducing or preventing the generation of electrostatic charges, the relevant phenomena and mechanisms need to be clearly understood. To explore and understand charge generation mechanisms, an appropriate measurement technique is necessary. Thus, a primary objective of this thesis was to develop an improved measurement technique to gain better understanding of charge generation inside gas-solid fluidized beds.

6.1. Conclusions

A novel on-line measurement technique was developed based on the Faraday cup method by constructing a copper fluidization column as the inner cup and a second surrounding copper column as the outer cup. The outer column was grounded to eliminate external electrostatic interferences, and the fluidization column was directly connected to a digital electrometer to measure the charges induced on the column wall. The Faraday cup fluidized bed was able to measure the net charges generated inside the fluidized bed, due to either charges leaving the system or being neutralized. This is the first study in which bi-polar charging and transport of charges by entrained fines have been measured.

Net charges generated inside fluidized beds due to particle-gas contacting were investigated for relatively large glass beads (566 μm mean diameter) fluidized by extra dry air. It was found that the air leaving top of the fluidization column did not carry any noticeable charges. Thus it was concluded that particle-gas contacting had a negligible effect on the particle charging mechanism for the conditions studied.

The likelihood of gas ionization due to frictional charging was also considered. However, information in the literature suggests that the fields generated by particle separation are too small to initiate discharges. Consequently, air ionization is expected to play a negligible role with respect to dissipation of particle charge.

In order to investigate whether net charges generated inside a fluidized bed could be due to the fines entrained from the fluidization column, free bubbling fluidization experiments were conducted with mono-sized and binary mixtures of particles consisting of relatively large glass beads (566 μm mean diameter) and fine glass beads (30 μm mean diameter). It was found that the entrained fines transported a net charge out of the fluidized bed, thereby leaving a net charge behind. Since fines are always carried over to a greater or lesser extent in fluidized bed processes, and also the capture efficiency of entrained fines is always less than 100% in practice, entrainment could be a major source of build-up of net charges inside fluidized beds.

The effect of adding fine particles on charge generation/dissipation inside the bed was studied by investigating the change of the electrostatic behaviour of fines after their addition to the fluidized bed. Free bubbling experiments were performed in the Faraday cup fluidization column after different fines were injected into beds of relatively large glass beads and polyethylene particles. Fines with different physical and chemical surface structures, Larostat 519, glass beads, silver coated glass beads, catalyst and silica, were examined.

It was found that Larostat 519, GB I, S-GB I, GB II and S-GB II fines carried positive charges out of the fluidized bed of relatively coarse glass beads at different relative humidities of the fluidizing air (0, 15, 35 and 60%). Comparison of Q/m ratios of different fines showed that the finer the particles, the higher the charges carried per unit mass. The physical surface structure of fines is believed to affect the number of their contacts and thus the amount of charges carried. Larostat fines helped to dissipate the initial bed charges by attaching themselves to the large glass beads. It was found that the higher the surface conductivity of the fines, the easier it was for them to lose their

charges to the column walls, thereby dissipating the initial bed charges. As the relative humidity of the fluidizing gas increased, the charge-to-mass ratios decreased, as expected. Bi-polar charging was also investigated. For both the coarse glass beads and polyethylene particles tested smaller particles were charged positively and larger particles negatively.

Free bubbling fluidization of binary mixtures of fines (Larostat 519, catalyst, silica and S-GB I) with relatively large polyethylene particles showed that the added fines carried different polarity of charges out of the fluidized bed, depending on the relative humidity of the fluidizing gas. It was concluded that the relative humidity of the fluidizing gas can affect the bed material (polyethylene particles) and/or the electrical behaviour of added fines. Catalyst and S-GB I fines behaved similarly, probably due to their similar surface electrical conductivities. Charge-to-mass ratios were higher for the catalyst and silica particles than for the other fines. Observations after fluidizing the binary particles mixtures confirmed that there were fewer polyethylene particles clinging to the column walls when Larostat 519 and S-GB I fines were present.

Bench-scale shaking experiments were performed to elucidate the charging mechanisms. Although there were uncertainties associated with the test results, the results confirmed that the fines used in previous fluidization experiments gained positive charges as they came into contact with relatively large glass beads. Further, the large glass beads became negatively charged upon contacting the copper walls. Larostat 519 (of the three types of fines tested) acted as an antistatic agent by helping to dissipate charges and preventing further charge generation. The charges carried by fines appeared to be due to charge separation, rather than charge transfer, since their polarity was opposite to that of the charges carried by the large glass beads. Particle-wall contacting, or particle motion and mixing in the Faraday cup fluidization equipment, could differ significantly from the bench-scale shaking experiments. In particular, particle-wall contacts were likely to have been much stronger in the small flasks than in the fluidization column. Since electrostatic charge generation is a complex phenomenon, dependent on many different factors,

caution was needed when applying the bench-scale experiments to the Faraday cup fluidized bed system.

Bench-scale copper plate contacting experiments were performed to help understand the charging mechanisms between the column walls and the fine and coarse particles. As the fine particles came into contact with a copper plate, charge transfer occurred, with fines carrying away almost all of the charges initially on the plate, leaving the plate nearly neutral. After that, Larostat 519, silver-coated glass beads, catalyst and silica particles became further charged due to charge separation, whereas fine glass beads maintained their initial charges. Due to charge separation, Larostat 519 particles became positively charged, whereas silver-coated glass bead, catalyst and silica fines became negatively charged. Charge separation was determined to be the dominant charging mechanism between the coarse glass bead and the polyethylene particles and the copper plate, with the particles becoming negatively charged.

Different fines charging mechanisms and their significance were investigated. Both charge transfer and charge separation are important. In the binary system of fines-large glass bead particles, for Larostat 519 fines, charge transfer and charge separation between the fines and the column walls were the dominant mechanisms. On the other hand, for glass beads and silver-coated glass beads, charge separation between the fines and large glass beads and also charge transfer between the fines and column walls appeared to be the leading mechanisms. In binary particle systems of fines-coarse polyethylene particles, when the fluidizing gas relative humidity was 0%, fines charged by charge transfer between the fines and coarse polyethylene particles for Larostat 519 fines, by charge separation between fines and the polyethylene particles and charge transfer between the fines and column walls for catalyst and S-GB I fines, and by charge separation between fines and column walls and also charge transfer between fines and polyethylene particles for the silica fines. When the relative humidity of the fluidizing gas increased to 60%, charge separation between the fines and column walls and also charge transfer between fines (but not Larostat 519) and polyethylene particles appeared to be the principal charging mechanisms. Since polyethylene particles appeared to have surface structures

similar to those of the catalyst and silica fines, it was expected that there would be more contacts between them than for the S-GB I fines. Therefore, it was speculated that for catalyst fines, charge separation between fines and polyethylene particles would be more dominant than charge transfer between fines and column walls. Also, for the silica fines, charge transfer between fines and particles would be more important than charge separation between the fines and the column walls.

Although, the role of each charging mechanism (charge transfer and charge separation) on electrical behavior of fines was individually investigated, net charges carried by entrained fines may have resulted from both mechanisms. Therefore, it is not easy to generalize the charging mechanism results so that they can be applied to other fluidization systems. However, the results found in this project help to determine and understand the possible mechanisms and provide a novel approach to the problem. Furthermore, frictional and triboelectrifications charging, and thus the charge polarity of contacting surfaces, are complex phenomena influenced by many factors such as surface finish, material purity, particle shape and moisture content.

The fines charging mechanisms considered in this study have included particle-particle, as well as particle-wall, interactions. The latter were important here because the fluidization column in this study was of laboratory scale, so that particle-wall contacts were also significant. However, in large industrial units, particle-particle interactions are likely to be dominant. Thus, although similar charging generation mechanisms exist in all fluidized beds, their significance depends on such factors as the scale of the column and the material, physical and chemical surface properties of the solid phases, as well as the moisture content of the fluidizing gas.

Overall it was concluded that fines added to an initially charged fluidized bed carry significant but different amounts of charges from the column, depending on their sizes, physical and chemical structure of particle surfaces, as well as the moisture content of the fluidizing gas. This is a significant finding since fines are always elutriated in fluidized bed processes. It also suggests that since electrostatic forces play a role in determining

the flux of entrained fines from a fluidized bed, they should be incorporated into models developed to predict entrainment flux and, perhaps also, transport disengagement height.

6.2. Recommendations

Further work is required to identify missing information such as the charge build-up on column walls and the initial and final charges on large particles for free bubbling fluidization of binary particles mixtures.

In order to better understand the charging mechanisms of the fines, other surface properties of particles such as surface work function should be determined. Further, measurements should be conducted at ambient pressure for similar relative humidities as in the Faraday cup fluidization experiments, to ensure comparability of the results.

In order to eliminate the variation of the ambient relative humidity, which could have affected the charge measurements in present study, the bench-scale shaking experiments and the copper plate contacting tests should be conducted in a dry box environment. In this manner, the relative humidity of the environment could also be controlled to achieve similar operating conditions to the experiments performed in the Faraday cup fluidization system. In order to increase the efficiency of separating the fine and coarse particles in the shaking experiments, a better method of pouring particles into the double Faraday cup should be considered by perhaps designing an automated device. Furthermore, work should be considered to develop a method to measure either the weight or the particle size distribution of particles collected in each cup of the double Faraday cup system.

Future work can be carried out to investigate the effect of fluidizing gas velocity on the charges generated inside the fluidized bed. This would also help understanding the significance of frictional charging in comparison with triboelectrification in gas-solid fluidized beds.

Since in this project, the Faraday cup fluidized bed system was able to measure the charges leaving with the fluidizing gas, the effect of ionized gas on reducing or eliminating charge generation inside the fluidized beds should be investigated.

This study led to some insight on the role of catalyst fines on the net charges generated inside a bed of polyethylene particles. Since electrostatic phenomena cause major problems in the polymerization industries, the same polyethylene and catalyst particles utilized in industrial reactors should be examined in the Faraday cup fluidization system to investigate and further understand the charge generation mechanisms involved. This would also shed some light on finding new ways (e.g., a new antistatic agent) of reducing and preventing charge generation in gas-solid fluidized beds used for polymerization processes.

Further work can be undertaken to integrate the electrostatic forces into entrainment models to determine the flux of entrained particles from fluidized beds.

Literature Cited

Ali, F.Sh., Ali, M.A., Ali, R.A. and Inculet, I.I., Minority Charge Separation in Falling Particles with Bipolar Charge, *Journal of Electrostatics,* **45**, 139-155, 1998.

Boland, D. and Geldart, D., Electrostatic Charging in Gas Fluidized Beds, *Powder Technology,* **5**, 289-297, 1971/1972.

Briens, C.L., Bergougnou, M.A. and Inculet, I.I., Size Distribution of Particles Entrained from Fluidized Beds: Electrostatic Effects, *Powder Technology,* **70**, 57-62, 1992.

Burdett, I.D., Eisinger, R.S., Cai, P. and Lee, K.H., Gas-Phase Fluidization Technology for Production of Polyolefin, *Fluidization X,* ed. M. Kwauk, J. Li and W.C. Yang, New York, 39-52, 2001.

Castle, P., University of Western Ontario, Personal Communication, 2004.

Chen, A., Bi, X. and Grace, J.R., Measurement of Particle Charge-to-Mass Ratios in a Gas-Solids Fluidized Bed by a Collision Probe, *Powder Technology,* **135-136**, 181-191, 2003.

Ciborowski, J. and Wlodarski, A., On Electrostatic Effects in Fluidized Beds, *Chemical Engineering Science,* **17**, 23-32, 1962.

Cross, J.A., Electrostatics: Principles, Problems and Applications, Adam Higler, Bristol, 1987.

Fan, Liang-shih and Zhu, Chao, Principles of Gas-Solid Flows, Cambridge University Press, New York, 1998.

Fasso, L., Chao, B.T. and Soo, S.L., Measurement of Electrostatic Charges and Concentration of Particles in the Freeboard of Fluidized Bed, *Powder Technology,* **33**, 211-221, 1982.

Fujino, M., Ogata, S. and Shinohara, H., The Electric Potential Distribution Profile in a Naturally Charged Fluidized Bed and its Effects, *International Chemical Engineering,* **25**, 149-159, January 1985.

Goode, M.G., Hasenberg, D.M., McNeil, T.J., and Spriggs, T.E., Method for Reducing Sheeting during Polymerization of Alpha-olefins, U.S. Patent, 4803251, (1989).

Goode, M.G., Williams, C.C., Hussein, F.D., McNeil, T.J., and Lee, K.H., Static Control in Olefin Polymerization, U.S. Patent, 6111034, (2000).

Grace, J.R., and Baeyens, J., Instrumentation and Experimental Techniques, chapter 13th in Gas Fluidization Technology, ed. D. Geldart, Wiley, Chichester, U.K., 1986.

Guardiola, J., Ramos, G. and Romero, A., Electrostatic Behavior in Binary Dielectric/Conductor Fluidized Beds, *Powder Technology,* **73**, 11-19, 1992.

Guardiola, J., Rojo, V. and Ramos, G., Influence of Particle Size, Fluidization Velocity and Relative Humidity on Fluidized Bed Electrostatics, *Journal of Electrostatics,* **37**, 1-20, 1996.

Ham, R.W., Galtier, R.A. and Bergougnou, M.A., Electrostatics in an Air/Catalyst Fluidized Bed at Ambient Temperature and Pressure, Fluidization VII, ed. O.E. Pother and D.J. Nicklin, Engineering Foundation, NY, 611-620,1992.

Harper, W.R., *Contact and Frictional Electrification*, Oxford University Press, London, 1967.

Hori, Y., The Lateral Migration of Surface Charges on Poly(methyl methacrylate) Graft-Copolymerized onto Polypropylene Film, and its Dependency on Relative Humidity, *Journal of Electrostatics,* **48**, 127-143, 2000.

Jones, T.B., Electrostatic and Dust Explosions in Powder Handling, in Selected Topics on Fluidization, Solids Handling, and Processing, Noyes Publications, Park Ridge, NJ, 817-871, 1997.

Katz, H. and Sears, J.T., Electric Field Phenomena in Fluidized and Fixed Beds, *Canadian Journal of Chemical Engineering,* **47**, 50-53, 1969.

Kittel, Charles, Introduction to Solid State Physics, 7th Ed., Wiley, New York, 1996.

Kunii, D. and Levenspiel, O., *Fluidization Engineering*, 2nd Edition, Butterworth-Heinemann, USA, 1991.

Montgomery, D.J., Static Electrification of Solids, *Solid State Phys.*, **9**, 139-196, 1959.

Park, A., Bi, H. and Grace, J.R., Reduction of Electrostatic Charges in Gas-Solid Fluidized Beds, *Chemical Engineering Science,* **57**, 153-162, 2002.

Revel, J., Gatumel, C., Dodds, J.A. and Taillet, J., Static Charge Elimination in a Slugging Fluidized Bed, *4th World Congress on Particle Technology,* Sydney, 1-8, 2002.

Riley, N.A., Projection sphericity, J. Sedimentary Petrology, **11**, v. 2, 94-97, 1941.

Smeltzer, E.E., Weaver, M.L. and Klinzing, G.E., Pressure Drop Losses due to Electrostatic Generation in Pneumatic Transport, *Ind. Eng. Chem. Process Des. Dev.,* **21**, 390-394, 1982.

Song, G.H., Rhee, A.S. and Lowder, G.R., Method for Reducing Sheeting and Static Charges during Polymerization of Ethylene Polymers, U.S. Patent, 5391657, 1995.

Tardos, G., and Pfeffer, R., A Method to Measure Electrostatic Charge on A Granule in a Fluidized Bed, *Chem. Eng. Commun.*, **4**, 665-671, 1980.

Trigwell, S. and Mazumder, M.K., Tribocharging in Electrostatic Beneficiation of Coal: Effects of Surface Composition on Work Function as Measured by X-ray Photoelectron Spectroscopy and Ultraviolet Photoelectron Spectroscopy in Air, *J. Vac. Sci. Technol. A.*, **19 (4)**, 1454-1459, 2001.

Wolny, A. and Kazmierczak, W., Triboelectrification in Fluidized Bed of Polystyrene, *Chemical Engineering Science,* **44**, 11, 2607-2610, 1989.

Wolny, A. and Opalinski, I., Electric Charge Neutralization by Addition of Fines to a Fluidized Bed Composed of Coarse Dielectric Particles, *Journal of Electrostatics,* **14**, 279-289, 1983.

Zhao, H., Castle, G.S.P., Inculet, I.I. and Bailey, A.G., Bipolar Charging in Polydisperse Polymer Powders in Industrial Processes, *Conference Record of the 2000 IEEE,* **2**, 835-841, 2000.

Zimmer, E., Die Elektrostasche Aufladung von Hochpolymeren Isolierstoffen, *Kustoffe*, **60**, 465-468, 1970.

Appendix A- Equipments Photographs

A.1. Experimental apparatus

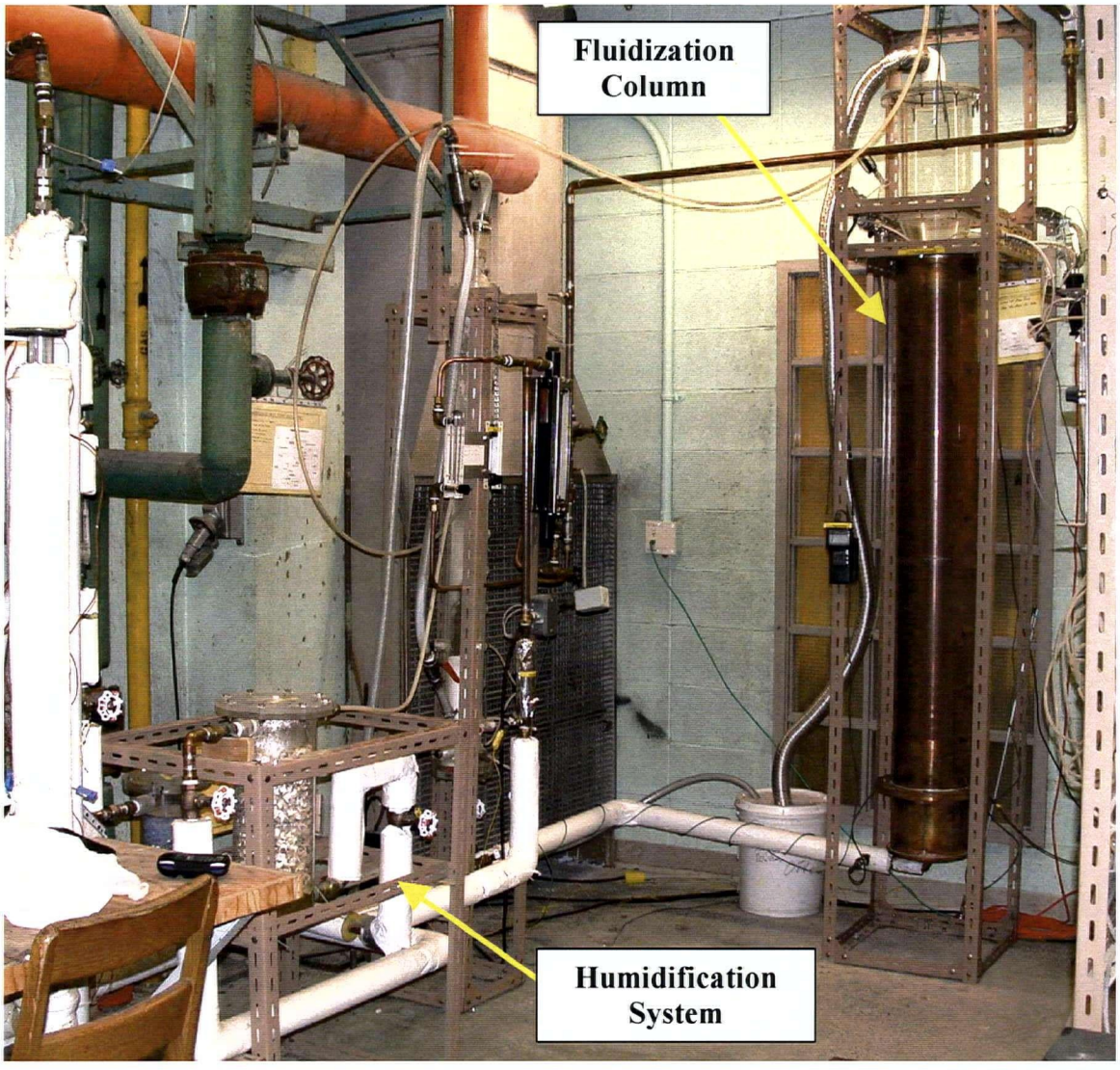

Figure A.1. Photograph of the experimental apparatus.

A.2 . Faraday cup fluidization column

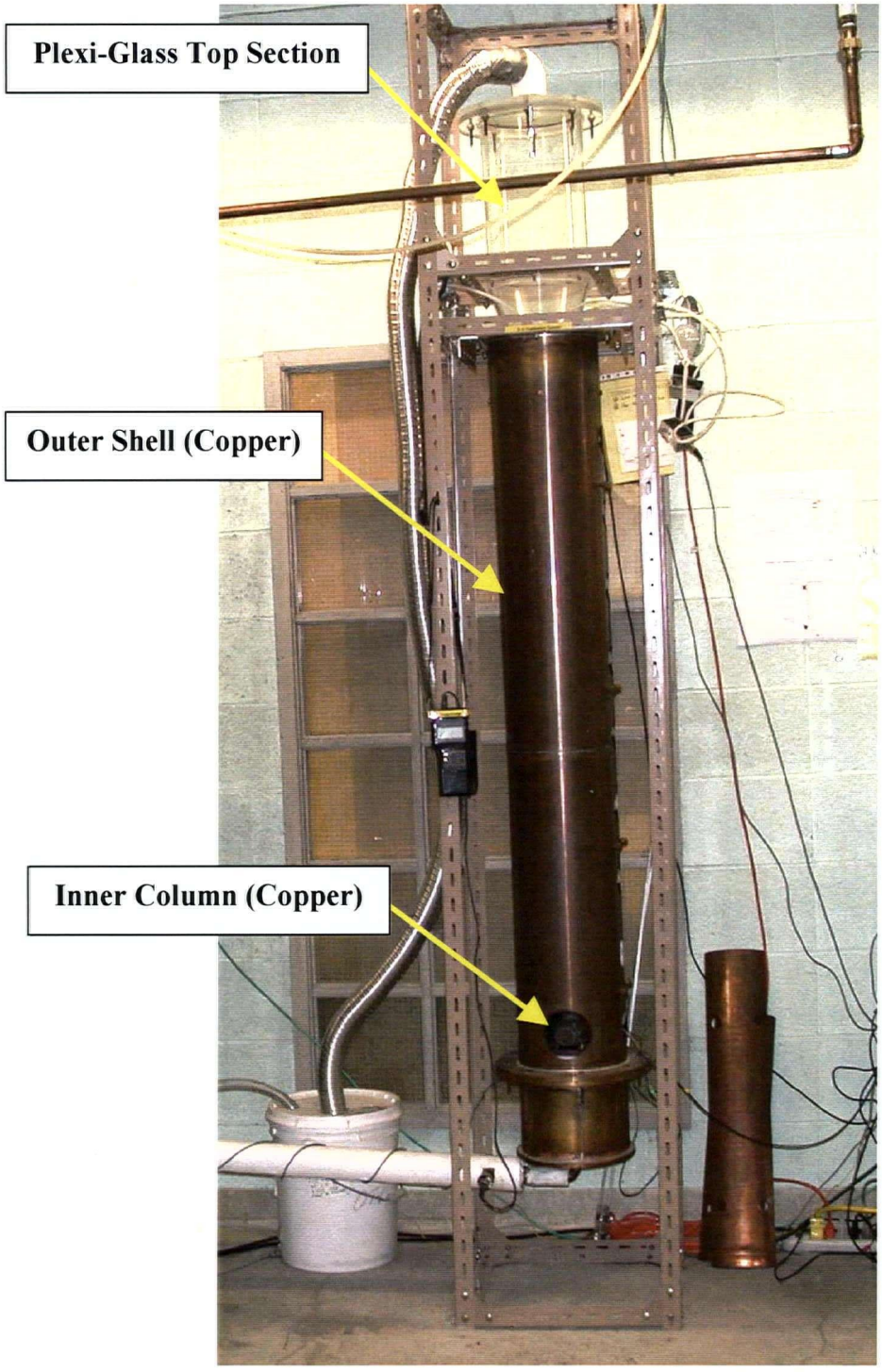

Figure A.2. Photograph of Faraday cup fluidization column (front view).

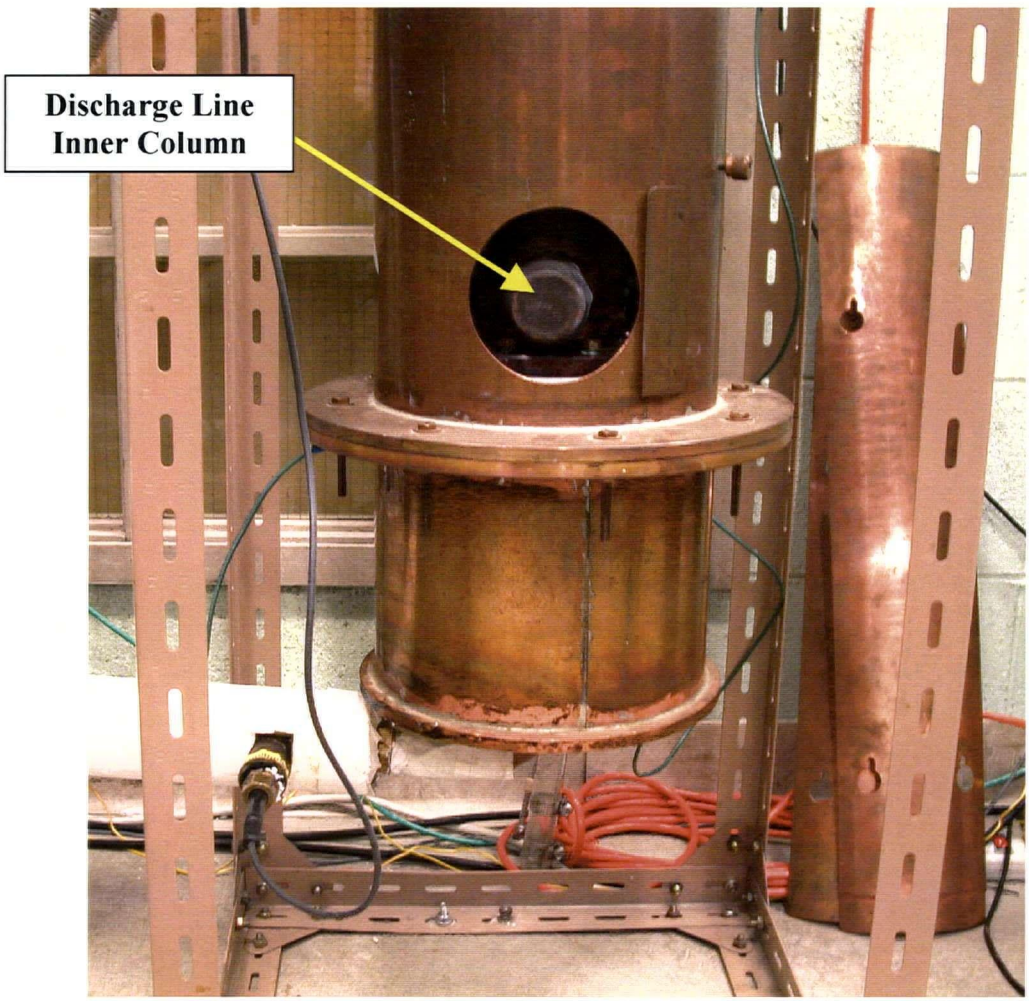

Figure A.3. Photograph of Faraday cup fluidization column showing the discharge line of the inner column (front view).

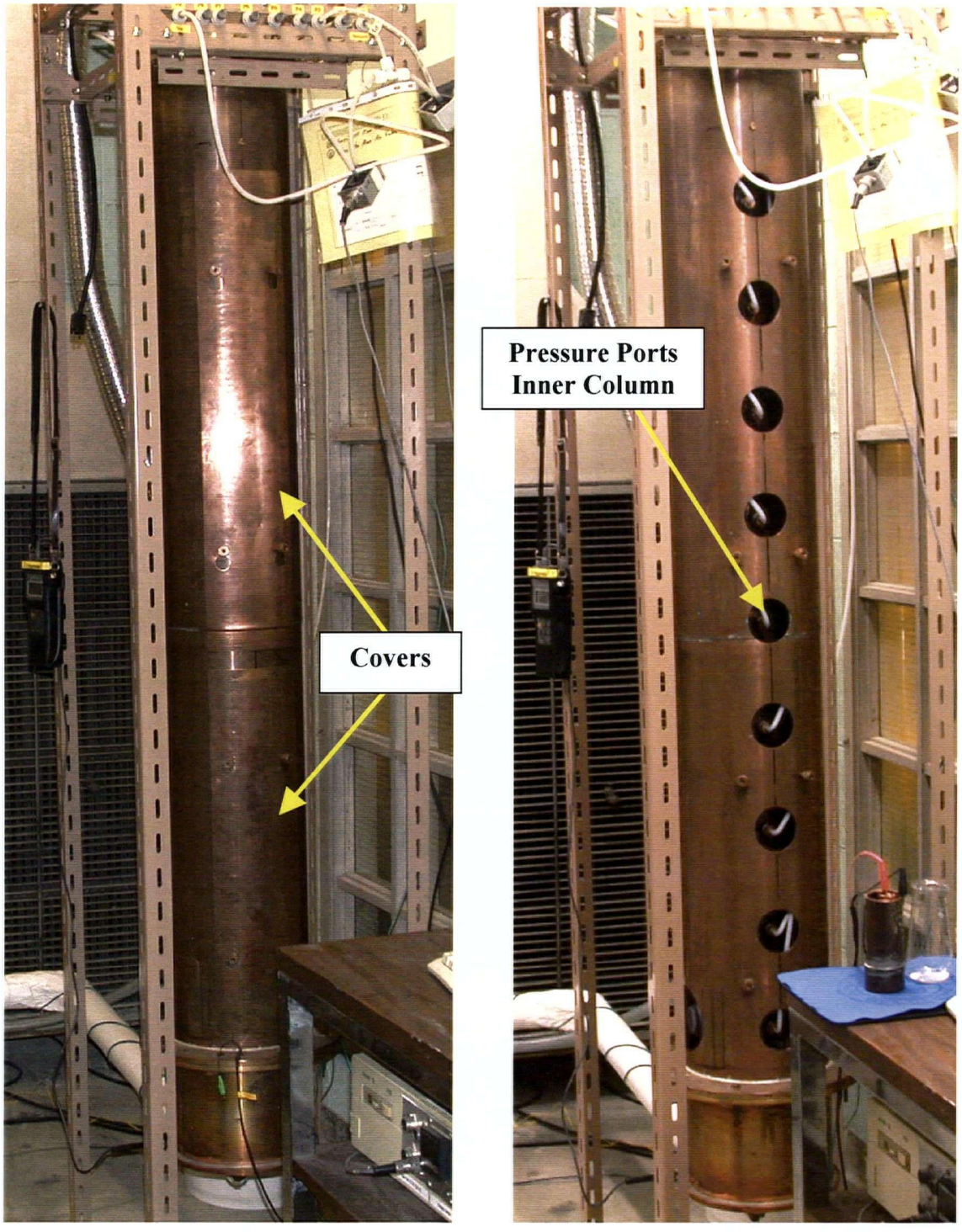

(a) (b)

Figure A.4. Photograph of Faraday cup fluidization column (side view). (a) With cover; (b) without cover.

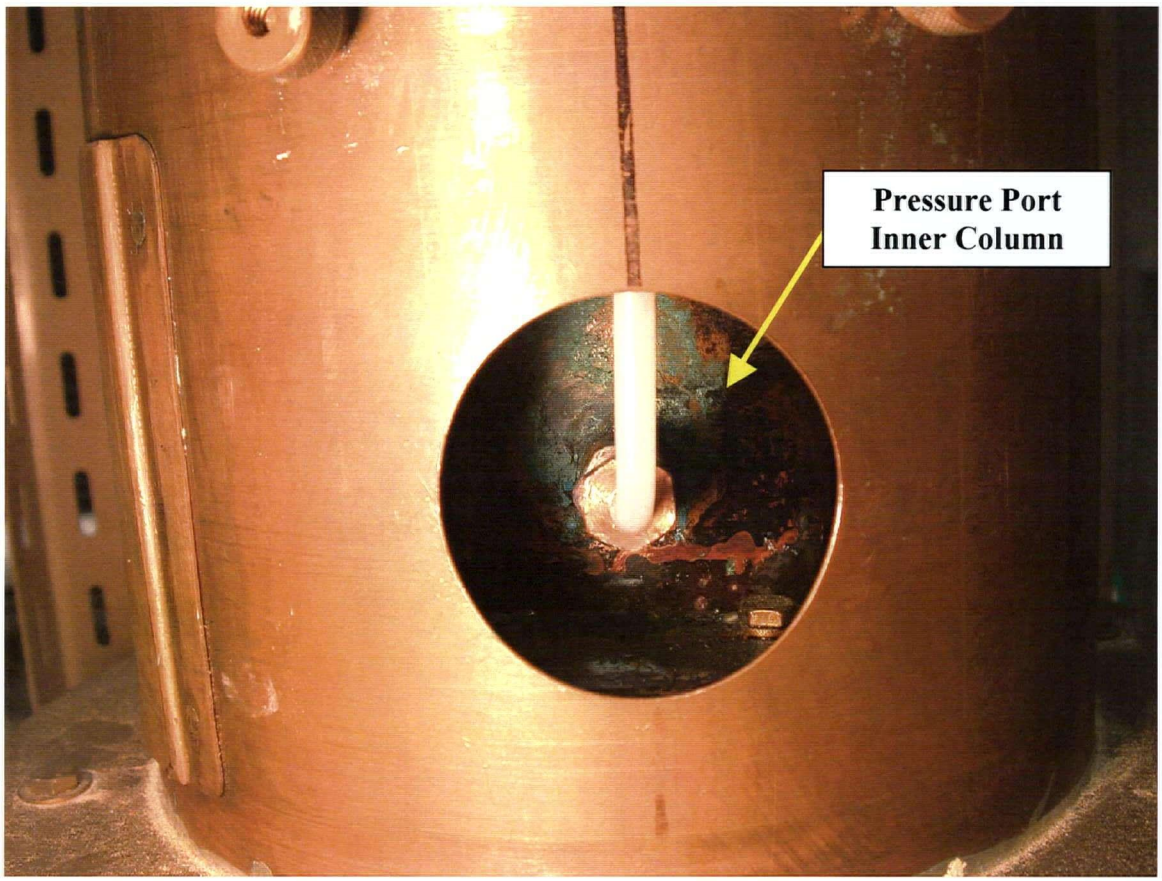

Figure A.5. Close-up of Faraday cup fluidization column (side view).

A.3 . Humidification system

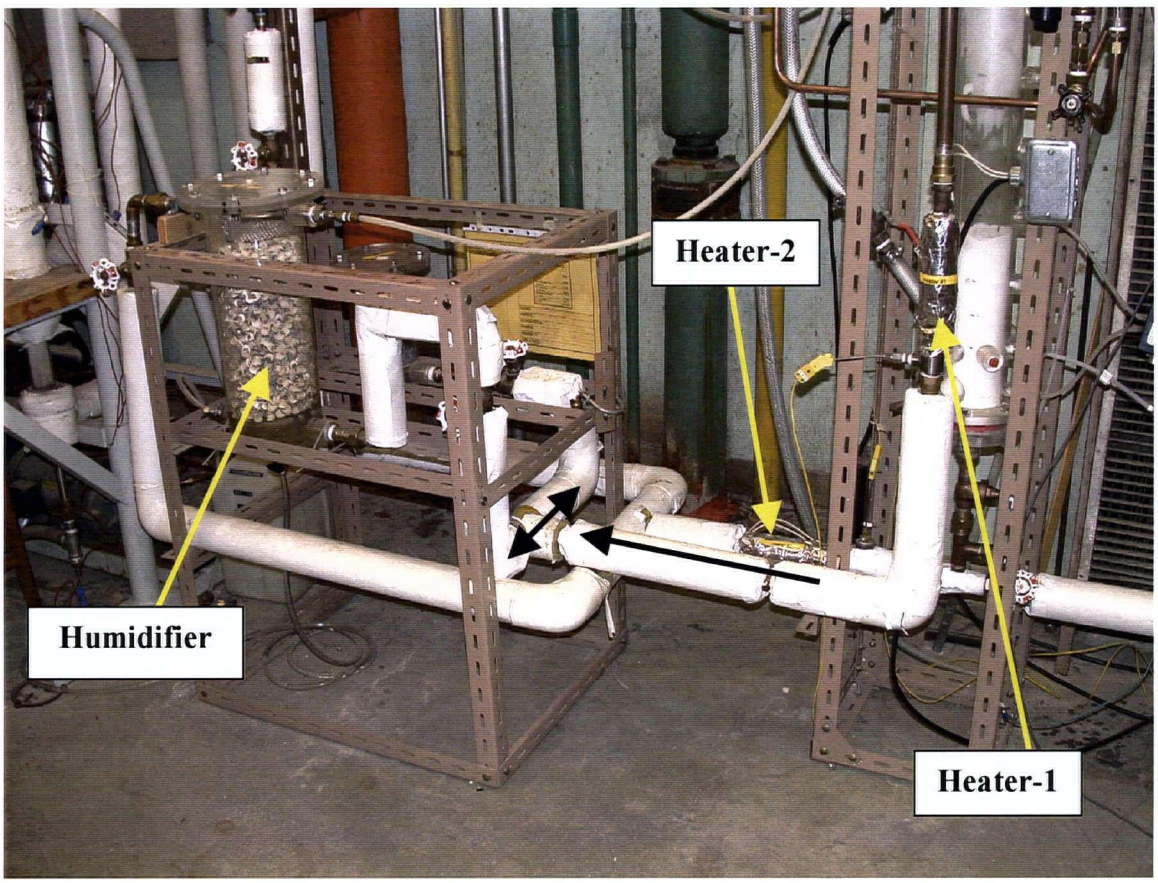

Figure A.6. Fluidizing gas humidification system.

A.4 . Double Faraday cup system

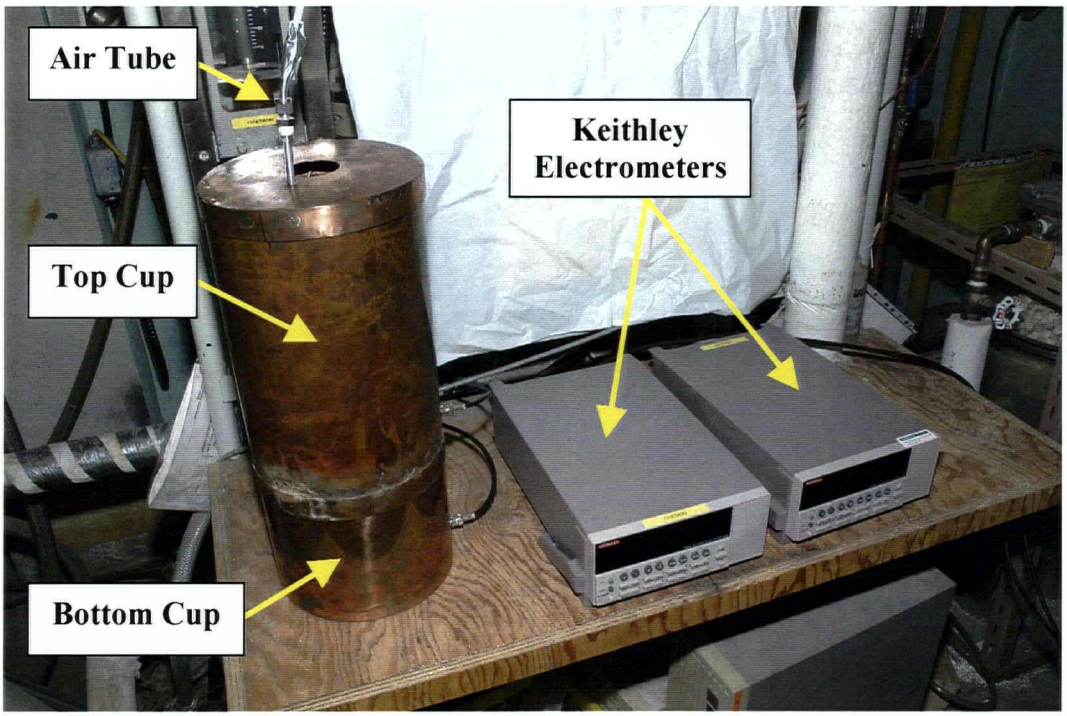

Figure A.7. Photograph of double Faraday cup system.

Figure A.8. Photograph of double Faraday cup system (with two cups separated).

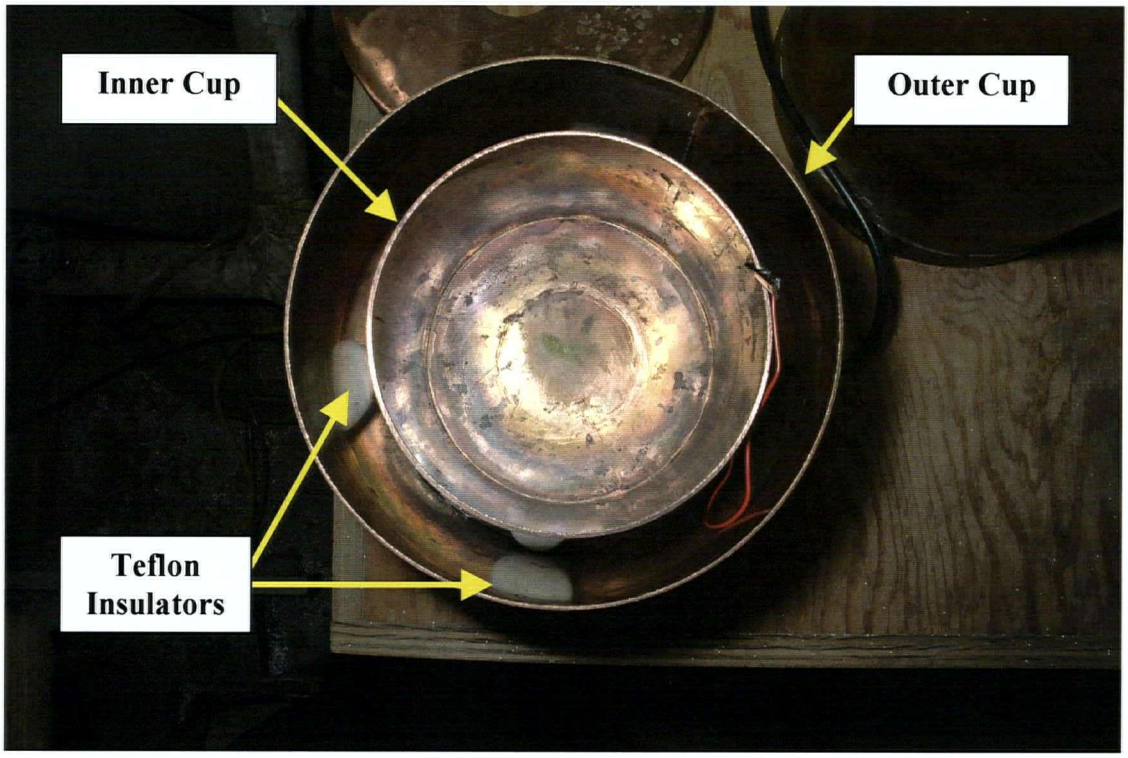

Figure A.9. Bottom Faraday cup.

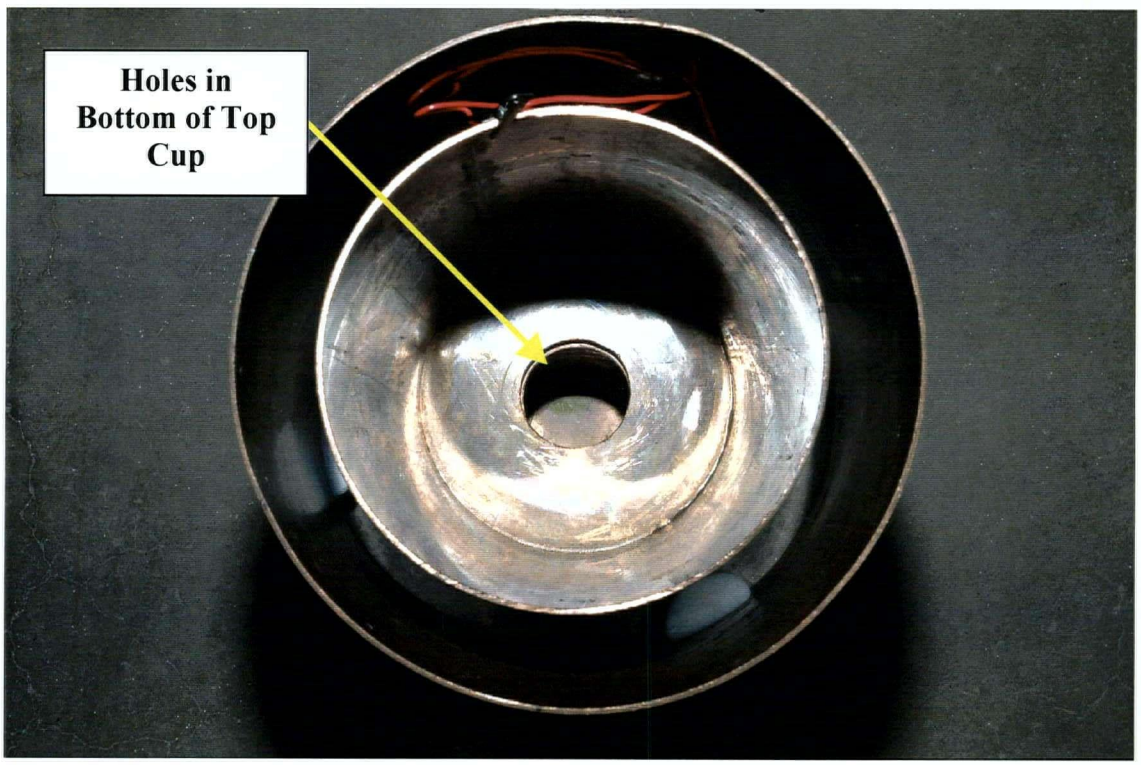

Figure A.10. Top Faraday cup.

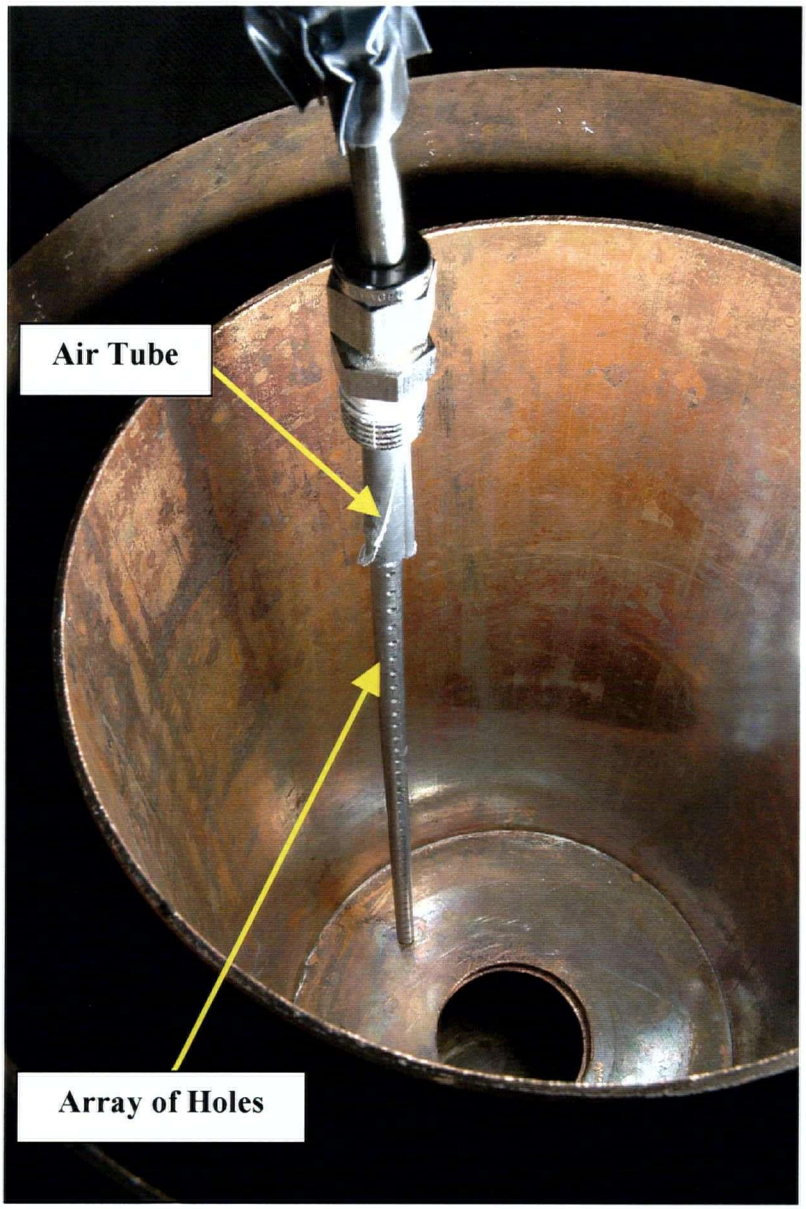

Figure A.11. Photograph of air tube inside top cup.

Appendix B- Particles Size Distribution Graphs

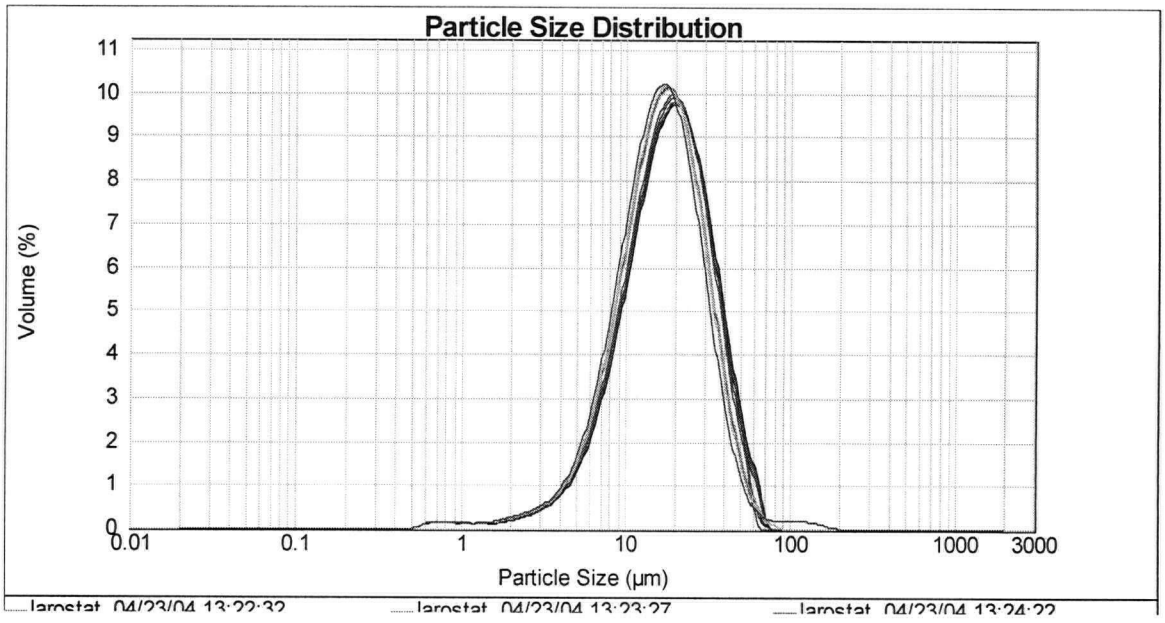

Figure B-1. Particle size distribution of Larostat 519 particles.

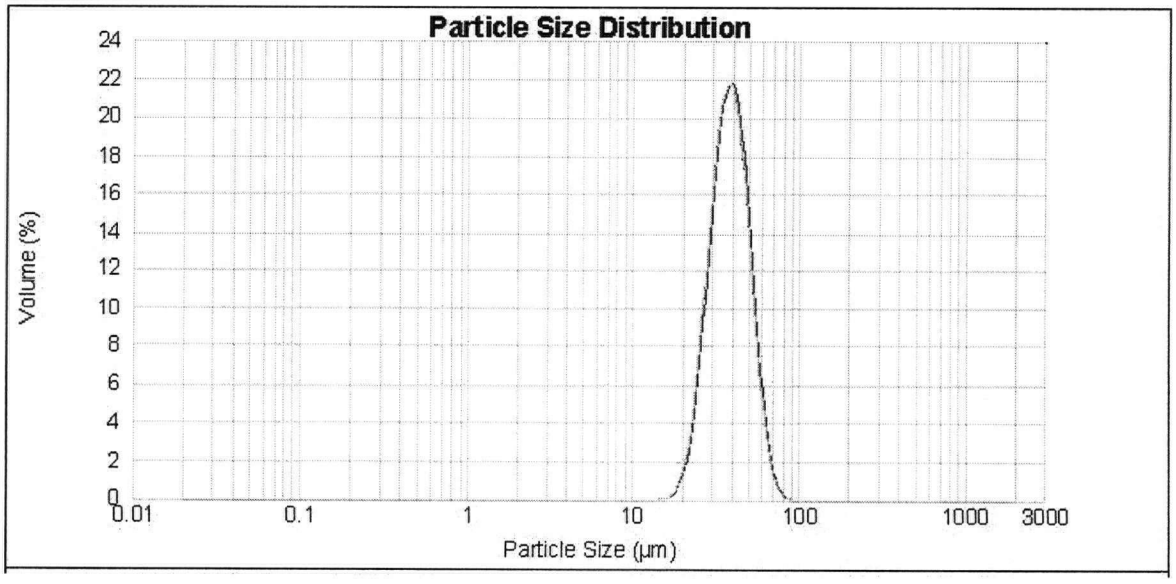

Figure B-2. Particle size distribution of GB I particles.

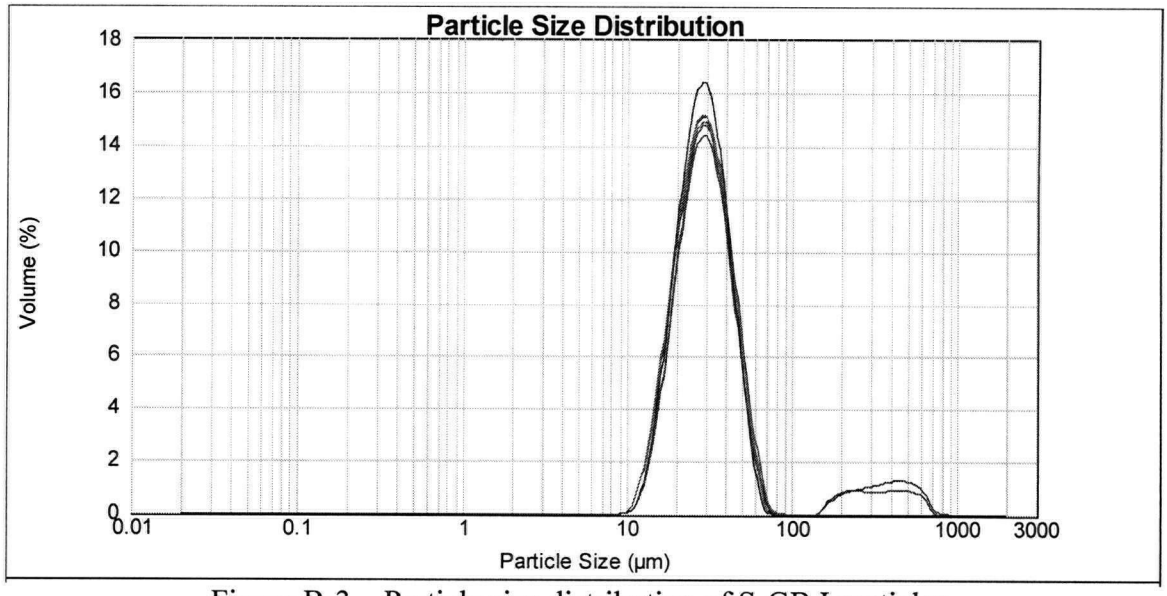

Figure B-3. Particle size distribution of S-GB I particles.

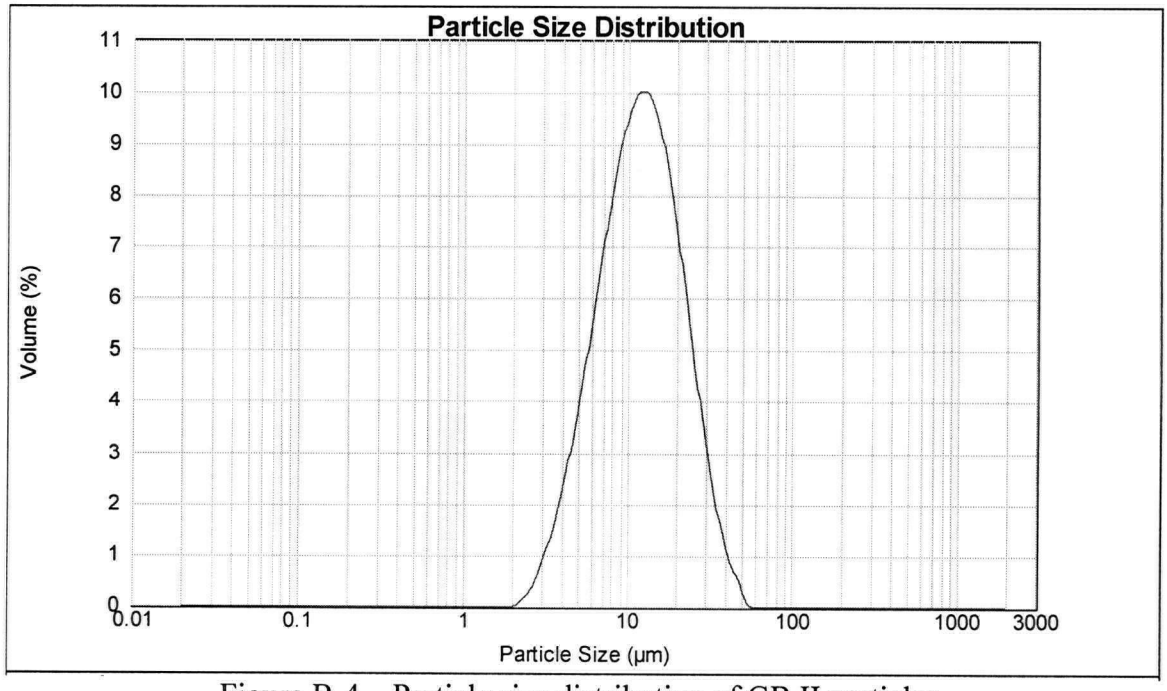

Figure B-4. Particle size distribution of GB II particles.

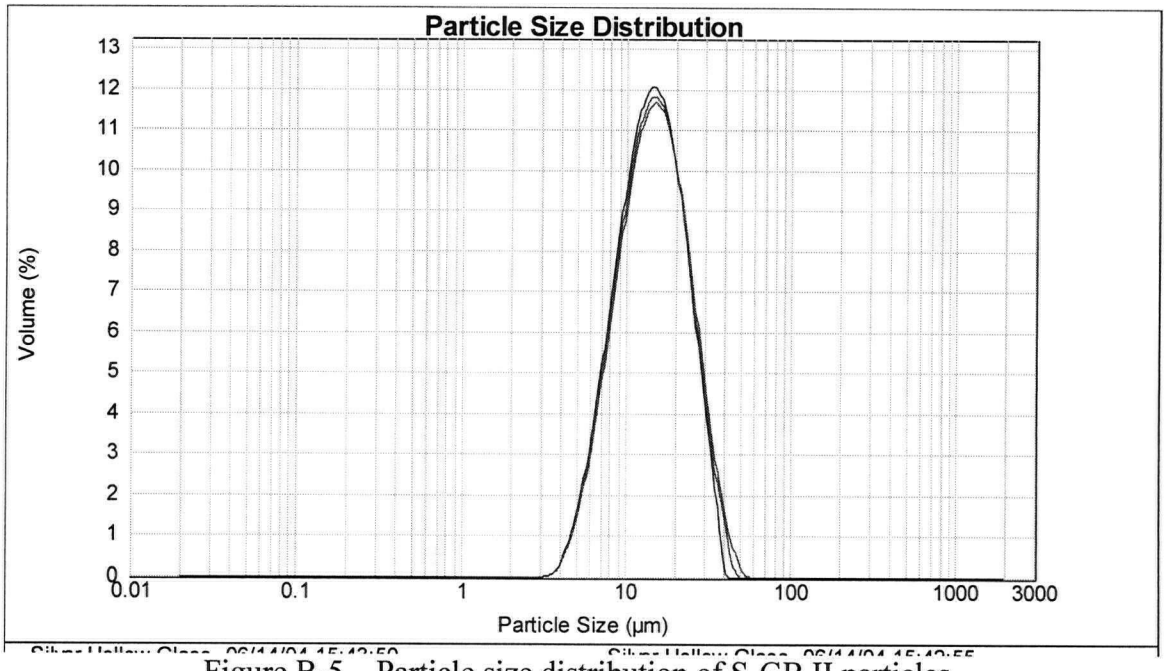

Figure B-5. Particle size distribution of S-GB II particles.

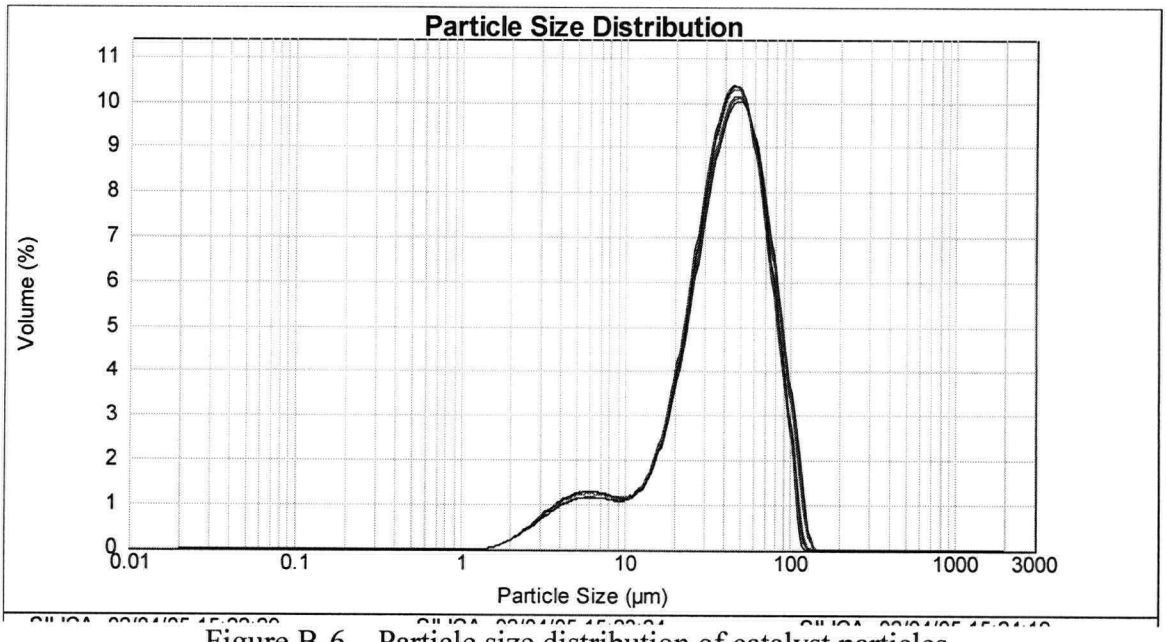

Figure B-6. Particle size distribution of catalyst particles.

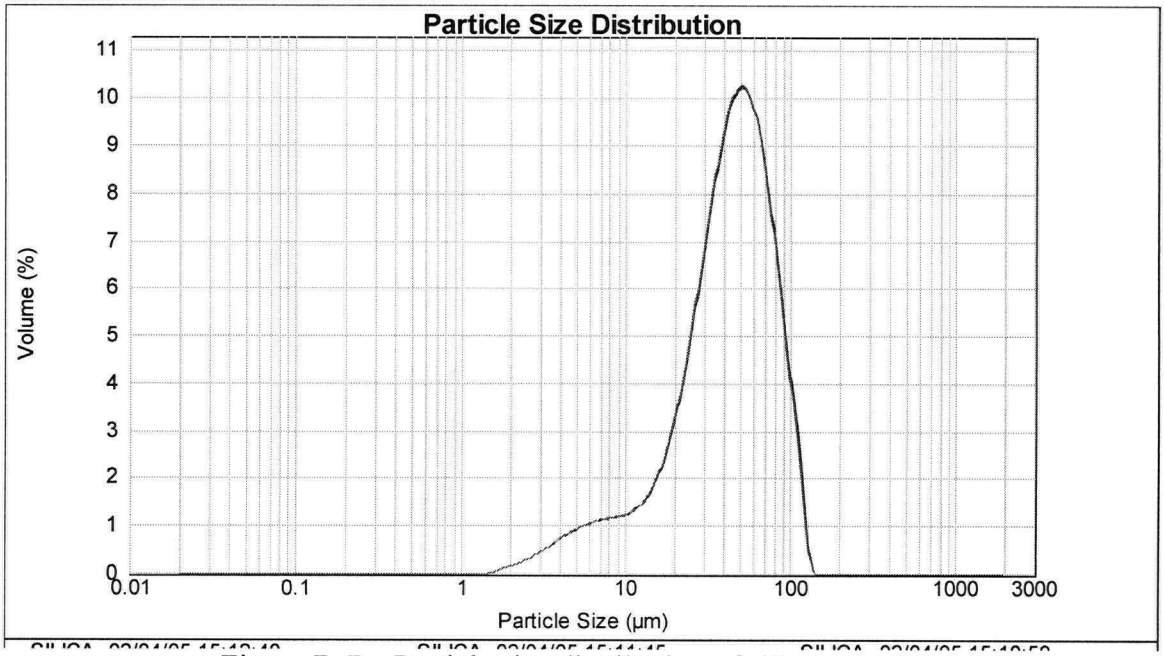

Figure B-7. Particle size distribution of silica particles.

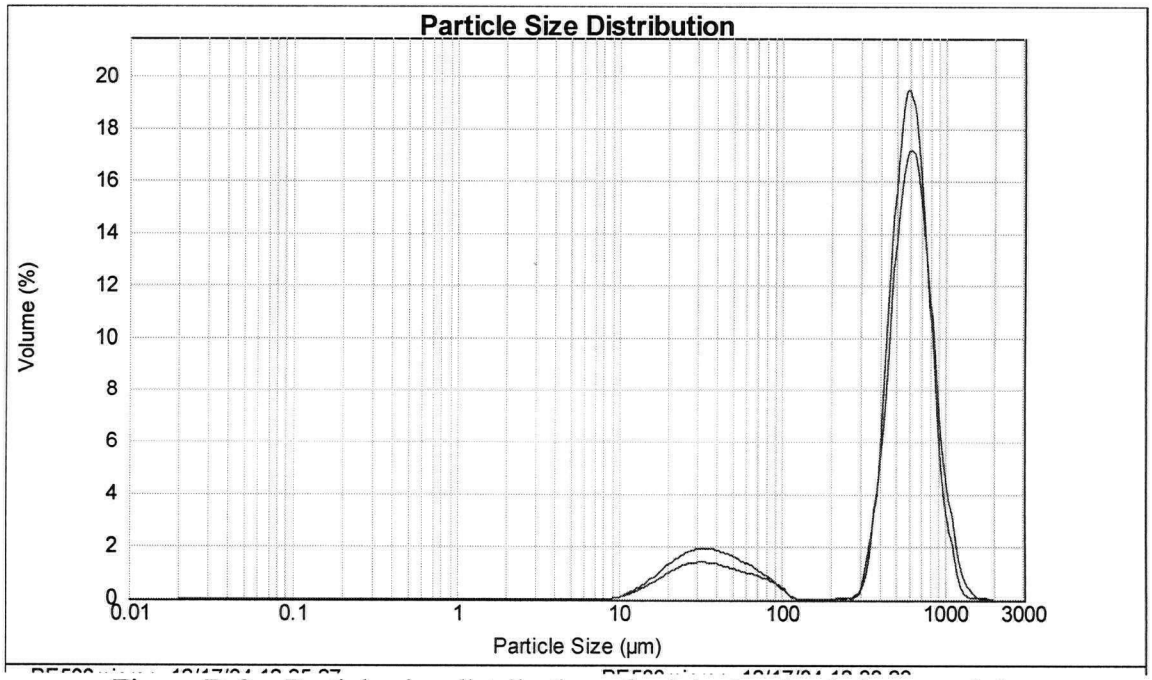

Figure B-8. Particle size distribution of original polyethylene particles.

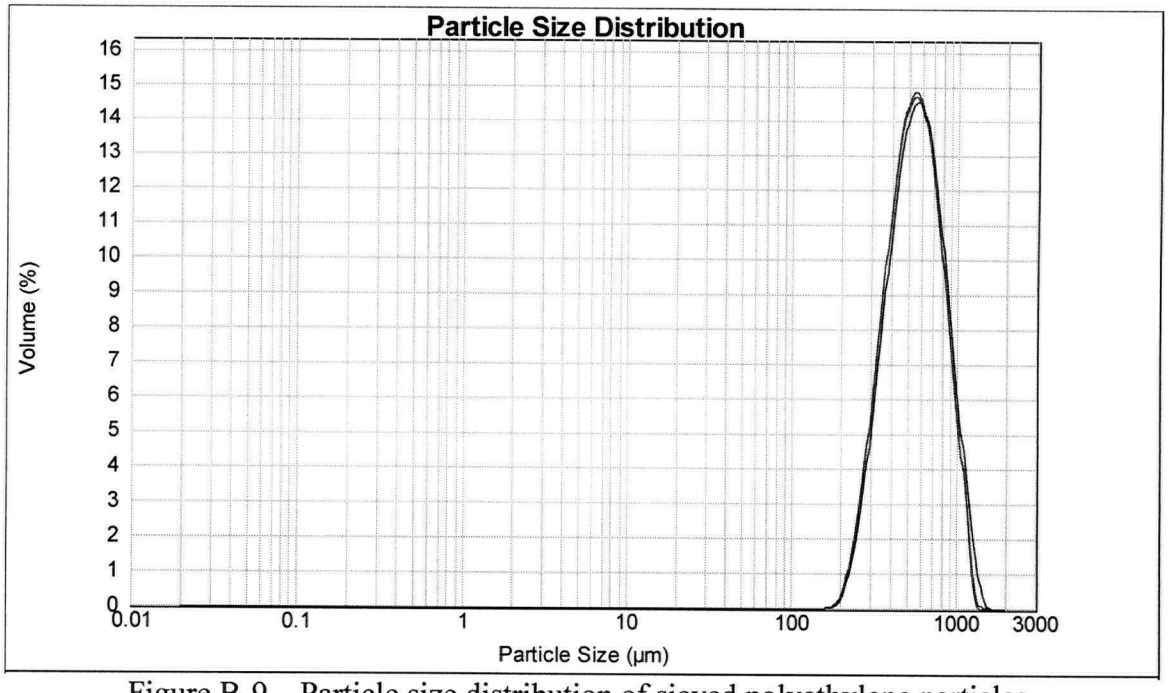

Figure B-9. Particle size distribution of sieved polyethylene particles.

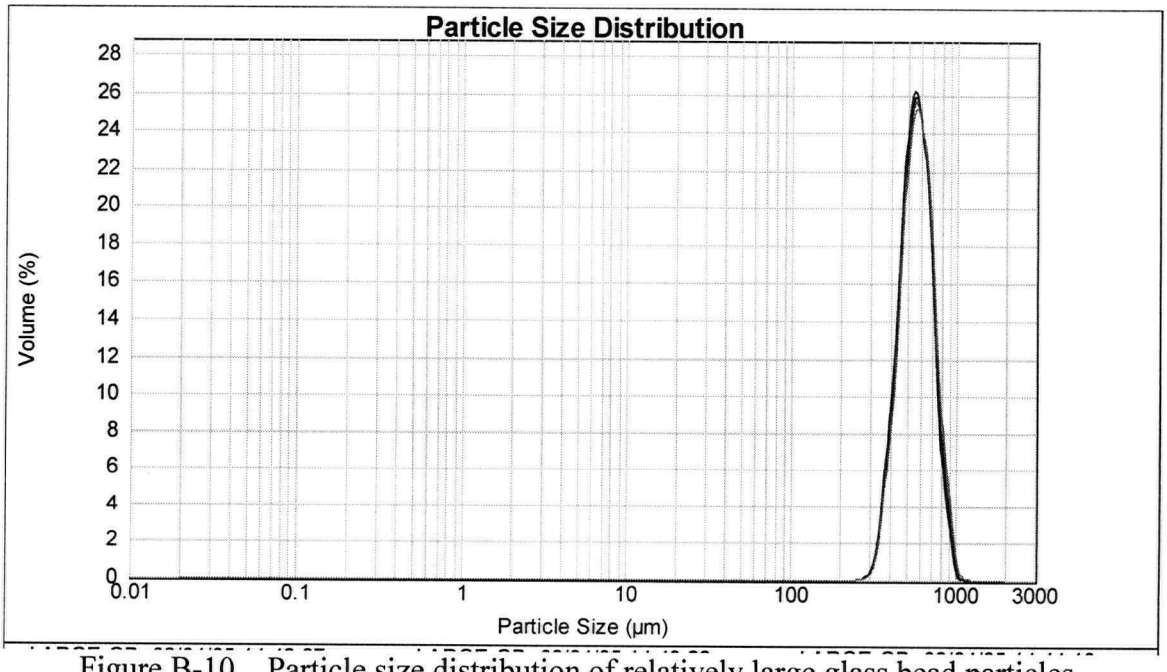

Figure B-10. Particle size distribution of relatively large glass bead particles.

Appendix C- Effect of the Removal of Teflon Piece from Inner Column

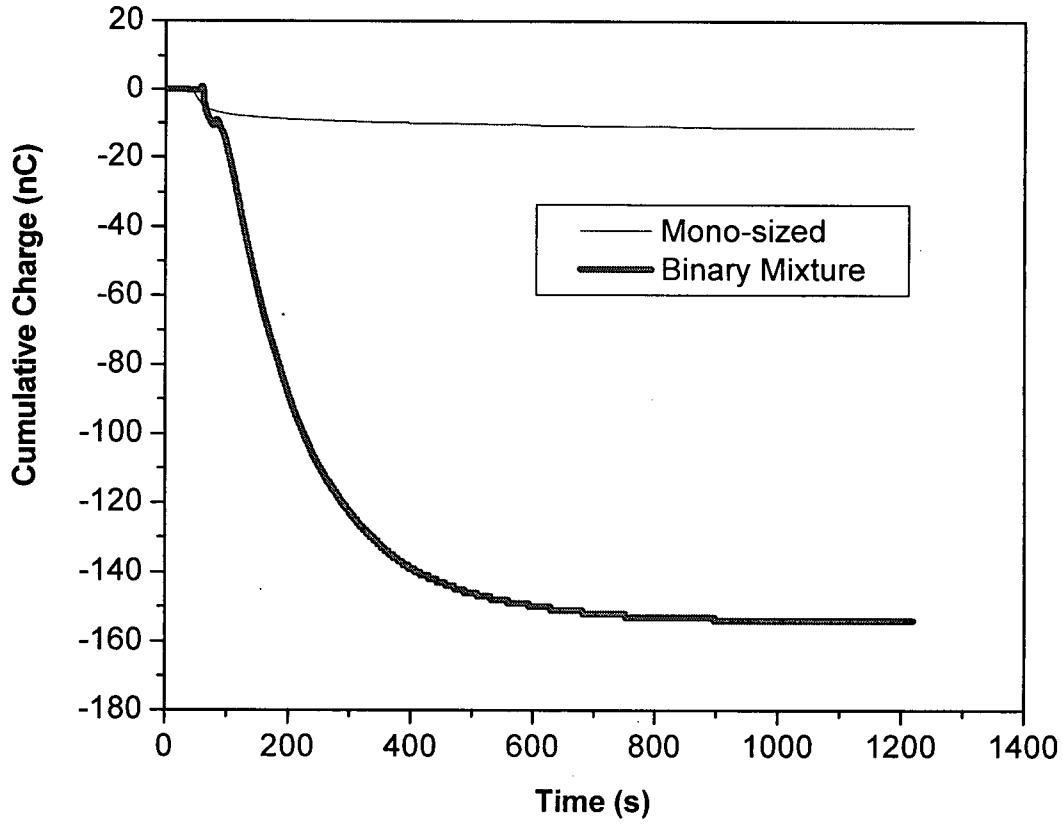

Figure C.1. Charges measured while fluidizing mono-sized and binary mixture of large glass beads with GB I as added fines without the Teflon piece but with filter system. RH=0%; superficial air velocity: 0.22 m/s; bed depth: 0.2 m; fines proportion: 0.2 wt%.

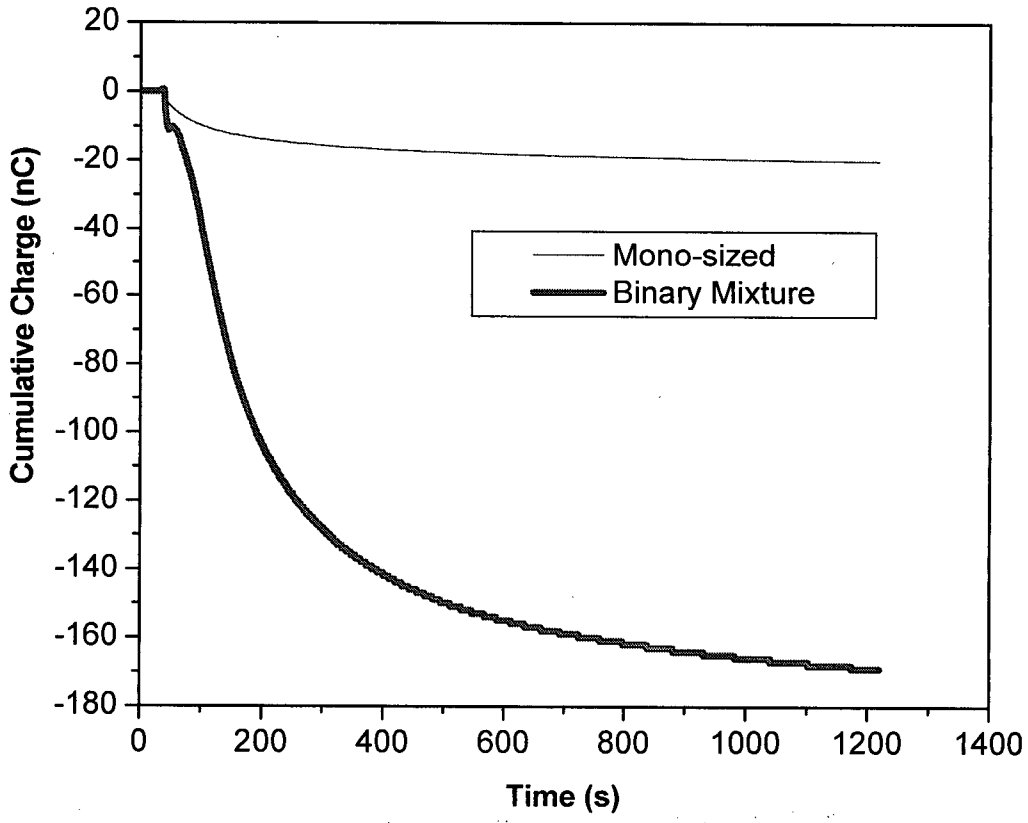

Figure C.2. Charges measured while fluidizing mono-sized and binary mixture of large glass beads with GB I as added fines without the Teflon piece and filter system. RH=0%; superficial air velocity: 0.22 m/s; bed depth: 0.2 m; fines proportion: 0.2 wt%.

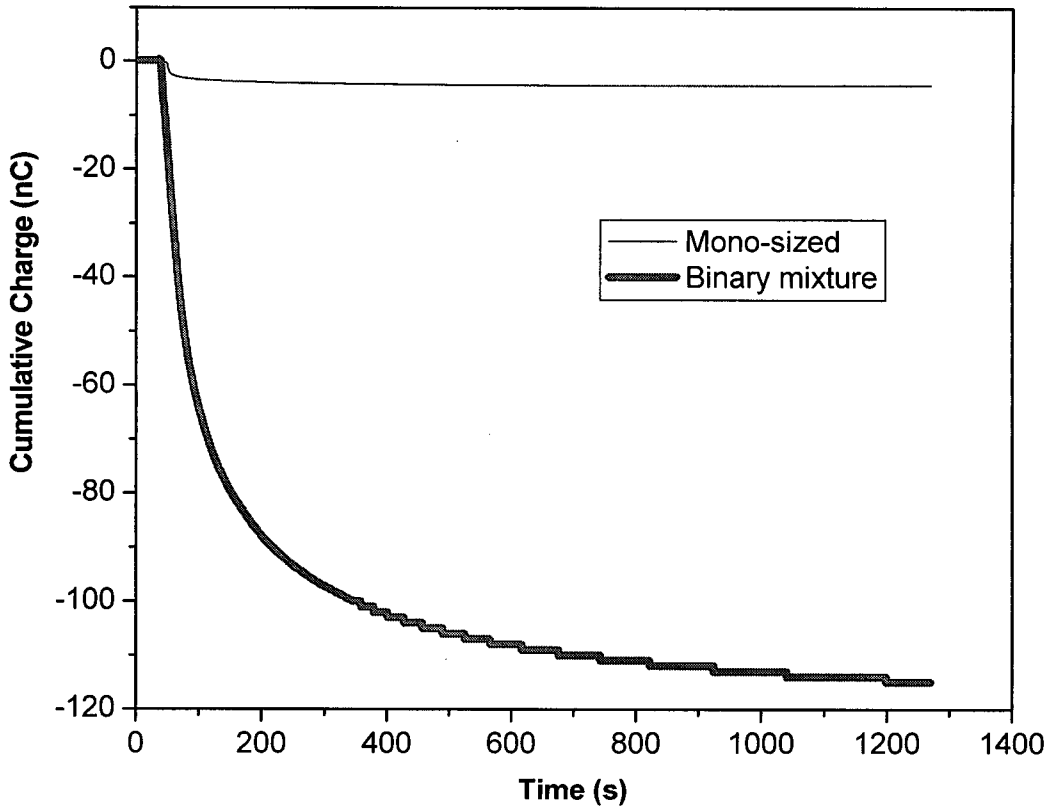

Figure C.3. Charges measured while fluidizing mono-sized and binary mixture of large glass beads with GB I as added fines with the Teflon piece and filter system in place. RH=0%; superficial air velocity: 0.22 m/s; bed depth: 0.2 m; fines proportion: 0.2 wt%.

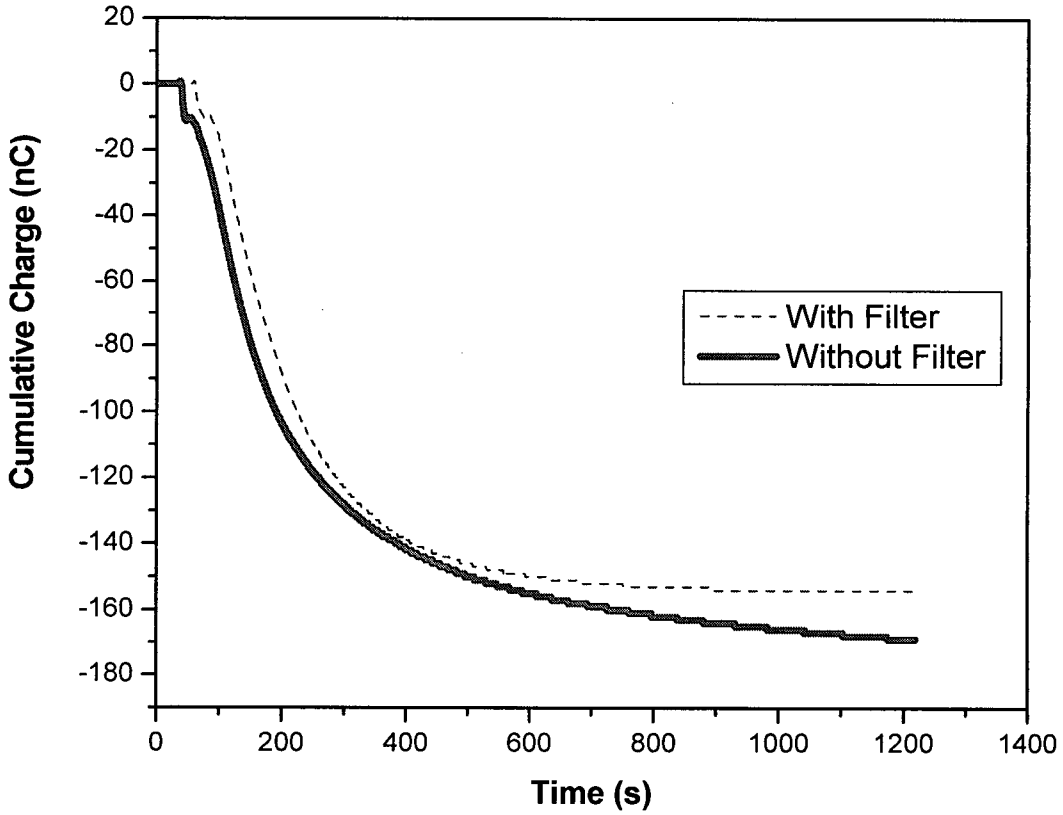

Figure C.4. Charge measurement reproducibility based on the results presented in Figures C1 and C2.

Appendix D- Bench-Scale Laboratory Results with Error Bars Present

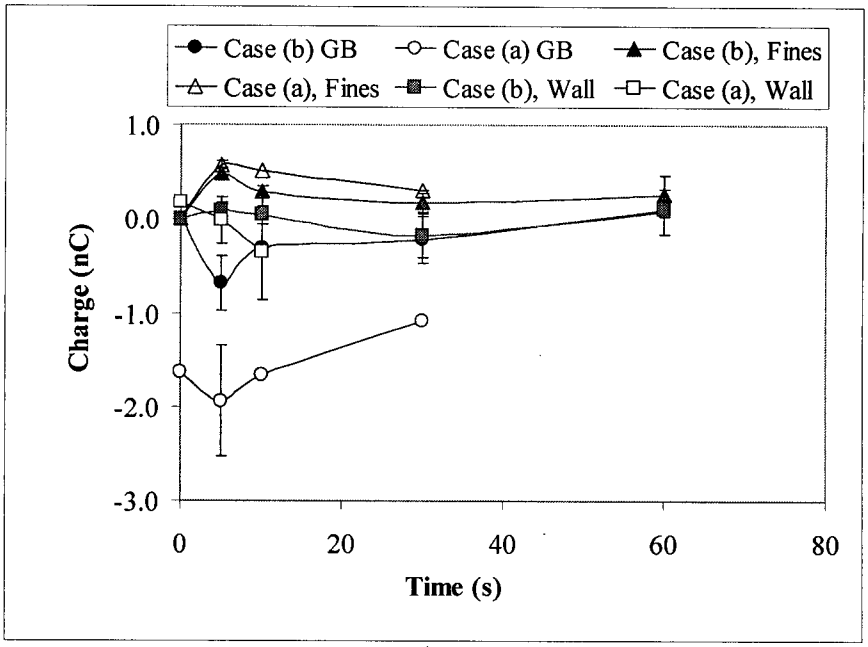

Figure D.1. Effect of addition of Larostat 519 for cases (a) & (b) in glass flask (otherwise = Figure 4.4). (Case (a): 09/09/05, Ambient RH ≈ 35%; Case (b): 09/03/04, Ambient RH ≈ 40%)

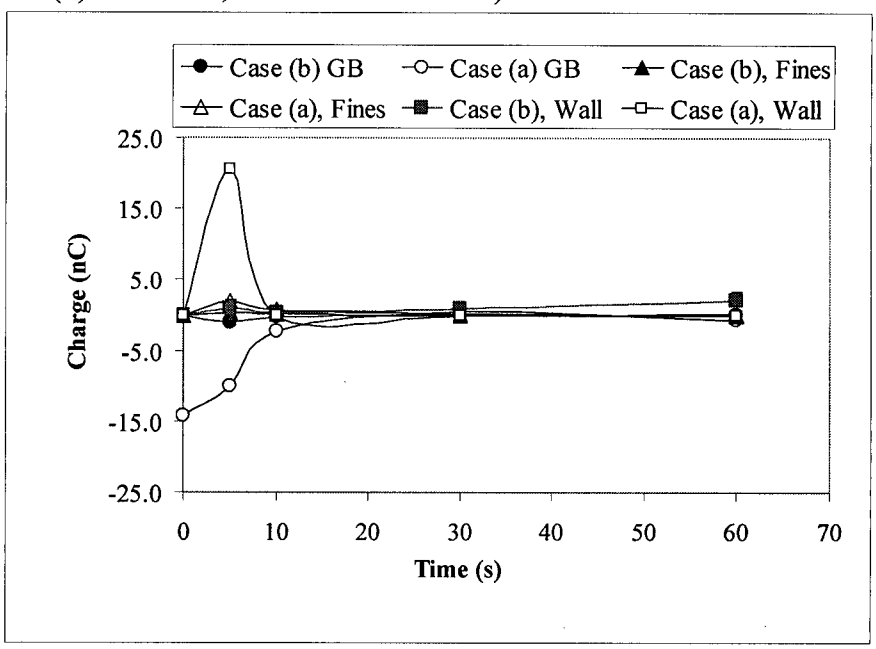

Figure D.2. Effect of addition of Larostat 519 for cases (a) & (b) in copper flask (otherwise = Figure 4.5). (Case (a): 09/09/05, Ambient RH ≈ 35%; Case (b): 09/03/04, Ambient RH ≈ 40%)

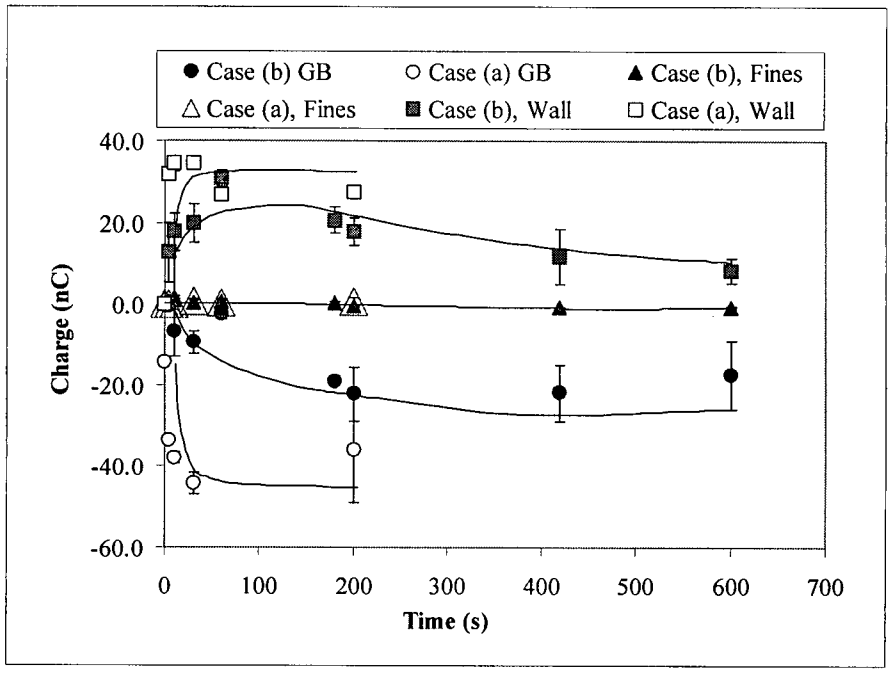

Figure D.3. Effect of addition of glass bead fines for cases (a) & (b) in glass flask (otherwise = Figure 4.6). (Case (a): 09/09/05, Ambient RH ≈ 35%; Case (b): 09/06/04, Ambient RH ≈ 55%)

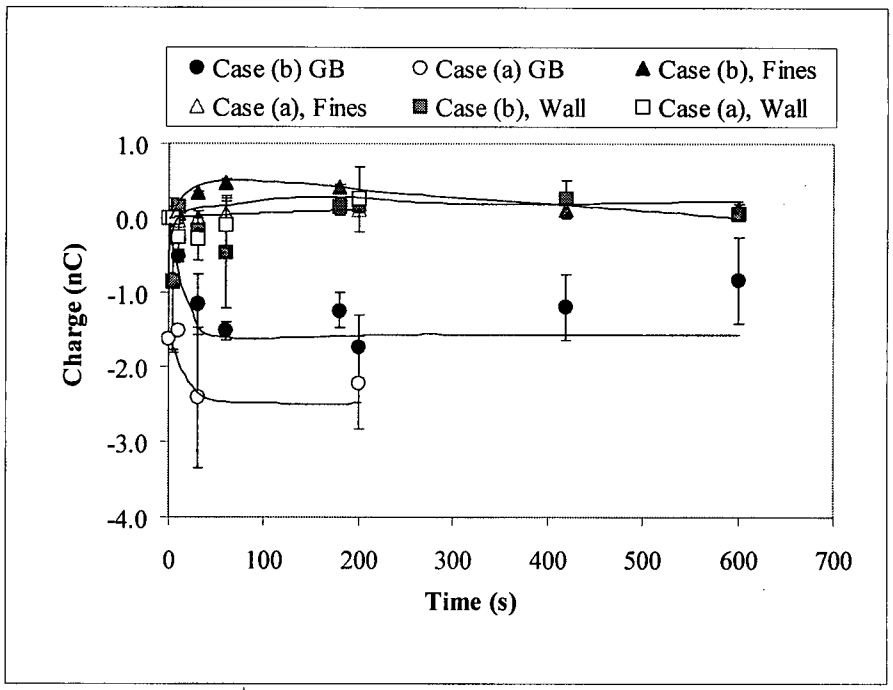

Figure D.4. Effect of addition of glass bead fines for cases (a) & (b) in copper flask (otherwise = Figure 4.7). (Case (a): 09/09/05, Ambient RH ≈ 35%; Case (b): 09/06/04, Ambient RH ≈ 55%)

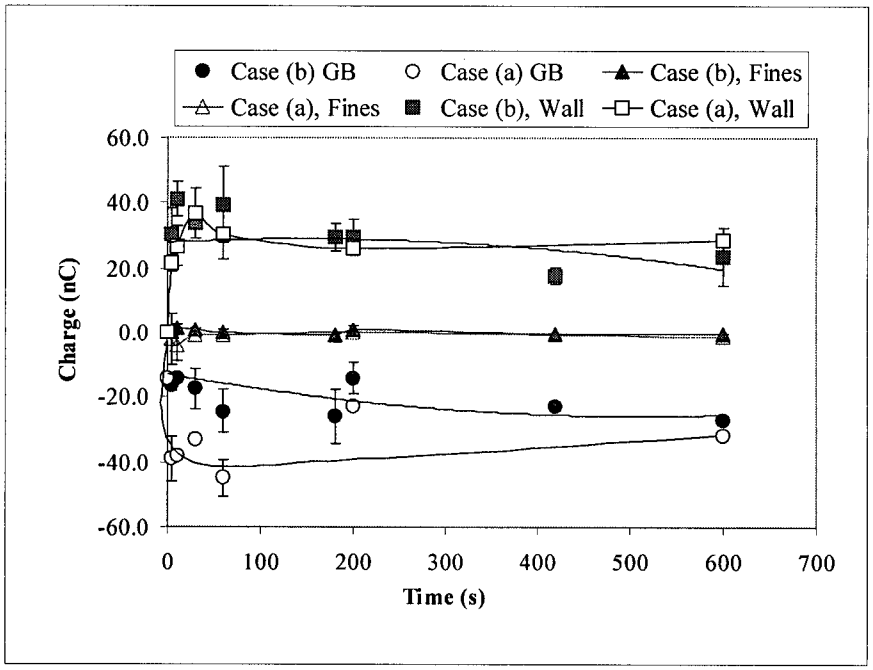

Figure D.5. Effect of addition of silver-coated glass bead fines for cases (a) & (b) in glass flask (otherwise = Figure 4.8). (Case (a): 09/09/05, Ambient RH ≈ 35%; Case (b): 09/07/04, Ambient RH ≈ 45%)

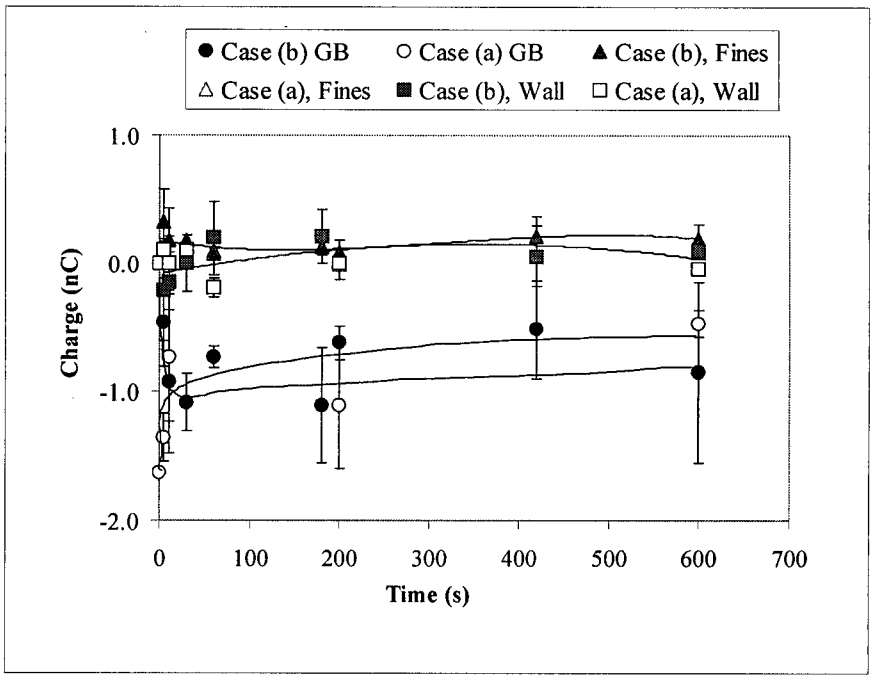

Figure D.6. Effect of addition of silver-coated glass bead fines for cases (a) & (b) in copper flask (otherwise = Figure 4.9). (Case (a): 09/09/04, Ambient RH ≈ 35%; Case (b): 09/07/04, Ambient RH ≈ 45%)

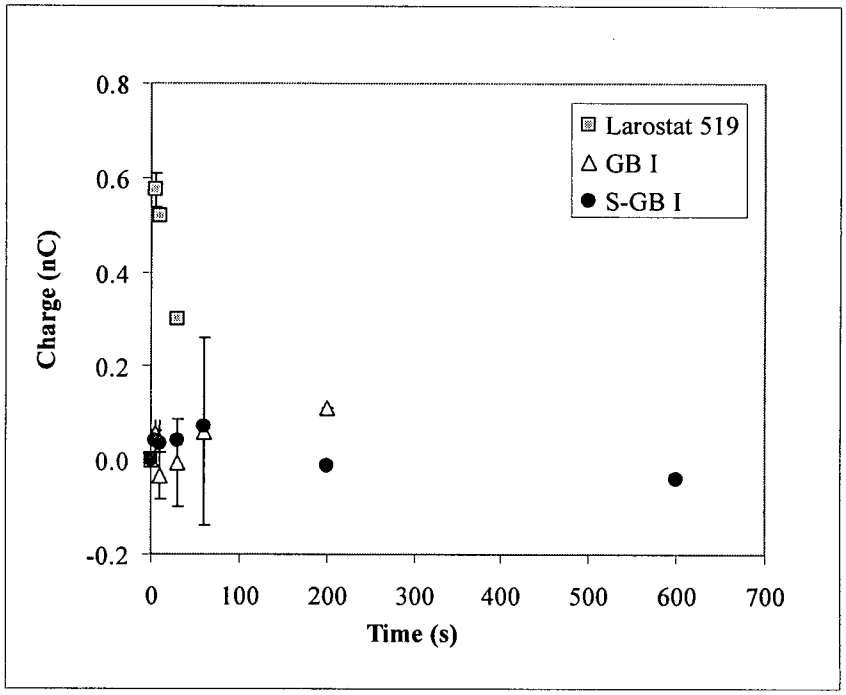

Figure D.7. Charges carried by different fines for case (a) in copper flask (otherwise = Figure 4.10).

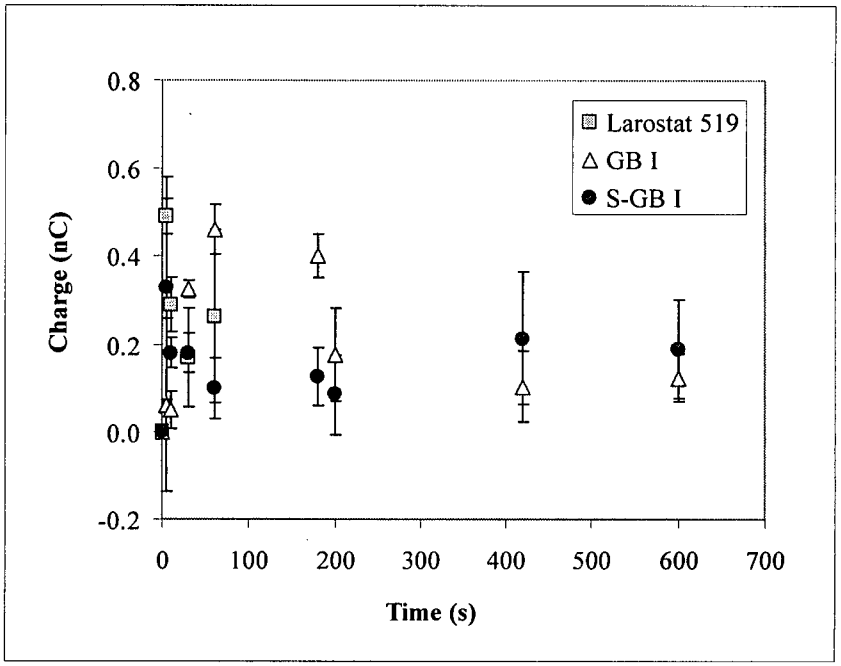

Figure D.8. Charges carried by different fines for case (b) in copper flask (otherwise = Figure 4.11).

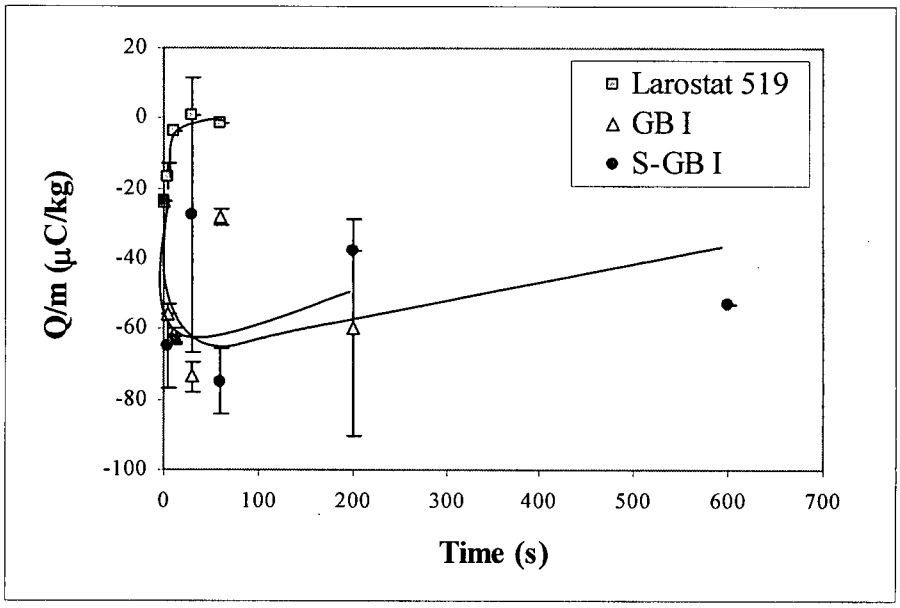

Figure D.9. Effect of addition of different fines on large glass beads for case (a) in glass flask (otherwise = Figure 4.12).

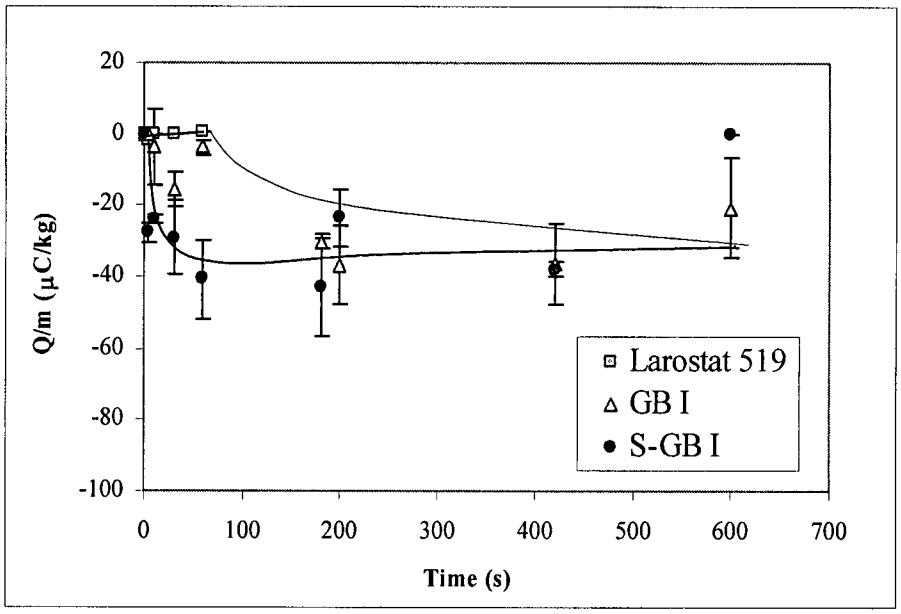

Figure D.10. Effect of addition of different fines on large glass beads for case (b) in glass flask (otherwise = Figure 4.13).

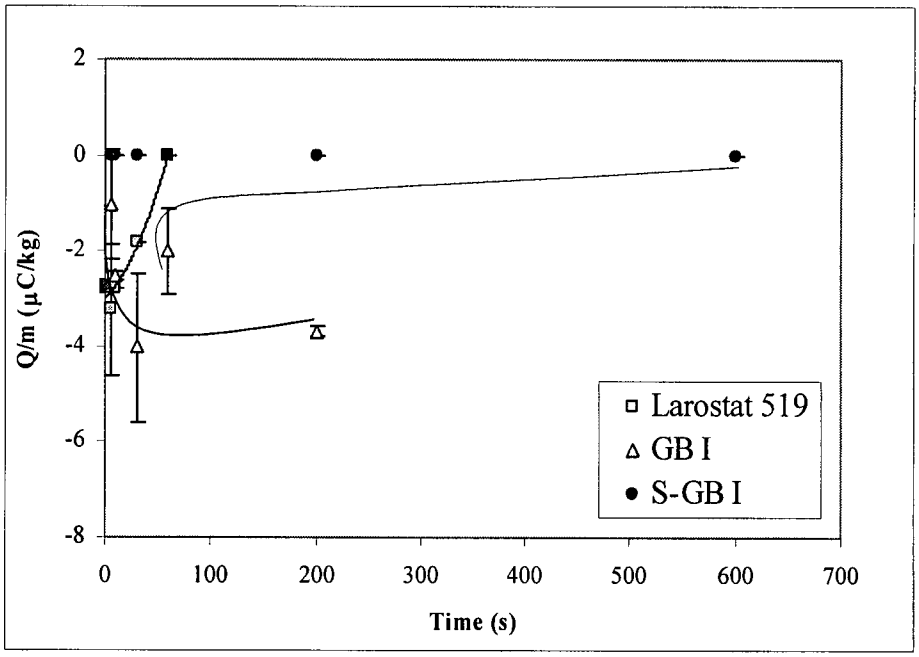

Figure D.11. Effect of addition of different fines on large glass beads for case (a) in copper flask (otherwise = Figure 4.14).

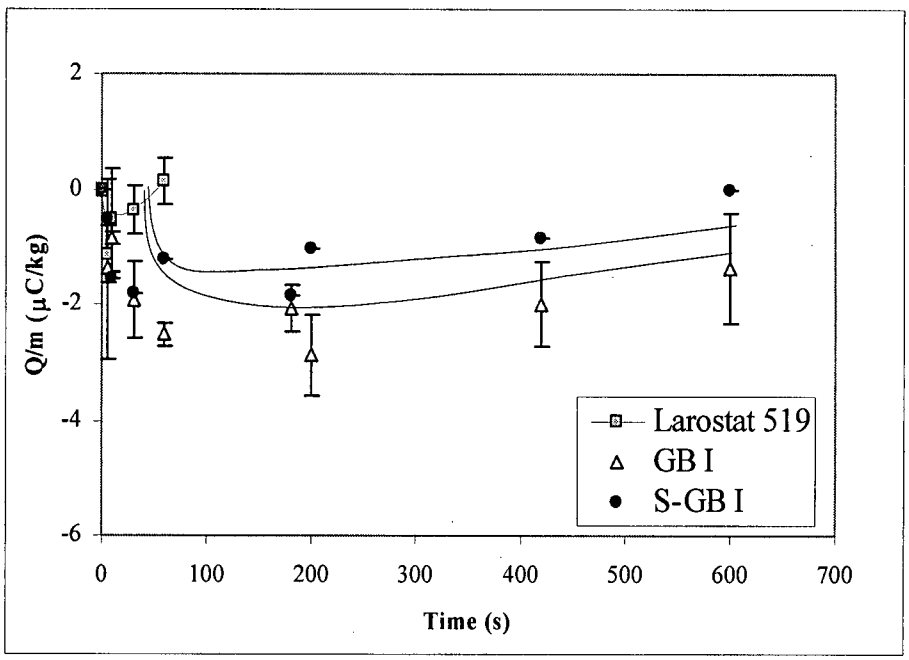

Figure D.12. Effect of addition of different fines on large glass beads for case (b) in copper flask (otherwise = Figure 4.15).

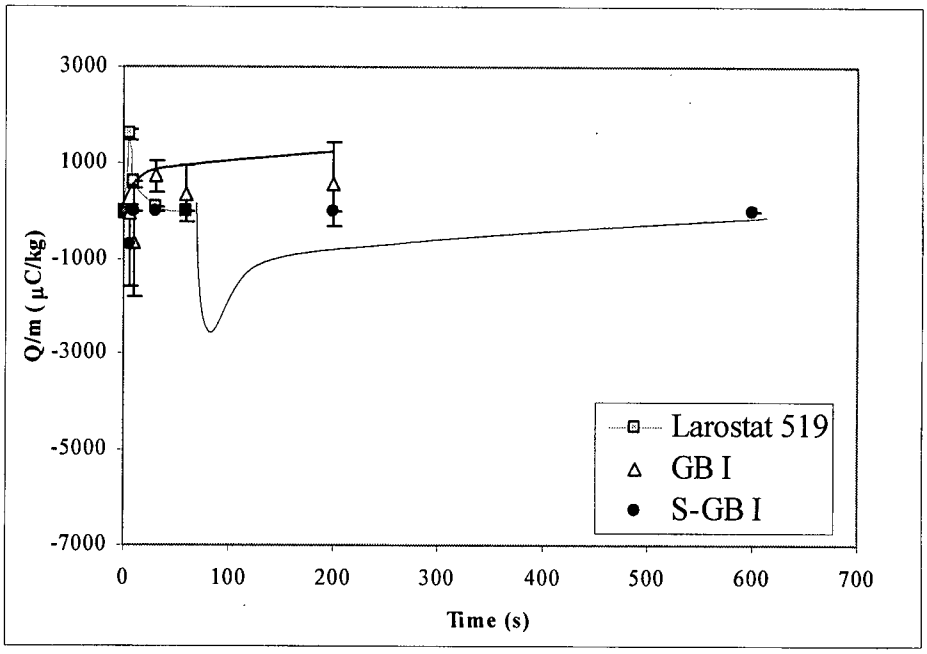

Figure D.13. Charges carried by different fines for case (a) in glass flask (otherwise = Figure 4.16).

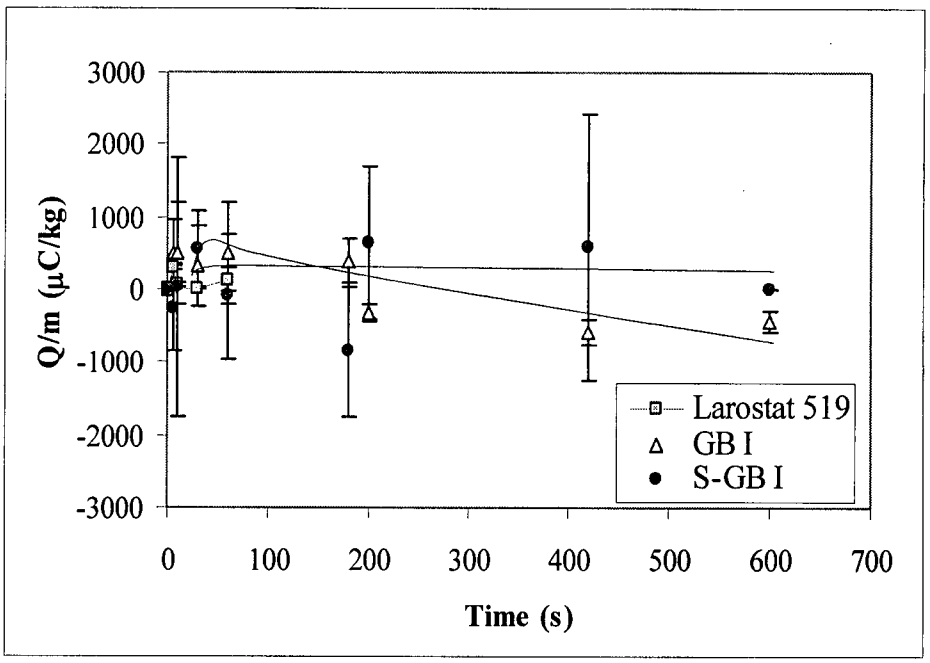

Figure D.14. Charges carried by different fines for case (b) in glass flask (otherwise = Figure 4.17).

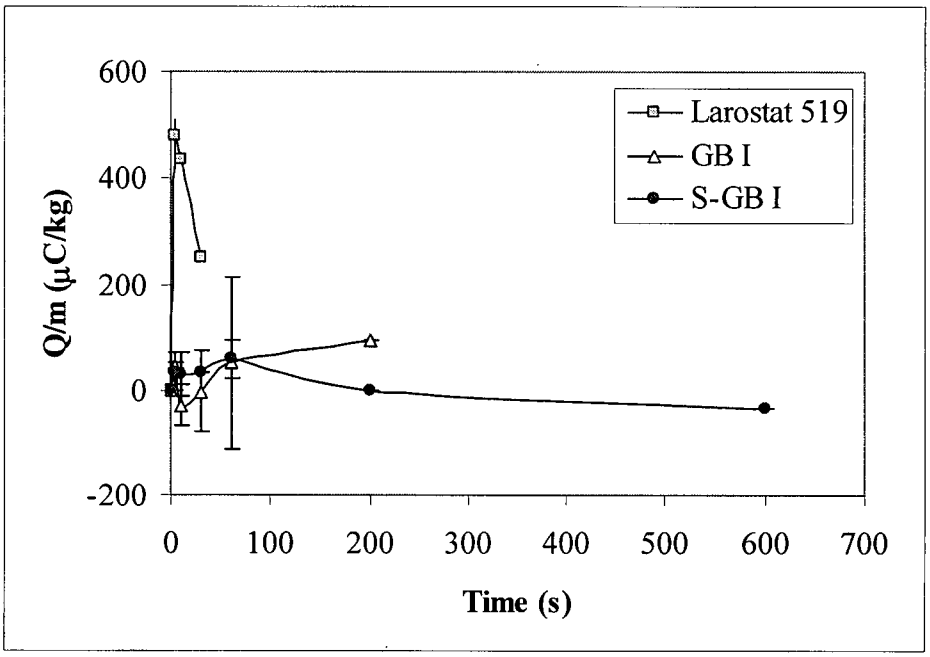

Figure D.15. Charges carried by different fines for case (a) in copper flask (otherwise = Figure 4.18).

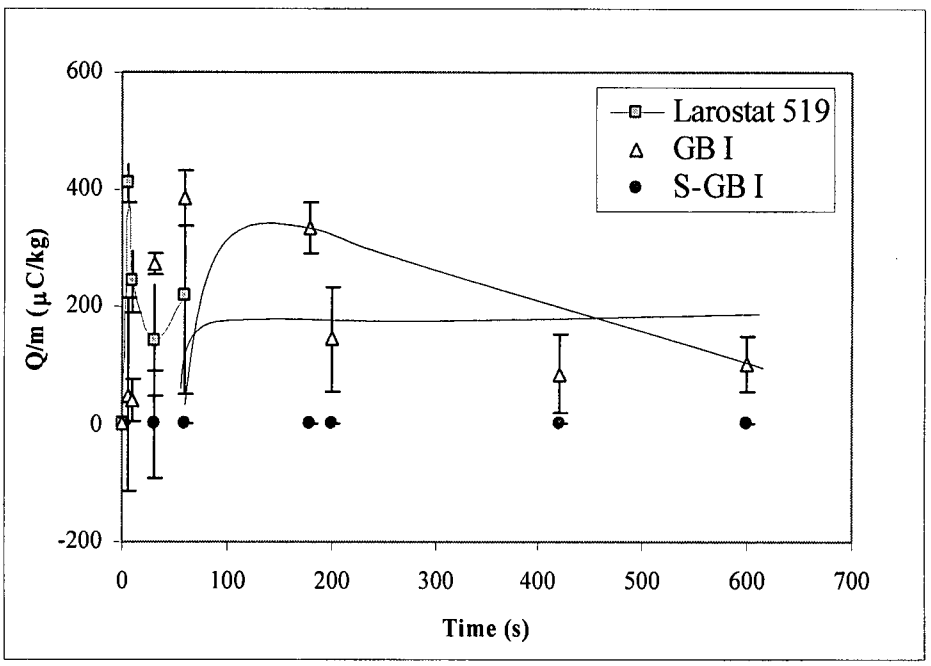

Figure D.16. Charges carried by different fines for case (b) in copper flask (otherwise = Figure 4.19).

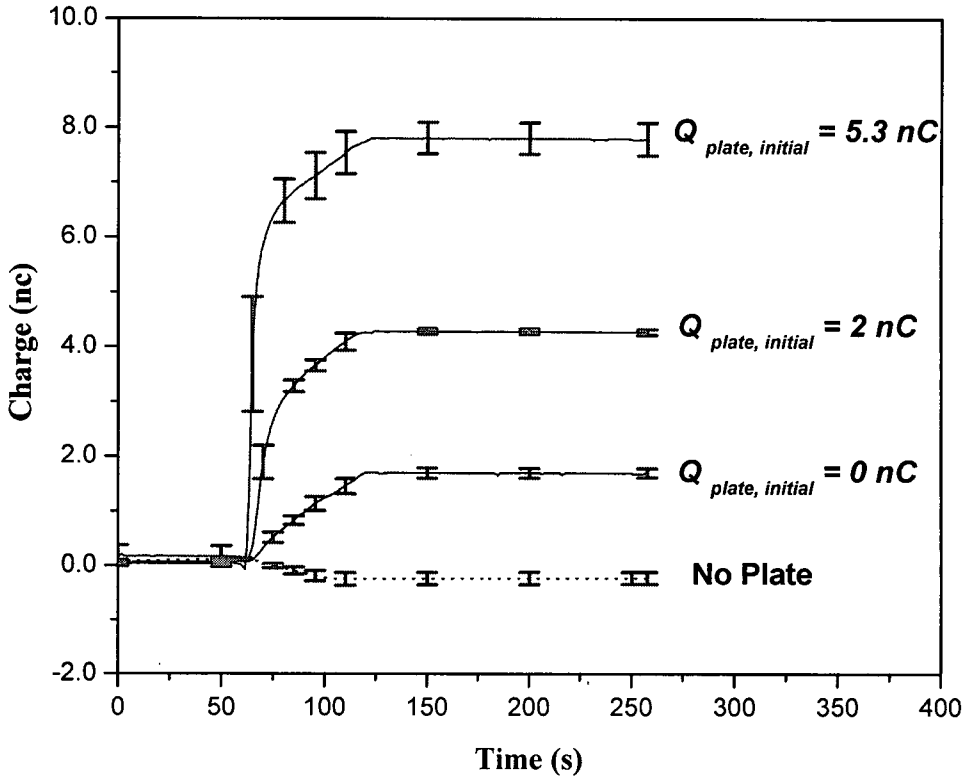

Figure D.17. Charges carried by Larostat 519 particles due to contact with copper plate of different initial charges with error bars shown (otherwise = Figure 4.22).

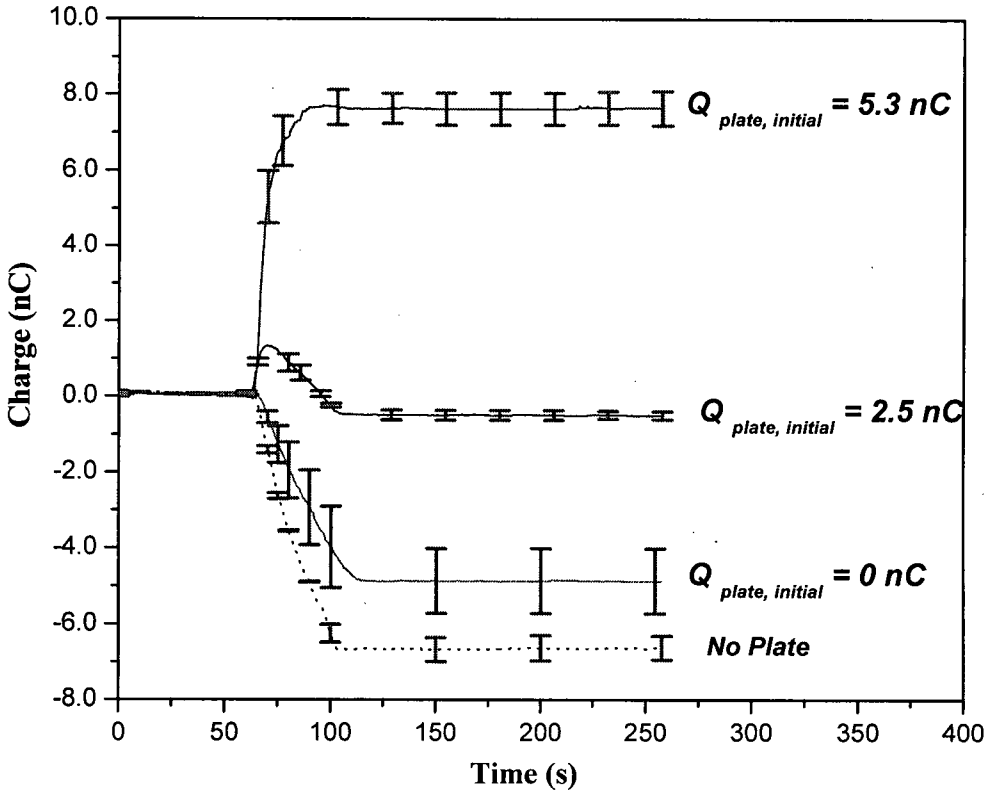

Figure D.18. Charges gained by fine glass beads due to contact with copper plate of different initial charges with error bars shown (otherwise = Figure 4.23).

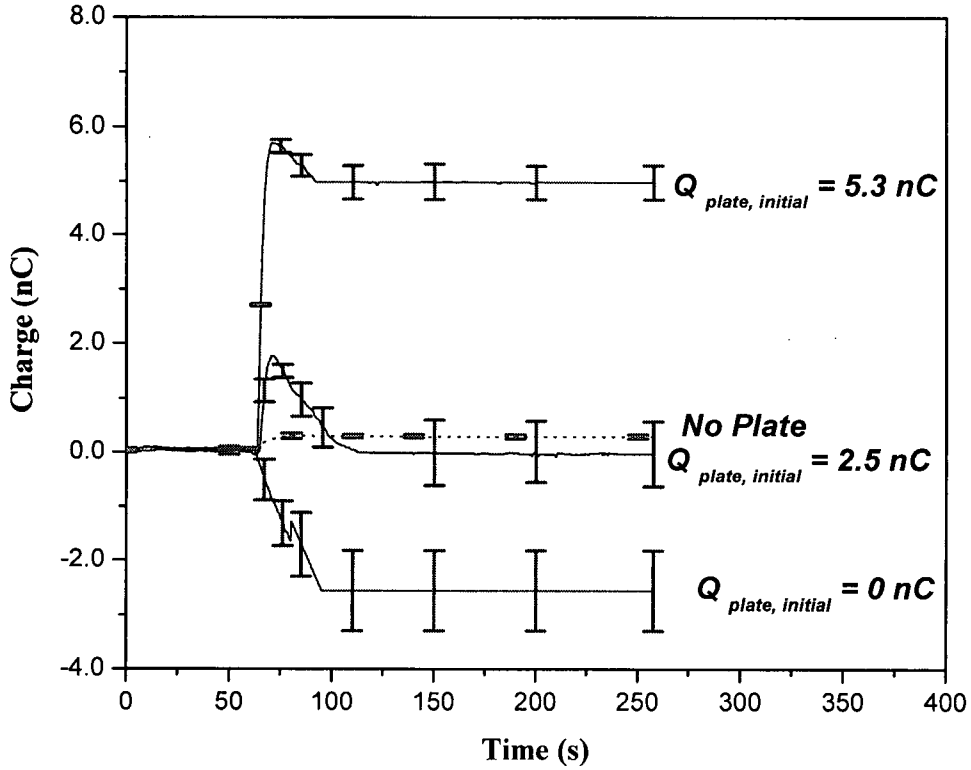

Figure D.19. Charges gained by silver-coated fine glass beads due to contact with copper plate of different initial charges with error bars shown (otherwise = Figure 4.24).

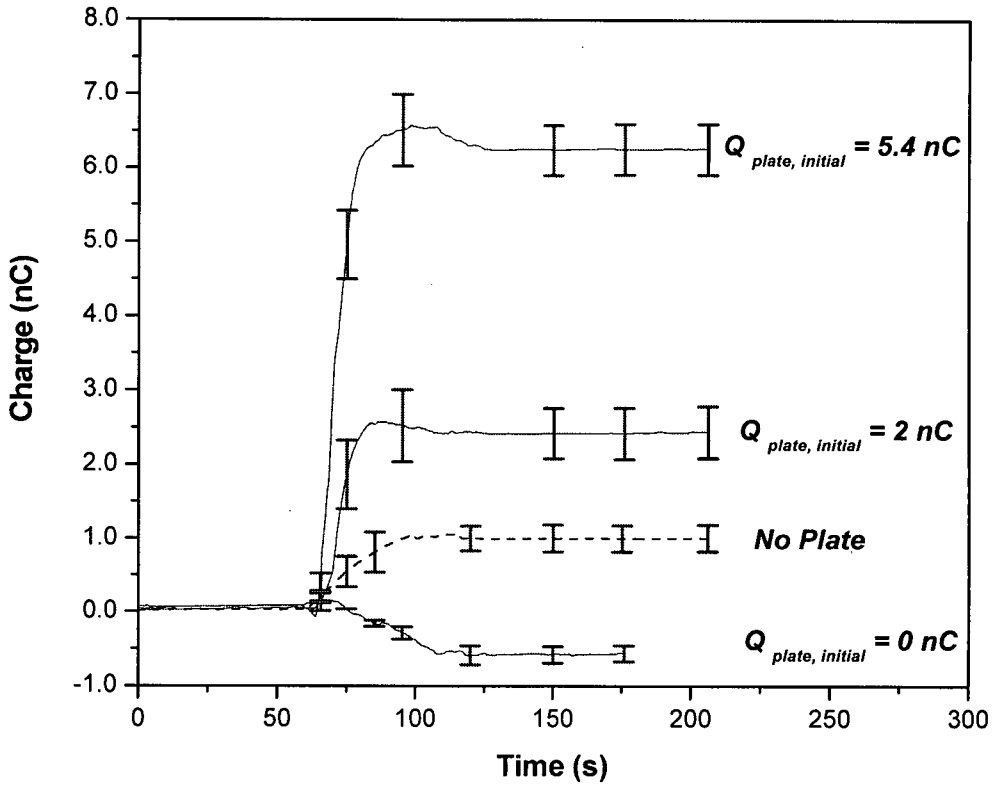

Figure D.20. Charges gained by catalyst particles due to contact with copper plate of different initial charges with error bars shown (otherwise = Figure 4.25).

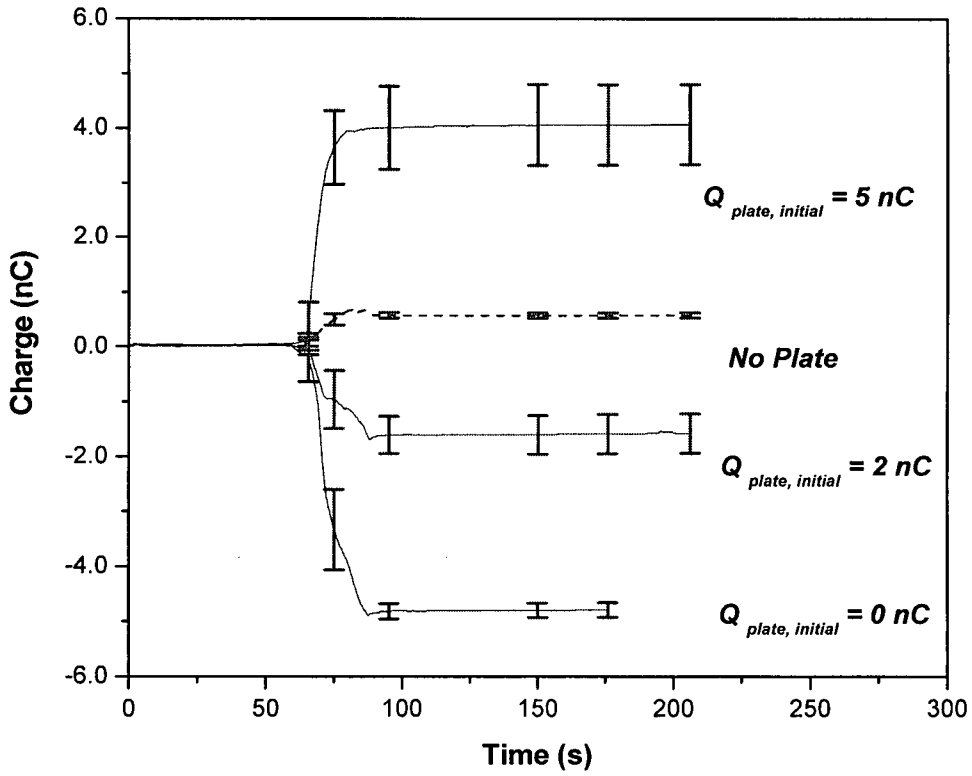

Figure D.21. Charges gained by silica particles due to contact with copper plate of different initial charges with error bars shown (otherwise = Figure 4.26).

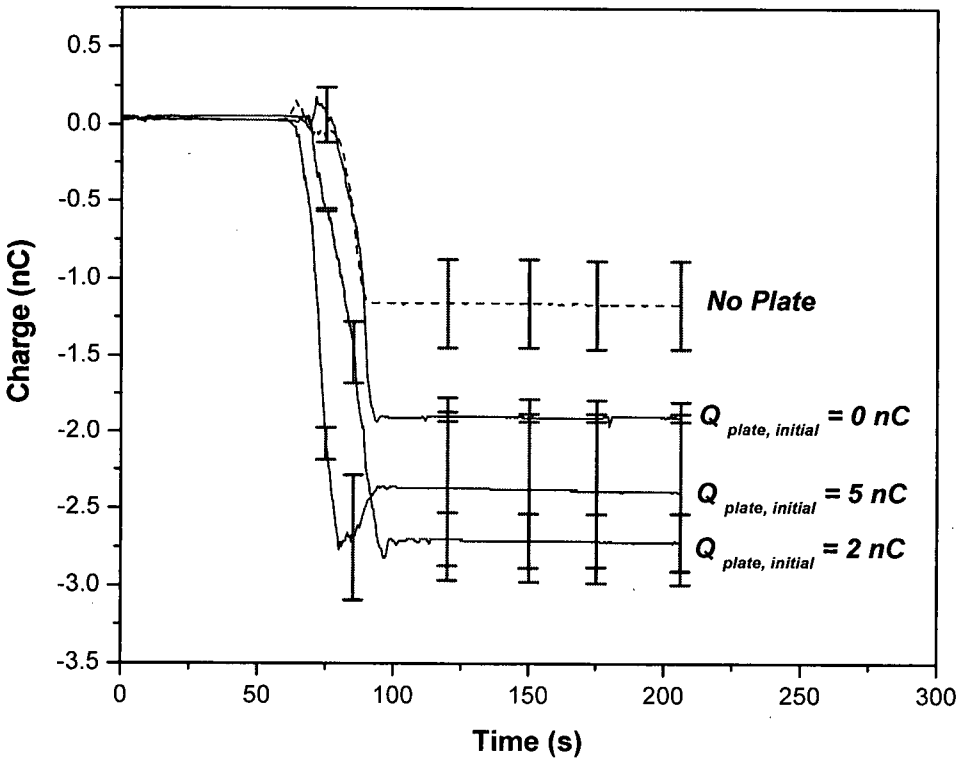

Figure D.22. Charges gained by polyethylene particles due to contact with copper plate of different initial charges with error bars shown (otherwise = Figure 4.27).

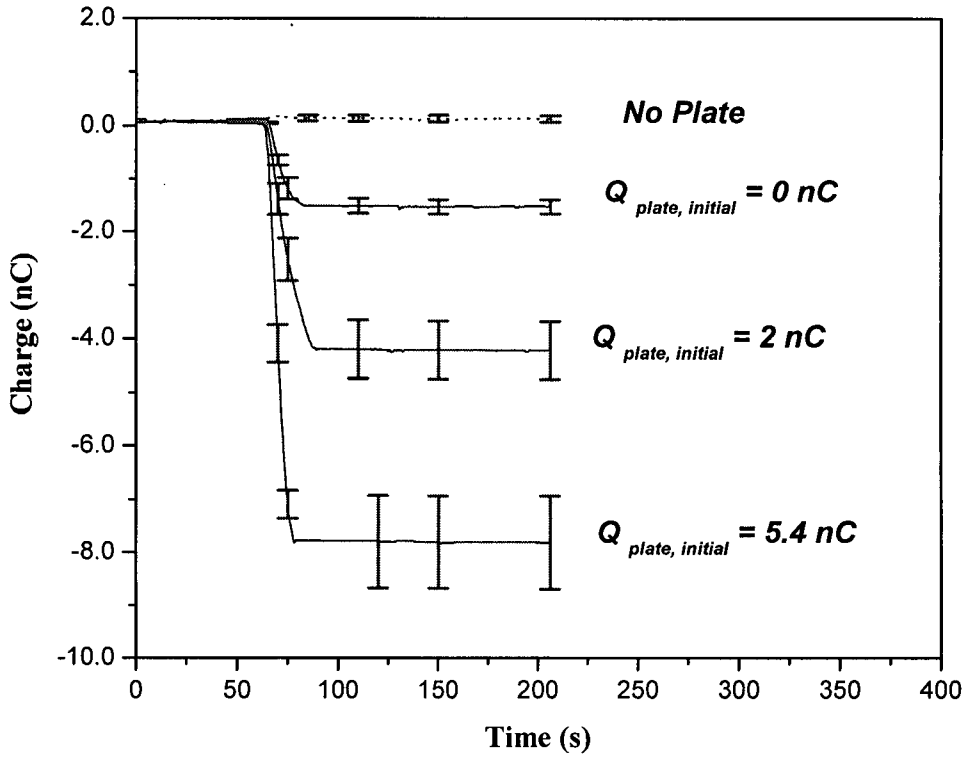

Figure D.23. Charges gained by large glass beads due to contact with copper plate of different initial charge with error bars shown (otherwise = Figure 4.28).